SCIENTIFIC COMMITTEE WORKING GROUP ON PILOT WHALES

24–27 November 2025

Greenland Representation, Copenhagen, Denmark (hybrid)

REPORT

Presented to the 32nd meeting of the Scientific Committee as NAMMCO/SC/32/08

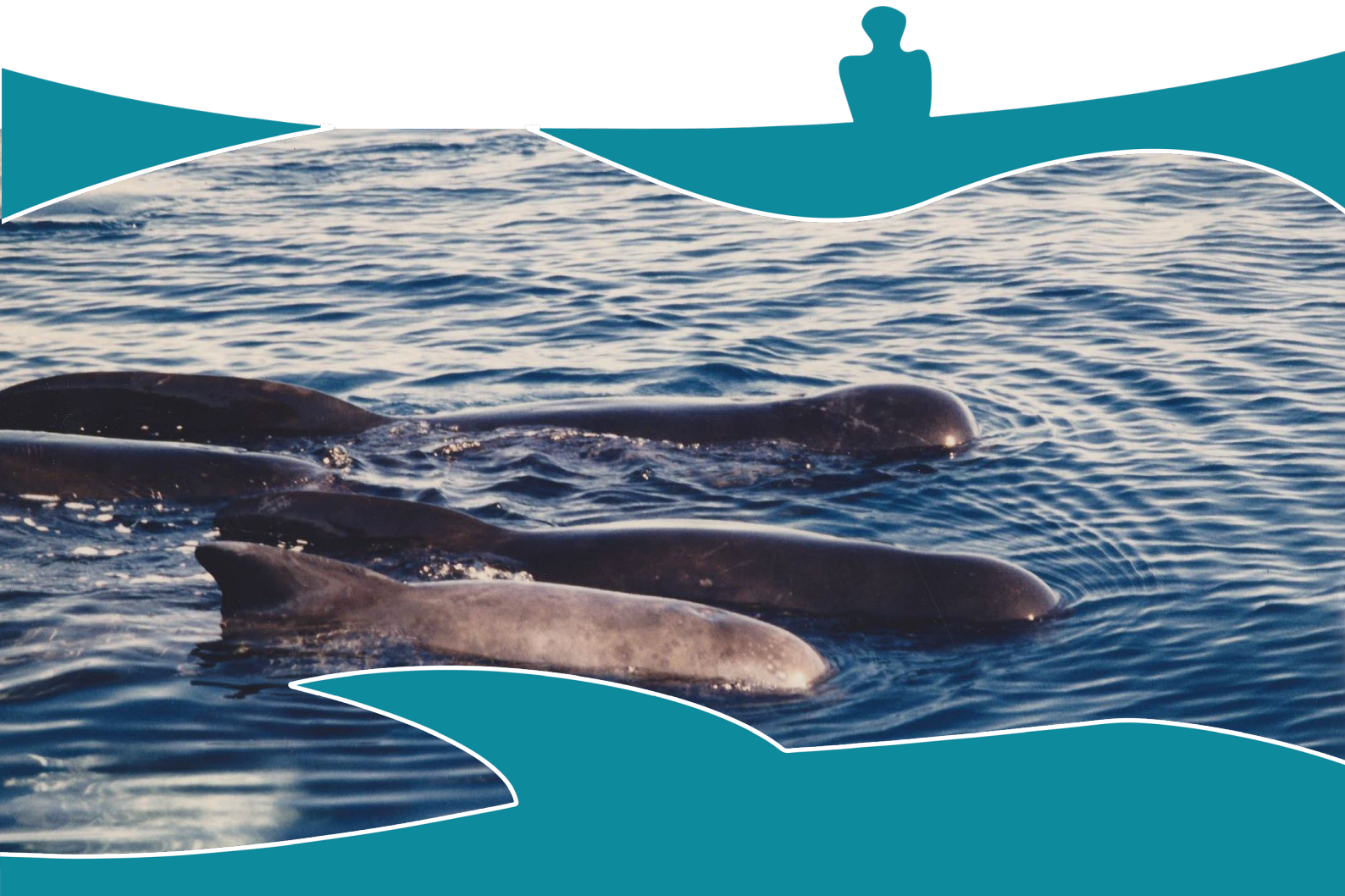

DISCLAIMER:

The content of this report contains the views of the Working Group and does not necessarily represent the views of the NAMMCO Scientific Committee or Council.

Cite this report as: NAMMCO (2025). *Report of the NAMMCO WG on Pilot Whales* (NAMMCO/SC/PWWG/2025-01). NAMMCO-North Atlantic Marine Mammal Commission. Tromsø. Norway. 140 pp. https://nammco.no/wp-content/uploads/2025/12/report_pwwg_2025-01.pdf

All reports of the Scientific Committee Working Group on Pilot Whales are available at https://nammco.no/pwwg_reports/

Chair

Philip Hammond

Rapporteur

Maria Garagouni

Authors

Matthieu Authier, Rachel Ball, Geneviève Desportes, Anne Kirstine Frie, Maria Garagouni, Philip S. Hammond, Mads Peter Heide-Jørgensen, Marie Louis, Bjarni Mikkelsen, Lise Helen Ofstad, Stine Petersen, Gudjón Már Sigurdsson, Fernando Ugarte, Sven Winter, Lars Witting

TABLE OF CONTENTS

EXECUTIVE SUMMARY

The NAMMCO Working Group on Pilot Whales (PWWG) met at the Greenland Representation in Copenhagen, Denmark, on 24–27 November 2025. The meeting was chaired by Philip Hammond, and the aim of the meeting was to conduct an assessment of long-finned pilot whales in the North Atlantic, with a focus on the Faroe Islands and Greenland.

Stock definition

Comprehensive **genomic analyses** of 172 pilot whales sampled across the North Atlantic and Spanish Mediterranean show the Mediterranean population as genetically distinct from animals in the North Atlantic. Within the North Atlantic, there is no evidence of genetic population structure, only a subtle differentiation of pilot whales in the Bay of Biscay and North America from the rest of the region.

Satellite telemetry data from 83 pilot whales tagged primarily in the Faroe Islands, but also East Greenland, Iceland, and Norway, show a distribution continuum across the eastern North Atlantic. Temporal and geographic limitations of most tag deployments precludes any robust inference on sub-structuring and seasonal movements of pilot whales in the North Atlantic.

With the exception of the Mediterranean and Bay of Biscay, neither the genetic nor the telemetry evidence support the existence of differentiated pilot whale stocks in the central and eastern North Atlantic. As such, it was decided to assess pilot whales as a single unit in the region of interest (central and eastern North Atlantic).

Biological parameters

Information on **age, growth, maturation, and pregnancy rates** was collected from pilot whales taken in the drive hunt in the Faroe Islands over two time periods, 1986–1988 and 2011–2023. The maximum ages were estimated in the early samples, at 59 years for females and 46 for males, while maximum body size was 554 cm for females and 635 cm for males. Females were estimated to reach sexual maturity at 7.1 years, corresponding to a body length of 395.7 cm. Ovulation rate was estimated at 0.4 year-1, annual pregnancy rate at 0.36, and mean calving interval at 2.8 years, in the recent time period. Survivorship analysis of the demographic parameters from the Faroese datasets resulted in similar estimates of biological parameters to those agreed as input to the assessment model. Sampling biases and methodological issues with ageing and allocating females to reproductive states were discussed; techniques should be standardised to prevent similar issues in future.

Distribution and abundance

Abundance estimates derived from the 2024 North Atlantic Sightings Survey (NASS) had previously been endorsed by the Working Group on Abundance Estimates. Aerial surveys in East and West Greenland resulted in estimates of 2,025 (95% CI: 585–7,012) and 7.595 (95% CI: 3.084–18.707) pilot whales, respectively. Shipboard surveys around the Faroe Islands and Iceland resulted in a bias-corrected estimate of 262,387 (95% CI: 134,027–513,681) pilot whales; this estimate is likely to be negatively biased because of poor coverage of previous high-density areas for this species. Estimates from 2015 and 2024 were agreed as input to the assessment model. Trend information from a commonly surveyed area in all NASS from 1987 to 2015 was also incorporated in the assessment model.

Direct and indirect removals

Catch statistics for the Faroese drive hunt are available unbroken from 1709 onwards. On average, catch was 831 pilot whales taken in 6.3 drives annually. Short- and long-term fluctuations in catch levels reflect both the availability of animals for the hunt and the demand for whale meat and blubber. Catch ranged from 1 to 1,200 animals per drive, with 52% of the drives taking fewer than 100 animals. Most drives took place (and highest catch numbers were recorded) in July, August, and September.

Catch records for pilot whales taken in East and West Greenland are available from 1923. For West Greenland, annual catches have been reported since 1996, often from drive hunts, ranging from 2 to 272 individuals. In East Greenland, reduced summer sea ice has coincided with increasing catches since

2001, through targeted, open water rifle hunts. Catches in both regions were primarily taken from July to October. Based on anecdotal evidence, it was agreed to adjust the catches in East Greenland by 10% to account for struck and lost animals. Such an adjustment was not applicable to drive hunts in West Greenland.

Catch histories for Iceland, Norway, and the UK and Ireland compiled by ICES varied considerably by year, but all ended before 1975. These data were included in the assessment model covering this period (see below).

Estimates of by-catch rates by the ICES WG on By-catch (WGBYC) for 2017–2024, as well as sporadic records from various countries, suggest low by-catches of pilot whales in European waters. No estimates were included in the assessment model.

Other anthropogenic stressors

Contaminant levels in pilot whales in the Faroe Islands have been monitored regularly since 1997 under the Arctic Monitoring and Assessment Programme (AMAP). Pilot whale tissues have been analysed for heavy metals (mercury, cadmium, selenium) and various persistent organic pollutants (such as organochlorinated pesticides). Mercury levels in adult muscle tissue have increased significantly since 1997 and are considered above the threshold for negative effects. Persistent organic pollutants that have been regulated for several decades are starting to decrease in pilot whale tissues, but this is not clearly evidenced for more recently emerged pollutant compounds. The effects of these various contaminants on hormone, vitamin, and enzyme levels in pilot whales are being investigated, but this is difficult to achieve without uncontaminated "control" specimens.

Little to no information about the impacts of **climate change, underwater noise, and other anthropogenic stressors** on pilot whales was available to the WG.

Population modelling and assessment

As supported by the genetic and telemetry evidence, pilot whales from Norway to West Greenland were assessed as a single unit. Bayesian age-structured population models were constructed to estimate the **production in the population from 1985 to 2025**—including catches from the Faroe Islands and Greenland—using estimates of fecundity and age at maturity from the 1986–1988 and 2011–2023 data, corrected abundance estimates from 2015 and 2024 and relative estimates from 1987 to 2015 as a trend, and age data from 1986–1988 with different likelihood weightings. The three agreed most suitable models estimated a slowly increasing population, with an overall annual production of 2.0% (90% CI: 0.4%–3.8%) and an abundance of 320,000 (90% CI: 196,000–530,000) pilot whales in 2025.

Depletion levels in the current population were explored with two density regulated models, which included the same biological and abundance data as above: the first model began in 1700 from a population presumed to be at carrying capacity (including catch data from Iceland, Norway, and the UK and Ireland); the second model began in 1985 from a population presumed to be below carrying capacity. The two models estimated an average depletion level of 91% (90% CI: 69%–98%).

Recommendations regarding removals

The data-based production estimates of the agreed models show that an annual total removal of 1570 pilot whales across the central and eastern North Atlantic allows the population to increase with 70% probability (the probability level applied in previous NAMMCO assessments). The current removals in all three hunts (average total of 956 animals in Faroe Islands, West and East Greenland, see below) are sustainable.

In relation to sustainability and to reduce the risk of local depletion, the WG recommends allocating future removals among the three hunting areas of West Greenland, East Greenland, and the Faroe Islands according to the average annual removals of the hunts during the last 10 years (i.e., from 2016 to 2025 for the Faroe Islands, and from 2015 to 2024 for Greenland). These average estimates are 679 for the Faroe Islands, 197 for West Greenland, and 80 for East Greenland (72 landed plus 10% struck

and lost). With the overall summed annual removal being 956 animals, this implies a ratio of 1570/956 = 1.6 between the estimated maximum sustainable removals and the current takes in each area.

Owing to the opportunistic nature of all three hunts, the advice is best implemented as a five-year limit that should not exceed 5*1.6*679 = 5432 removals over five years in the Faroe Islands, 5*1.6*197 = 1576 removals over five years in West Greenland, and 5*1.6*80 = 640 removals over five years in East Greenland (corresponding to 1576 and 576 landings for West and East Greenland, respectively). These recommendations assume no by-catch in the central and eastern North Atlantic. The advice should be reconsidered by the Scientific Committee, ideally within five years and no later than 10 years in the absence of new information.

Recommendations for conservation and management

To all Parties

- A survey to provide new information on abundance should be conducted within the next 10 years.
- More telemetry data should be collected from the Faroe Islands and additional areas across the North Atlantic to provide more representative geographical coverage. Tagging should aim to provide a more representative coverage of the whole year.

To the Faroe Islands

- Sampling and ageing of pilot whales should be conducted to provide a representative sample of the entire catch.

To Greenland

- Undertake sampling for biological parameters from the drive hunts in West Greenland.
- Collect and analyse more genetic samples from West Greenland.
- Collect samples and conduct analyses to better inform stock definition in East and West Greenland (e.g., long-term telemetry, stable isotopes, contaminant levels).

To Iceland

- Age existing tooth samples and collect data to inform biological parameters whenever possible.

Recommendations for research

To all Parties

- *(Reiterated from the WG on Genetics 2024)* Initiate a dedicated genetic monitoring programme based on archival and newly collected samples from harvested groups in Greenland and the Faroe Islands, as well as in mass stranding events wherever they occur, to determine:
  i. family groupings and social structure,
  ii. putative population of origin,
  iii. the influence of removing entire family units during pilot whale hunts, for instance in terms of genetic diversity, inbreeding levels, mutation load, and standing genetic variation.
- Review and standardise the techniques used for ageing and obtaining reproductive parameters and determine whether there may be a common methodological bias in existing data.
- Collect information on body condition (e.g., blubber thickness) to monitor the effects of environmental changes.

REPORT

The NAMMCO Working Group on Pilot Whales (PWWG) met at the Greenland Representation in Copenhagen, Denmark, on 24–27 November 2025. The meeting was chaired by Philip Hammond, with participants both in person and online (full list of participants is available in Appendix 3).

1 OPENING REMARKS

The Chair welcomed participants to the meeting and called for a round of introductions. He noted that meeting etiquette should be observed, as laid out in document PWWG/2025-01/FI/01.

2 ADOPTION OF AGENDA

Hammond reminded the group of the meeting aim, namely, to conduct a stock assessment of long-finned pilot whales in the North Atlantic, with a focus on making recommendations on the sustainability of catches in the Faroe Islands and Greenland. The items on the agenda are intended to facilitate an assessment model for the region.

The agenda was adopted with no modifications, as shown in Appendix 1.

3 APPOINTMENT OF RAPPORTEURS

In time-honoured tradition, Deputy Secretary Maria Garagouni was appointed rapporteur, with support from other participants as needed, and with the contribution of written summaries from the authors of any presentations given.

4 REVIEW OF AVAILABLE DOCUMENTS

The WG was reminded of the list of available meeting documents (as shown in Appendix 2, with some additions later in the day). It was noted that document PWWG/2025-01/10 on biological parameters became available to the group on the first day of the meeting.

5 ASSESSMENT OF LONG-FINNED PILOT WHALES IN THE NORTH ATLANTIC

5.1 STOCK DEFINITION

The identification of potentially distinct populations will inform the WG's decision on which areas to use for a stock assessment, e.g., whether to assess the entire North Atlantic as one unit and/or more than one region separately.

5.1.1 Genetic information

Sven Winter presented recent analysis of pilot whale genetic samples from around the North Atlantic, including the latest report of the Genetics WG (PWWG/2025-01/6a) and further analyses completed since that meeting (PWWG/2025-01/6b).

Summary

Long-finned pilot whales (*Globicephala melas*) have previously been shown to exhibit low genetic diversity across the North Atlantic, with subtle regional structuring, and a genetically distinct, low-diversity Mediterranean population. However, genome-wide patterns of population structure and diversity remain largely unexplored. Here, we present whole-genome sequence data from 172 individuals sampled across the North Atlantic and Spanish Mediterranean. Analyses reveal two clearly separated populations, with the Mediterranean population exhibiting reduced diversity consistent with historical bottlenecks and genetic drift, which may amplify its apparent divergence. Within the North Atlantic, population differentiation is weak, PCA and admixture analyses suggesting a potential east–west differentiation. However, genomic regions with elevated divergence identified by window-based

PCA do not correspond to geographic separation. Genome-wide heterozygosity and demographic reconstructions support these patterns, while mitochondrial genomes confirm low diversity and mostly shared haplotypes. These results provide the first genome-wide perspective on long-finned pilot whales, highlighting Mediterranean distinctiveness and a weak, subtle east–west gradient, with subtle differentiation of Bay of Biscay individuals and USA/Canada individuals from the rest of the North Atlantic.

Discussion

It was asked whether the (potential) east–west gradient in the admixture analysis could be explained by neighbouring populations exchanging genetic material at the edge of their respective ranges. Theoretically, that could be possible, but high levels of mating would be required to produce such a pattern; it is more likely that excluding the French samples from the pool would remove any signal of such a geographic gradient, due to their shared ancestry with Mediterranean pilot whales.

The WG agreed that in the results presented, there is little to no evidence to support any genetic structure in the North Atlantic, in particular around the Faroe Islands, Iceland, and Greenland, which are of focus for this assessment. The WG agreed that a comparison with samples from the Southern Hemisphere, as well as other areas of the Mediterranean, would be of interest but beyond the scope of the present assessment. It was noted that some of the genetic variability seen could result from social structure and, despite the considerable effort required, this would be worth investigating further. It should also be noted that while samples from all regions were taken from different groups over several years, the samples from West Greenland come from a single group.

5.1.2 Telemetry information

Bjarni Mikkelsen presented working document PWWG/2025-01/09 on the movements and distribution of pilot whales tagged in the Faroe Islands and Iceland.

Summary

On fourteen different occasions, over the period 2000–2024, pods were driven into shallow waters of the Faroe Islands, where a total of 58 pilot whales were tagged. Tags used were fin-mounted SPOT and SPLASH satellite transmitters from Wildlife Computers and four fin-mounted satellite tags from Telonics. Also, three animals were tagged in Iceland in 2023, with WC LIMPET tags, darted from a distance. These satellite-linked recorders transmit data via the Argos satellite system. Argos position data vary in accuracy, and to remove unrealistic positions, data were filtered with the sda filter in R, which uses the Freitas et al. (2008) algorithm. Of the 61 transmitters deployed in total, ten provided locations for more than three months, while seven tags (11%) failed or transmitted only on the first day. The longest track duration was 292 days. Average duration for the longest lasting tag in each group was 111 days. Tagged groups ranged from 7 to 80 animals, with a mean of 31. Groups were tagged in all months from May to November, mostly between June and August. The tagged pods all left the Faroe Shelf just after tagging, moving to deeper slope waters with subsequent variation in movements. Four general movement patterns can be identified: 1) moving north to the southern slope of the Norwegian Sea and along the northern slope of the Faroe–Iceland Ridge and moving along the Faroe–Shetland Channel, 2) moving south to the Faroe, Bill Bailey, and Lousy Banks and around the Rockall Plateau and along the offshore waters of the UK Shelf, 3) moving south to the deeper waters beyond the Rockall Bank, and 4) moving west to the deep waters of the Iceland Basin, the Reykjanes Ridge, and Irminger Sea. The tracked animals did not show any clear seasonality in distribution. Notably, the results demonstrated that pilot whales occur north of the Faroes year-round, and that they make long-distance movements to lower latitudes in high summer. The lack of seasonality in distribution indicates that pilot whales do not make distinct feeding migrations or have specific feeding areas but rather find food over a wide range in all seasons.

Discussion

The WG debated whether the tracked animals could be said to show seasonal movement patterns or not; migration similar to that observed in baleen whales is certainly not apparent. On the one hand,

based on the small number of tagged animals compared to the total population, the mostly relatively short tag longevity, and the common starting point in the Faroe Islands (except for the three animals tagged in Iceland), it was argued that seasonal variation could not be excluded. On the other hand, the tracks indicate that some slight north–south movements could be apparent, potentially reflecting animals following prey. Movements of blue whiting and *Todarodes* squids have been shown to correlate with higher pilot whale numbers around the Faroe Islands (Jákuppstovu, 2002). Information on diet is limited to around the Faroe Islands and not available to inform whether the tracks in the southwest of the region could be linked to specific prey movements.

In relation to social aspects that might also inform genetics studies, it was asked whether animals tagged in the same groups that subsequently split off from each other did so shortly after the tagging event. Mikkelsen clarified that animals that separated from each other did so generally three to five days after the tagging event, possibly because they did not belong to the same small family units to begin with, but to different family units within the larger groups.

Information was available to the WG on movements of animals tagged in northern Norway (from Audun Rikardsen and the MINTAG project) and East Greenland (from the Faroese/Greenland TOPLINK project), as shown in Figure 1. Tracks were shown from 11 animals tagged in northern Norway between 2022 and 2025, lasting from 20 days to over 5 months; these animals remained on the continental shelf for the duration of tag transmission. Five more pilot whales were tagged using MINTAGs in northern Norway, ranging in transmission times from two hours to 48 days. Four of these individuals remained close to the Norwegian coastline throughout, while one was tracked moving to the Shetland Isles. Six pilot whales were tagged in East Greenland in 2023–2025, for a duration of between 1 and 61 days. The movements of all six were concentrated on the continental shelf.

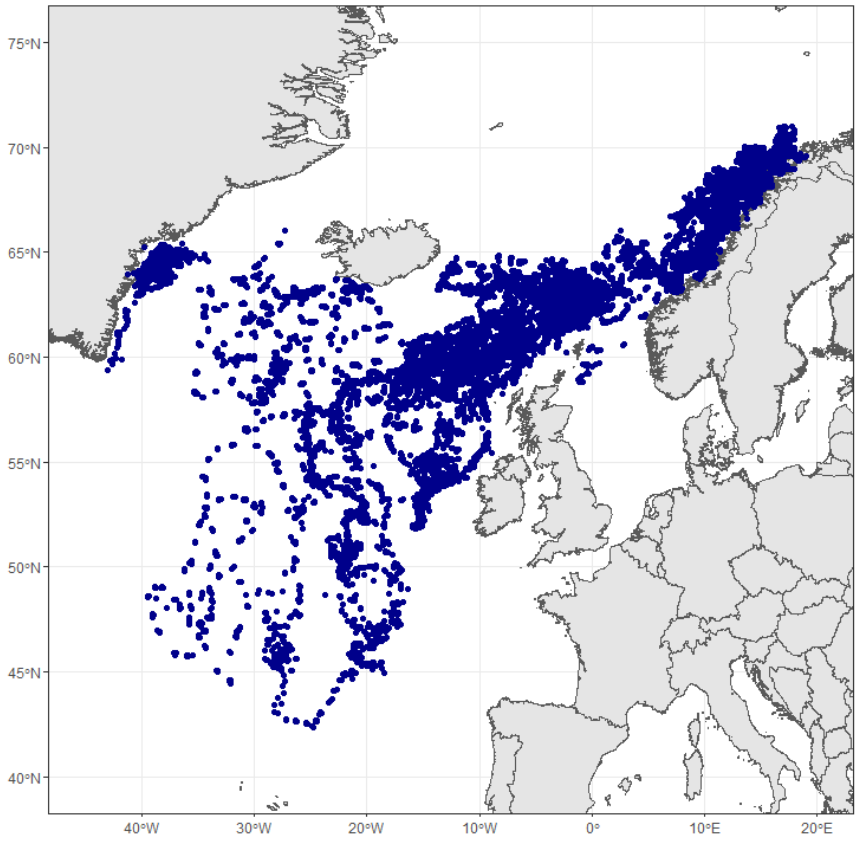

Figure 1. Telemetry data showing locations of long-finned pilot whales tagged in East Greenland (TOPLINK project), the Faroe Islands (Faroe Marine Research Institute), Iceland (University of Iceland Research Centre in Vestmannaeyjar), and Norway (MINTAG project and University of Tromsø Department of Arctic and Marine Biology).

Overall, the location data show a distribution continuum from Greenland to Norway. The limited duration and geographical extent of most telemetry deployments precludes robust inference about sub-structuring of pilot whales in the North Atlantic.

5.1.3 Conclusion

The genetic and telemetry evidence does not support the existence of any stock differentiation in the eastern and central North Atlantic, with the exception of the Spanish Mediterranean and some animals in the Bay of Biscay.

5.2 BIOLOGICAL PARAMETERS

Mikkelsen presented working document PWWG/2025-01/10 which provided data on age, growth, and female reproductive parameters of pilot whales taken in the traditional drive hunt in the Faroe Islands. *[In an earlier version of this report, this document was provided as an Appendix. This has now been removed for confidentiality reasons, but could be made available on request to the author.]*

Summary
Age was estimated from growth layer groups (GLGs) in teeth, with 354 females and 110 males aged in the period 2011–2023. Also, ages were available for the period 1986–88 (N = 2423), from an international study on pilot whales in the Faroe Islands. Length (N = 18553) and weight (N = 621) data were available from the official catch statistics, from the period 1986–2025. Female ovary pairs from 639 animals were examined for evidence of pregnancy and lactation; ovaries were also weighed and the number of corpora determined. Attainment of sexual maturity (A50) for females was estimated to occur at an average age of 7.1 years, and at a body length of 359.7 cm. The oldest female in the sample was 59 years (for males 46 years), and maximum measured body size from the biological samples was 554 cm for females and 625 cm for males (from the official data 600 cm and 1320 kg for females and 650 cm and 2320 kg for males). Ovulation rate was estimated to 0.40 year-1. The total number of corpora increased with age up to around age 23; thereafter it levelled out, which could indicate that corpora do not persist throughout life. Estimated annual pregnancy rate was 0.36 (based on a gestation period from the 1986–1988 study of 12 months) and the calving interval 2.8 years. Tiny and full borne foetuses were most frequently present in August and September, indicating that parturition occurs mainly in late summer.

Discussion
It was noted that younger age classes, at least 0 to 6 years, are underrepresented in the 2011–2023 data as a result of not being included in samples and/or a non-random selection of animals to be aged. This affected the calculation of age at maturity and pregnancy rate, if animals that may have matured or become pregnant at younger ages were missed.

The 2011–2023 age data presented were clearly not representative of the population and cannot be used in the assessment model. However, if there were data from drives in which it was known that all, or almost all, of the animals were taken as samples and also aged, these could potentially be used. Mikkelsen and Ofstad selected data from four drives which seemed to meet these conditions. However, even this sub-sample of ages were clearly not representative of the population. The WG concluded that, unfortunately, the 2011–2023 age data could not be used in the assessment model.

Potential issues with the ageing techniques and allocating females to reproductive states were discussed. It has been observed in harbour porpoises that GLGs are formed differently in relation to the calving season, and may also differ by population (Frie and Lindström, 2024). It was clarified that, in this dataset, the number of GLGs refers to the number of completed GLGs, but no other information was included about the timing of the sample collection. With regards to ovulation rate, it was noted that the 2011–2023 data indicate a higher rate of 0.4 corpora per year (PWWG/2025-01/10, Figure 13) than the 1986–1988 data, 0.25 corpora per year (Martin & Rothery, 1993). This could potentially result from different or problematic methods of identifying corpora in the ovaries; in harbour porpoises it has been documented that misidentification of accessory corpora, staining, and magnification methods,

could all contribute to erroneous results (Frie and Lindström, 2024), something which could also be the case here. This should be investigated further for pilot whales. Finally, it was pointed out that corpora luteum that did not result in pregnancies, as well as potentially high abortion rates (Desportes et al., 1994), were not accounted for in the data (although for the population model, these will be incorporated in the first-year survival parameter; see item 5.6).

To enable accurate calculation of age at first parturition, smaller foetuses should be allocated as being born in the next year, whereas larger ones would presumably be born in the same year in which they were recorded. While this was not achieved in the available dataset, it should be standard practice in future.

Matthieu Authier presented a survivorship analysis using demographic parameters from the Faroese data.

Summary
Data on age of long-finned pilot whales taken in the traditional drive hunt in the Faroe Islands (Mikkelsen et al. 2025) were analysed using time-to-event methods to estimate age-specific vital rates (survival and female maturity). Survivorship was estimated from age-at-death with the parametric method described in Rouby et al. (2021): model fit, when compared to a non-parametric estimate (Kaplan & Meier 1958), was good when data from 1986–1988 and 2013–2023 were analysed separately. The 1986–1988 data displayed the expected bath-tub pattern for age specific mortality, but not the 2013–2023 data, suggesting sample selection issues and a deficit of young age classes in the recent data. Female maturity was estimated with time-to-event methods taking into account left-censoring (females that matured before being taken) and right-censoring (females that would have matured later had they not been taken). This approach assumed that count of a single corpus corresponds to the age at which females matured, although maturation may have occurred one or more years before. Nevertheless, this approach yielded estimates of age at maturity similar to those reported in Mikkelsen et al. (2025). The results from these analyses aligned with the decisions taken with respect to the samples to include in the assessment model to inform on demographic parameters.

5.3 DISTRIBUTION AND ABUNDANCE

Abundance estimates derived from the latest North Atlantic Sightings Survey (NASS) were presented by Mads Peter Heide-Jørgensen for Greenland and Stine Petersen for the Faroe Islands and Iceland. These had already been endorsed by the Working Group on Abundance Estimates (NAMMCO 2025).

Summary
An aerial line transect survey of cetaceans was conducted in coastal waters off West and East Greenland during August–September 2024. The survey aimed to assess whale populations in nearshore and offshore zones, covering areas extending up to 100 km from the West Greenland coast and up to 50 km from the East Greenland coast. There were a total of 5 and 17 pilot whale encounters in East and West Greenland, respectively. Abundance estimates were corrected for perception and availability bias where possible, using data from satellite-linked time-depth recorders and observations of cue rates. Options for estimation methods were presented, and the preferred estimates are 7,595 (95% CI: 3,084–18,707) pilot whales in West Greenland and 2,025 (95% CI: 585–7,012) in East Greenland. In East Greenland, the abundance estimate for pilot whales was higher in 2024 compared to 2015, while West Greenland showed a decline in estimated abundance relative to previous surveys.

Data from the NASS 2024 Icelandic and Faroese ship surveys were analysed to estimate pilot whale abundance. Surveys were carried out in double platform mode (IO configuration). The available data required some processing before analysis, which was done in collaboration with the data providers from the Faroes and Iceland. The survey effort included designed transects and some additional transects. All on-effort data, including 123 sightings of groups, were used to estimate detection probability. Only the data from designed transects were used to estimate abundance; these included 7,091 km of effort and sightings of 42 groups with mean group size of 17.8. The data were first analysed

to estimate abundance uncorrected for animals missed on the transect line using a single platform approach by combining data from both platforms on each ship. The top-ranking detection function included vessel as a covariate and fitted the data well. Within the nominal survey strip defined by the largest perpendicular distance of 1,686m, average detection probability was estimated as 0.207 (CV = 0.241). Total uncorrected abundance was estimated as 174,246 individuals (CV = 0.302; 95% CI: 95,569–317,696). The data were then analysed to estimate abundance corrected for perception bias using a double platform approach. The top-ranking conditional detection function included Beaufort as a covariate and fitted the data well. Average conditional detection probability was estimated as 0.688 for both platforms combined, giving an overall average detection probability of 0.207 * 0.688 = 0.142 (CV = 0.244). Total corrected abundance was estimated as 262,387 individuals (CV = 0.339; 95% CI: 134,027–513,681).

Discussion

It was highlighted that animals present in August in the area covered by aerial surveys off East Greenland may not be different from animals present in the shipboard survey conducted in July (specifically, block IDW2); therefore, the 2024 estimates were not summed in calculating total abundance. For consistency, the WG agreed not to include the 2015 estimates from East Greenland in calculating total abundance for the North Atlantic.

The lack of effort in block IR_N and the lack of sightings on designed transects in block FM, areas of high pilot whale density in previous surveys, mean that total estimated abundance in 2024 is likely negatively biased.

The 1987–2015 trend analysis in document PWWG/2025-01/FI/04 (Pike et al. 2019) was discussed. For the purposes of incorporating trend information in the assessment model, the WG agreed to include uncorrected estimates of abundance for the common 6 Survey Index Area described in that paper (see also Appendix 4). The WG also agreed to use corrected abundance estimates for those years with the most extensive survey coverage (2007, 2015, and 2024), as shown in Appendix 4.

5.4 DIRECT AND INDIRECT REMOVALS

5.4.1 Faroese catch history

Mikkelsen presented working document PWWG/2025-01/08, which provided an overview of the catches of long-finned pilot whales from the traditional drive hunt in the Faroe Islands.

Summary

Catch statistics exist back to 1584, and records are unbroken since 1709, i.e. for more than 300 years. This may be the longest series of hunting statistics existing today. The statistics include about 269,181 pilot whales taken in 2,033 drives, with an average of 132 animals in each drive, and an average of 609 pilot whales taken in six drives per year. Since 1709, the average annual catch has been 831 whales and 6.3 drives. Both short- and long-term fluctuations are apparent in the harvest. After 1709, the period 1750–90 had no or few catches, while catches were high in the periods 1830–50 and 1940–80. In intermediate periods, and the most recent thirty years, catches have been around the long-term average. Group size has ranged from 1 to 1,200 animals; however, 52% of the catches have consisted of fewer than 100 animals. Most catches are taken in July, August, and September, when 67% of all drives have occurred.

Discussion

It was underlined that the catch size in each year reflects a combination of the availability of pilot whales around the Faroe Islands, the relative demand for pilot whale meat and blubber (e.g., increased food needs during and after World War II correspond to very large catches), and some management measures. Mikkelsen informed the WG that the peak in catch numbers observed in the 1980s has been found to correlate with an increase of *Todarodes* squids over the continental shelf, as recorded in fishery data, and that such a large influx of pilot whales has not been observed since. Although demand may be slightly reduced in more recent years—especially after the health authorities started advising

limited consumption due to high mercury loads in the meat and blubber—interest and involvement in the hunt remains. The number of pods driven compared to the total available cannot be determined because there is no systematic record of pods that are sighted but not hunted (particularly for earlier periods).

It was noted that average group size in the last 25 years appears smaller compared to previous centuries, but it is unclear whether that is an artefact of data categorisation. The opportunistic nature of the hunt, with approximately five drives per year, indicates that it is unlikely to be a result of the community targeting smaller pods due to reduced demand.

5.4.2 Greenlandic catch history

Heide-Jørgensen presented working document PWWG/2025-01/13 on pilot whale catch statistics from Greenland.

Summary
Statistics on reported pilot whale catches from East and West Greenland were compiled from Heide-Jørgensen & Bunch (1991) for the years 1923–1986 and from the official hunters' reporting system, Piniarneq (1993–2024), for the period after 1993. The Piniarneq records include information on municipality, town or settlement, and month of harvest.

Pilot whales were only sporadically caught—or reported caught—in West Greenland between 1921 and 1986. No official statistics are available for 1987–1993, and reporting from the early years of the Piniarneq system may be incomplete. Since 1996, however, pilot whales have been taken annually in West Greenland, with the year 2000 as the only exception. Annual catches range from 2 to 272 whales, reflecting the variable occurrence of pilot whales in West Greenland coastal waters.

No pilot whale catches were reported from East Greenland before 2001. The subsequent increase in catches coincides with the disappearance of summer sea ice along the coast and the increasing inflow of Atlantic Water (Heide-Jørgensen et al. 2022).

Hunting methods differ markedly between East and West Greenland. In East Greenland, pilot whales are known to occur in specific offshore areas 30–50 km from the coast, enabling directed hunting. Whales are taken individually in offshore waters, often with several dinghies shooting at the pods. This method may result in considerable losses in addition to the whales brought to shore. No drive fishery for pilot whales occurs in East Greenland.

In West Greenland, pilot whales are also primarily found offshore and are not subject to a targeted hunt. Instead, whales occasionally enter the deep-water troughs between the West Greenland banks, possibly while following squid concentrations. When detected by coastal residents, the whales can be driven into bays or shallow areas where they are shot.

All catches reported from East Greenland originate from the Tasiilaq community. In West Greenland, catches are concentrated in coastal areas adjacent to the channels between the banks, with the largest numbers taken in the northernmost communities. A few catches reported from Qaanaaq require verification.

The seasonal distribution of catches in both East and West Greenland is strongly concentrated in the open-water period from July to October. Occasional reports of winter catches also require confirmation.

Discussion
The WG discussed the need to adjust removals by struck and lost rates and what rates were appropriate to use. There are no data to inform struck and lost rates for pilot whales. In East Greenland, observations of the hunt by researchers suggest low rates, and pilot whales are reportedly easier to hunt than other species: hunters have described them as larger, slower, and easier to approach and secure than, e.g., dolphins, with only 5–10% of the animals sinking after being shot. The WG agree to use a base 10% loss rate to adjust East Greenland catches. However, as this is based on anecdotal

evidence, the WG agreed to the use of a second catch data series adjusted by a struck and lost rate calculated for the narwhal hunt by the WG on Narwhal in East Greenland (NEGWG) in 2023, equal to a multiplier of 1.3 (NAMMCO 2023). For West Greenland, struck and lost rates are expected to be low in the drive hunts. The communal nature of the drive hunts could potentially lead to over-reporting. The WG was not in a position to adjust the catch series for West Greenland.

5.4.3 By-catch

A summary of recorded by-catches and estimated total animals by-caught by the ICES WG on By-catch (WGBYC) for the period 2017–2024 suggests low by-catches of pilot whales in European waters. The highest risk appears to be posed by pelagic fishing gear such as trawlers. Sporadic reports of individual and group by-catches were discussed, but no estimates were available for the assessment.

5.4.4 Removals from other areas in the eastern North Atlantic

Besides the Faroe Islands and Greenland, the 1996 ICES Study Group for pilot whales (document PWWG/2025-01/FI/12) compiled catch records from Iceland, Norway, and Great Britain and Ireland. Catches vary considerably by year and area, but all ended before 1975 (Appendix 5). These catch histories were incorporated in the assessment models.

5.5 OTHER ANTHROPOGENIC STRESSORS

5.5.1 Contaminants

Katrin Hoydal (Faroe Environment Agency) presented recent findings by AMAP on contaminant loads in pilot whales caught in the Faroese drive hunt (PWWG/2025-01/FI/12).

Summary
Pilot whales have been part of the pollution monitoring on the Faroe Islands and have been monitored regularly since 1997. The monitoring is focusing on heavy metals and persistent organic pollutants, POPs and is part of the Arctic Monitoring and Assessment Programme (AMAP), which is a working group under the Arctic Council. The monitoring involves sampling every year of pilot whale muscle, blubber, liver and kidney. Sometimes also other tissues are sampled, e.g. blood for analyses of effects.

The tissues are analysed for the heavy metals mercury (Hg) and cadmium (Cd), as well as selenium (Se) and for the POPs PCBs, organochlorinated pesticides, such as DDTs, chlordanes, toxaphenes, etc., PBDEs, and PFASs.

Since we have monitored for many years (20+) now it is possible to analyse time-trends for the different contaminants. To avoid that the trend analyses are confounded by other factors such as age and sex, we only use juvenile males for the trend analyses in pilot whales.

The results show that Hg in pilot whale muscle seems to be significantly increasing from the mid-1990s until now. The concentrations of Hg in liver are at a much higher level than in muscle and above suggested negative threshold level in marine mammals (the contaminants in liver are analysed in adult whales).

The POP concentrations show decreasing time-trends for the legacy POPs, that have been regulated for the last 40-50 years, whereas for the emerging pollutants the trend is not as clear. However, PBDEs, which have been regulated since around 2002, have shown a decrease since their regulation. For PFAS it depends on the different compounds, and we need to analyse more samples to get a better trend analysis.

The contaminants can have effects both on the exposed pilot whales, but also on the humans using the pilot whales for food. We have done some effect analyses on pilot whales from the Faroe Islands, analysing hormones, vitamins and enzymes involved in metabolism of contaminants. It was however not possible to see clear overall negative effects on the analysed biomarkers, but more studies are needed and planned, but are dependent on funding.

Discussion
Some clarification was given regarding the data sources included in certain analyses. The WG thanked Hoydal for the comprehensive and interesting overview of this topic.

5.5.2 Climate change

There is little information on the potential impacts of climate change on pilot whales. An affinity for warmer sea surface temperature in the spring (as a proxy for prey availability in the summer) has been identified in the central and eastern North Atlantic (Ramirez-Martinez et al., 2024)). In the western North Atlantic, pilot whale distribution appears to have shifted northward despite their prey species' distribution shifting deeper in the water column but remaining in the same area (Thorne and Nye, 2021).

5.5.3 Other human impacts

No information was available to the WG on the potential impacts of underwater noise, tourism and other vessel traffic, etc., on pilot whales.

5.6 POPULATION MODELLING AND ASSESSMENT

5.6.1 Assessment units

The genetic data, supported by the telemetry data, show no evidence of anything other than a single biological population of pilot whales across the whole central and eastern North Atlantic, excluding Spain and possibly the Bay of Biscay (item 5.2.1). The WG therefore agreed that the assessment should be conducted on a single assessment unit in the region of interest.

Ugarte raised the possibility that animals taken in the East Greenland hunt could be part of a separate population based on the lack of overlap in tracks from animals tagged in the Faroes and in East Greenland, and that animals tagged in East Greenland remained in the area during summer. Counterarguments to this view were:

a) The telemetry data are limited by the tagging location, the number of animals tagged, and the short duration of most of the tags and therefore cannot be considered representative of year-round movement patterns across the whole central and eastern North Atlantic. Nevertheless, animals tagged in the Faroe Islands have been tracked up to the Greenland shelf edge and there is no reason to assume whales in this area do not mix with whales available to the hunt in East Greenland.
b) The most parsimonious explanation is that whales that began using waters off East Greenland after the sea ice receded in 2001 are part of a single population of whales and that their concentrated short-term movements on the continental shelf during summer reflect foraging in this area at that time.
c) Although the genetic sample of non-related individuals from West Greenland is small, those from East Greenland were from a range of years and areas and could not be differentiated from animals sampled in the Faroe Islands, thus providing no evidence that animals off East Greenland should be considered as a separate population. The samples from Canada and the USA were similar to the rest of the North Atlantic, so there is no reason to consider animals off West Greenland as genetically distinct. However, a recent separation, e.g. a subgroup of whales taking advantage of the receding ice in the past two decades, would not be detected by genomic analysis.

The WG reconfirmed that the only approach supported by the available evidence was to assess the central and eastern North Atlantic as a single stock. Concerns over local area depletion would need to be investigated with longer-term telemetry studies and other monitoring information.

5.6.2 Model structure and results

Working Paper PWWG/2025-01/07 (Appendix 6) developed the Bayesian assessment modelling based on the agreed structure of one overall population of long finned pilot whales across the North Atlantic

from Norway to West Greenland, with Canada and the USA not being assessed. Sub-paper 07a explored the construction of the age-structured simulation model, where it was necessary to downscale the weight of the log likelihood contribution from the age data by a multiplicative fraction to obtain appropriate fits to the age and abundance data.

By incorporating all catches from Greenland and the Faroe Islands, sub-paper 07b developed the assessment model using the available data to estimate the production in the population from 1985 to 2025. The model estimated the potential regulation of the growth rate by fitting a linear change in the birth rate and age of reproductive maturity to the pregnancy and maturity data of the early (assigned to 1987) and late (assigned to 2017) sampling periods in the Faroe Island, allowing also for a linear change in offspring survival. The model also integrated the early age data as separate age distributions for 1986, 1987, and 1988, and the agreed time-series of relative abundance estimates from 1987 to 2015, and three agreed corrected abundance estimates 2007, 2015, and 2024. This provided a model with strongly data-updated posterior distributions from uniform priors for all parameters, except that the 2017 prior on offspring survival was only weakly updated, and that a humped beta(2,2) prior for adult survival was centred around 0.96 and rescaled to cover the range from 0.93 to 0.99. This prior on adult survival was also firmly updated in the agreed models.

To resolve the issue of overlap in the time-series of relative and corrected abundance estimates in 2007 and 2015, the WG agreed to keep the complete relative time-series as an index of trend, and to use the average of the 2015 and 2024 corrected abundance estimates as an absolute scaler applied to 2020. Three versions of this model showed that weighting the log likelihood of the age data by 0.1, 0.25, or 0.5 had only a minor influence on the results, and the WG agreed to use these three models to provide informative estimates of the production in the population. These models applied a loss rate of 10% to the catches in East Greenland, with a sensitivity run with 30% showing hardly any influence on the results. These models estimated a slowly increasing population, given the catches from 1985 to 2025, with an overall yearly production of 2.0% (90% CI: 0.4%–3.8%) and a current 2025 abundance of 320,000 (90% CI: 196,000 – 530,000) animals (Figure 2).

Using the same biological and abundance data as the exponential model above, sub-paper 07c developed two density regulated models to estimate the current depletion of the population. The first model incorporated an extended catch history that includes all known catches from the central and eastern North Atlantic starting in year 1700, assuming an initial population at carrying capacity. The second model explored the fit to the recent data from a 1985 population assumed to be below the carrying capacity. The average estimate of the depletion level from the two models was 91% (90 CI: 69%–98%).

6 RECOMMENDATIONS FROM THE WORKING GROUP

6.1 RECOMMENDATIONS REGARDING REMOVALS

The WG agreed to use the data-based production estimate of the agreed models as an overall estimate of sustainable removals. These models show that an annual total removal of 1570 animals across the central and eastern North Atlantic allows the population to increase with 70% probability (the probability level applied in previous NAMMCO assessments). The current removals of all three hunts (average total of 956 animals in Faroes, West and East Greenland, see below) are sustainable.

In relation to sustainability and to reduce the risk of local depletion, the WG recommend allocating future removals among the three hunting areas of West Greenland, East Greenland, and the Faroe Islands according to the average annual removals of the hunts during the last 10 years (i.e., from 2016 to 2025 for the Faroe Islands, and from 2015 to 2024 for Greenland). These average estimates are 679 for the Faroe Islands, 197 for West Greenland, and 80 for East Greenland (72 landed plus 10% struck and lost). With the overall summed annual removal being 956 animals, this implies a ratio of 1570/956 = 1.6 between the estimated maximum sustainable removals and the current takes in each area.

Owing to the opportunistic nature of all three hunts, the advice is best implemented as a five-year limit that should not exceed 5*1.6*679 = 5432 removals over five years in the Faroe Islands, 5*1.6*197 = 1576 removals over five years in West Greenland, and 5*1.6*80 = 640 removals over five years in East Greenland (corresponding to 1576 and 576 landings for West and East Greenland, respectively). These recommendations assume no by-catch in the central and eastern North Atlantic. The advice should be reconsidered by the SC, ideally within five years and no later than 10 years in the absence of new information.

6.2 RECOMMENDATIONS FOR CONSERVATION AND MANAGEMENT

To all Parties

- A survey to provide new information on abundance should be conducted within the next 10 years.
- More telemetry data should be collected from the Faroe Islands and additional areas across the North Atlantic to provide more representative geographical coverage. Tagging should aim to provide a more representative coverage of the whole year.

To the Faroe Islands

- Sampling and ageing of pilot whales should be conducted to provide a representative sample of the entire catch.

To Greenland

- Undertake sampling for biological parameters from the drive hunts in West Greenland.
- Collect and analyse more genetic samples from West Greenland.
- Collect samples and conduct analyses to better inform stock definition in East and West Greenland (e.g., long-term telemetry, stable isotopes, contaminant levels).

To Iceland

- Age existing tooth samples and collect data to inform biological parameters whenever possible.

6.3 RECOMMENDATIONS FOR RESEARCH

To all Parties

- *(Reiterated from the WG on Genetics 2024)* Initiate a dedicated genetic monitoring programme based on archival and newly collected samples from harvested groups in Greenland and the Faroe Islands, as well as in mass stranding events wherever they occur, to determine:
  i. family groupings and social structure,
  ii. putative population of origin,
  iii. the influence of removing entire family units during pilot whale hunts, for instance in terms of genetic diversity, inbreeding levels, mutation load, and standing genetic variation.
- Review and standardise the techniques used for ageing and obtaining reproductive parameters and determine whether there may be a common methodological bias in existing data.
- Collect information on body condition (e.g., blubber thickness) to monitor the effects of environmental changes.

7 ANY OTHER BUSINESS

There was no other business discussed.

8 REPORT ADOPTION AND MEETING CLOSE

A draft report was adopted at 12:25 on November 27. Editorial changes were agreed upon and the final report was adopted via correspondence on xx December 2025.

Participants thanked the Greenland Representation for their gracious hosting of the meeting, and the Chair for running the meeting efficiently. The Chair in turn thanked the group for their contributions,

particularly Authier, Ofstad, and Witting for data processing and modelling during the meeting. The WG expressed appreciation for the significant amount of information available to be included in the pilot whale assessment, in contrast to assessments of more data-poor species.

REFERENCES

Desportes, G., Andersen, L. W., & Bloch, D. (1994) Variation in foetal and postnatal sex ratios in long-finned pilot whales, *Ophelia, 39*(3), 183-196.

Freitas, C., Lydersen, C., Fedak, M.A., & Kovacs, K. M. (2008) A simple new algorithm to filter marine mammal Argos locations. *Marine Mammal Science*, 24: 315-325. https://doi.org/10.1111/j.1748-7692.2007.00180.x

Frie, A. K., Lindström, U. (2024) Exploring the effects of methodological choices on the estimation and biological interpretation of life history parameters for harbour porpoises in Norway and beyond. *PLoS ONE 19*(7): e0301427. https://doi.org/10.1371/journal.pone.0301427

Heide-Jørgensen, M.P. & Bunch. C. (1991) *Occurrence and hunting of pilot whales in Greenland.* Working paper nr. 4 submitted to the ICES Study Group on Pilot Whales, Montreal 3-4 December 1991. 14 pp.

Jákupsstovu, S. H. í (2002) *The pelagic fish stocks, pilot whales and squid in Faroese waters - migration pattern, availability to fisheries and possible links to oceanographic events*. 2002 ICES Annual Science Conference, Copenhagen, Denmark. CM 2002/N:07. https://doi.org/10.17895/ices.pub.25443178

Kaplan, E. L. & Meier, P. (1958) Nonparametric estimation from incomplete observations. *Journal of the American Statistical Association,* 53(282), p. 457-481. https://doi.org/10.2307/2281868

Martin, A. R., Rothery, P. (1993) *Reproductive parameters of female long-finned pilot whales (*Globicephala melas*) around the Faroe Islands*. Report of the International Whaling Commission. 14:263–304.

Mikkelsen, B., Ofstad, L. H., & Akralið, R. (2025) *Age- and length distribution, sex ratio, growth and female reproduction of long-finned pilot whales in the Faroe Islands.* Working paper NAMMCO/SC/31/PWWG/10 presented at NAMMCO Pilot Whale Working Group, November 24–November 27, Copenhagen, Denmark.

NAMMCO (2025). *Report of the Working Group on Abundance Estimates* (NAMMCO/SC/AEWG/2025-03). NAMMCO-North Atlantic Marine Mammal Commission. Tromsø, Norway. https://nammco.no/abundance_estimates_reports/

Ramirez-Martinez, N. C., Víkingsson, G. A., Øien, N. I., Mikkelsen, B., Gunnlaugsson, T., & Hammond, P. S. (2024). Distribution and habitat use of deep-diving cetaceans in the central and north-eastern North Atlantic. *NAMMCO Scientific Publications, 13*. https://doi.org/10.7557/3.7416

Rouby, E., Ridoux, V. & Authier, M. (2021) Flexible Parametric Modeling of Survival from Age at Death Data: a Mixed Linear Regression Framework. *Population Ecology, 63*, p. 108-122. https://doi.org/10.1002/1438-390X.12069

Thorne, L. H., Nye, J. A. (2021) Trait-mediated shifts and climate velocity decouple an endothermic marine predator and its ectothermic prey. *Scientific Reports* 11(1): 18507. https://doi.org/10.1038/s41598-021-97318-z

APPENDIX 1: AGENDA

1. **Opening remarks**
2. **Adoption of agenda**
3. **Appointment of rapporteurs**
4. **Review of available documents**
5. **Assessment of long-finned pilot whales in the North Atlantic**
   - 5.1. Distribution
   - 5.2. Stock identity
   - 5.3. Biological parameters
   - 5.4. Abundance estimation
   - 5.5. Removals
     - 5.5.1. Catch
     - 5.5.2. By-catch
     - 5.5.3. Other
   - 5.6. Impacts from other anthropogenic stressors
     - 5.6.1. Contaminants
     - 5.6.2. Noise
     - 5.6.3. Tourism
     - 5.6.4. Climate change
     - 5.6.5. Other
   - 5.7. Population modelling and assessment
6. **Recommendations from the Working Group**
   - 6.1. Recommendations regarding removals
   - 6.2. Recommendations regarding conservation and management
   - 6.3. Recommendations for research
7. **Any other business**
8. **Report review and adoption**
9. **Closing remarks**

APPENDIX 2: LIST OF PARTICIPANTS

NAMMCO PARTIES

Anne Kirstine Frie (SC, NO, online)
Institute of Marine Research
anne.kirstine@hi.no

Bjarni Mikkelsen (SC, FO)
Faroe Marine Research Institute
bjarnim@hav.fo

Fernando Ugarte (SC, GL)
Greenland Institute of Natural Resources
feug@natur.gl

Gudjón Már Sigurdsson (SC, IS)
Marine and Freshwater Research Institute
gudjon.mar.sigurdsson@hafogvatn.is

Lars Witting (SC, GL)
Greenland Institute of Natural Resources
larsw@natur.gl

Lise Helen Ofstad (FO)
Faroe Marine Research Institute
liseo@hav.fo

Mads Peter Heide-Jørgensen (SC, GL)
Greenland Institute of Natural Resources
mhj@ghsdk.dk

Marie Louis (GL)
Greenland Institute of Natural Resources
marie.louis@natur.gl

Sven Winter (FO, online)
University of the Faroe Islands
sven.w@setur.fo

INVITED EXPERTS

Matthieu Authier
University of La Rochelle
matthieu.authier@univ-lr.fr

Rachel Ball
University of Glasgow
racheljb2708@gmail.com

Philip Hammond (Chair)
University of St Andrews
psh2@st-andrews.co.uk

Stine Petersen (online)
University of St Andrews
sop1@st-andrews.co.uk

NAMMCO SECRETARIAT

Geneviève Desportes
Secretary General
genevieve@nammco.org

Maria Garagouni
Deputy Secretary
maria@nammco.org

APPENDIX 3: LIST OF DOCUMENTS

Documents in italics were made available during the meeting.

Document Reference	Title	Agenda Item
Meeting/Working Documents		
PWWG/2025-01/01	Draft Agenda	2
PWWG/2025-01/02	Draft List of Participants	1–3
PWWG/2025-01/03	Draft List of Documents	4
PWWG/2025-01/04	Pilot whale abundance estimates: Faroe Islands–Iceland (Petersen & Hammond)	5.3, 5.6
PWWG/2025-01/05	Pilot whale abundance estimates: Greenland (Heide-Jørgensen)	5.3, 5.6
PWWG/2025-01/06a	Report of the Genetics WG (2025)	5.1, 5.6
PWWG/2025-01/06b	Pilot whale genetic structure in the North Atlantic–analysis updates (Winter)	5.1, 5.6
PWWG/2025-01/07a	On the construction of a Bayesian assessment model for long-finned pilot whales in the North Atlantic (Witting)	5.6
PWWG/2025-01/07b	*Bayesian assessment runs for long-finned pilot whales in the North Atlantic (Witting)*	5.6, 6
PWWG/2025-01/07c	*Density regulated models for long-finned pilot whales in the North Atlantic (Witting)*	5.6, 6
PWWG/2025-01/08	Catch history of long-finned pilot whales in the Faroe Islands (Mikkelsen, Ofstad, Akralíð)	5.4
PWWG/2025-01/09	Movements of long-finned pilot whales tagged in the Faroe Islands (Mikkelsen, Ofstad, de Clerck, Akralíð)	5.1, 5.3
PWWG/2025-01/10	*Age, growth, and reproduction of long-finned pilot whales in the Faroe Islands (Mikkelsen, Ofstad, Akralíð)*	5.2
PWWG/2025-01/11	Pilot whale tagging in Norway by UiT 2022–2025 (Rikardsen)	5.1, 5.3
PWWG/2025-01/12	Pilot whale by-catch in ICES waters (WGBYC)	5.4
PWWG/2025-01/13	Pilot whale hunting and catches in Greenland (Heide-Jørgensen)	5.4
For information documents		
PWWG/2025-01/FI/01	Meeting Code of Conduct (ICES)	All
PWWG/2025-01/FI/02	Report of the Pilot Whale WG (2008)	5
PWWG/2025-01/FI/03	Report of the Harbour Porpoise WG (2022)	5
PWWG/2025-01/FI/04	Pike et al (2019) Estimates of long-finned pilot whales in the Northeast Atlantic 1987-2015	5.3

PWWG/2025-01/FI/05	Pike et al (2019) Estimates of cetacean abundance in the central North Atlantic 2015 surveys	5.3
PWWG/2025-01/FI/06	Pike et al (2020) Estimates of cetacean abundance in the central North Atlantic 2007 surveys	5.3
PWWG/2025-01/FI/07	Hansen et al (2018) Abundance of whales in West and East Greenland in summer 2015	5.3
PWWG/2025-01/FI/08	ICES 1993 Assessment of pilot whales	5.6
PWWG/2025-01/FI/09a	ICES 1996 Assessment of pilot whales	5.6
PWWG/2025-01/FI/09b	*Pilot whale catch and stranding data by country (Ofstad)*	
PWWG/2025-01/FI/10	Selbmann et al (2022) Occurrence of long-finned pilot whales and killer whales in Icelandic coastal waters and their interactions	5.3
PWWG/2025-01/FI/11	Pampanin et al (2023) Pilot whale bile content – an indicator of ocean health	5.5
PWWG/2025-01/FI/12	Reinert et al (2023) AMAP Faroe Islands 2017–2020 Heavy metals and POPs Core Programme	5.5
PWWG/2025-01/FI/13	*Samarra et al (2024) Stable isotope trophic ecology of pilot whales stranded in Iceland*	
PWWG/2025-01/FI/14	*Paula Méndez-Fernandez (2025) Presentation on pilot whales in French waters at ECS conference*	
PWWG/2025-01/FI/15	*Xuereb et al (2023) POPs in mass stranded pilot whales in Iceland*	
PWWG/2025-01/FI/16	*Thorne and Nye (2021) Poleward shift of pilot whales vs their prey*	
PWWG/2025-01/FI/17	*Pilot whale life history data from Iceland*	
PWWG/2025-01/FI/18	*Desportes et al (1994) Variation in foetal and postnatal sex ratios in long-finned pilot whales*	
PWWG/2025-01/FI/19	*Modelling survivorship in pilot whales*	

APPENDIX 4: SURVEY AREAS USED TO CALCULATE ABUNDANCES

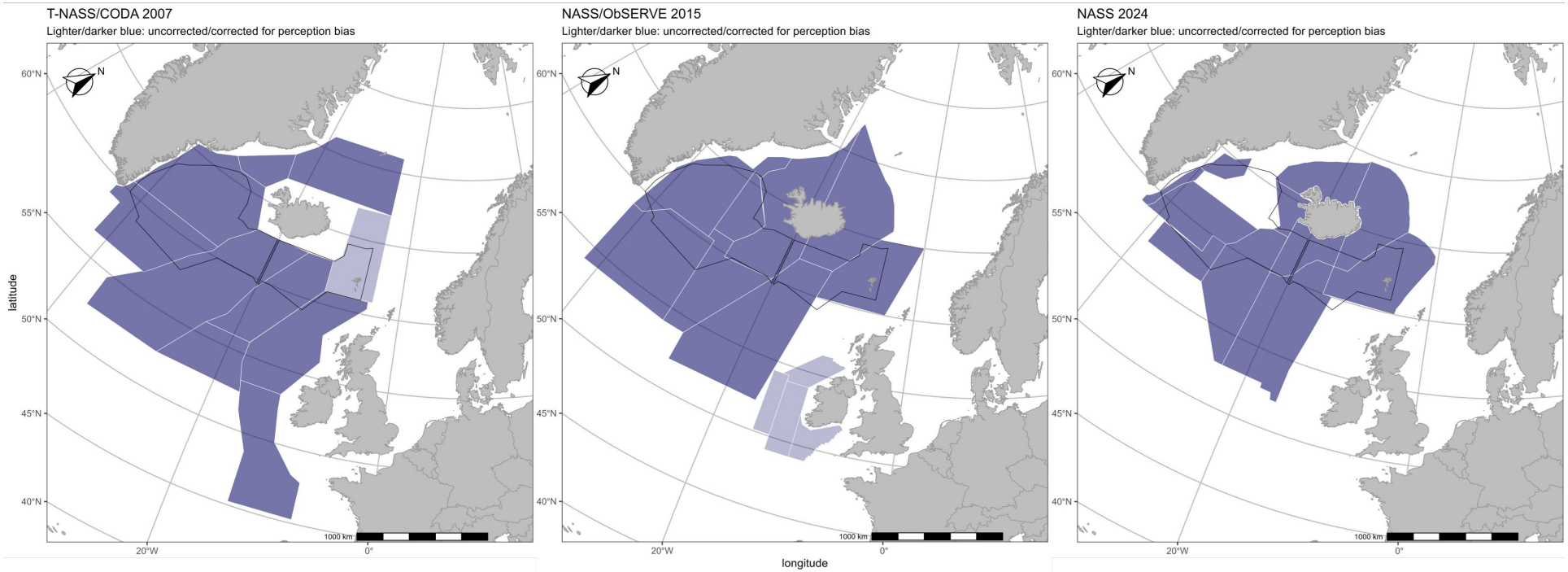

Figure A1. Survey blocks included in the calculation of pilot whale abundance estimates that were incorporated in the assessment models. *Left:* T-NASS and CODA surveys conducted in 2007. *Centre:* NASS and ObSERVE surveys conducted in 2015. *Right:* NASS conducted in 2024. Estimates for light blue strata were uncorrected for perception bias, while estimates for dark blue strata were corrected. The black outline denotes the 6 Survey Index Area that was used in the trend analysis by Pike et al. (2019).

APPENDIX 5: TABLE OF CATCHES AND STRANDINGS 1700–1995

Table A1. Records of pilot whale catches and strandings from 1700 to 1995, as compiled by the ICES Pilot Whale Study Group in 1996. Years with no recorded pilot whale catches or strandings in any of the listed countries have been excluded from the table. These catch data were included in the density-regulated population model (PWWG/2025-01/7c).

	Norway			Great Britan & Ireland		Faroe Islands	Iceland		Greenland
Year	Total catch	Males	Females	Total catch	Stranded	Total catch	Driven	Stranded	Catches
1704							37		
1709						1448			
1710						1430			
1711						715			
1712						385			
1713						1090			
1714						635			
1715						625			
1716						728			
1717						720			
1718						409			
1719						726			
1720						803			
1721						905			
1722						317			
1723						1320			
1724						1063			
1725						1359			
1726						688			
1727						835			
1728						236			
1729						1423			
1730						915			
1731						2188			
1732						277			
1733						1186			
1734						696			
1735						559			
1736						391			

	Norway			Great Britan & Ireland		Faroe Islands	Iceland		Greenland
Year	Total catch	Males	Females	Total catch	Stranded	Total catch	Driven	Stranded	Catches
1737						350			
1738						214			
1739						313			
1741						1460			
1743						622			
1744						1017			
1746						100			
1747						647			
1748						165			
1749						212			
1752						194			
1754						172			
1770						16			
1776						743			
1781						434			
1782						50			
1787						262			
1792						152			
1793						148			
1794						288			
1796						545			
1797						100			
1798						91			
1799						1370			
1800						53		45	
1801						154			
1802						752			
1803				40		1063			
1804						953			
1805				310		206			
1806				50		550			
1807						367			
1808						1145			

	Norway			Great Britan & Ireland		Faroe Islands	Iceland		Greenland
Year	Total catch	Males	Females	Total catch	Stranded	Total catch	Driven	Stranded	Catches
1809						226		1000	
1810						429			
1811				261		510			
1812						834	724	2814	
1813						281			
1814						261			
1815						543			
1816						812			
1817						652			
1818						917	100		
1819						1448			
1820						787			
1821						263			
1822						1647			
1823						1098			
1824						442	550		
1825						1935			
1826						714			
1827						711			
1828						725			
1829						556			
1830						1149			
1831				300		695			
1832				800		391			
1833						1455			
1834				330		1569			
1835						1338			
1836				380		1183			
1837				20		1221			
1838						1332			
1839				195		1614			
1840				38		2193			
1841				287		1651			

	Norway			Great Britan & Ireland		Faroe Islands	Iceland		Greenland
Year	Total catch	Males	Females	Total catch	Stranded	Total catch	Driven	Stranded	Catches
1842						645			
1843						3142			
1844				300		2171			
1845				1800		2541			
1846						1039			
1847						2675			
1848						1181			
1849						769			
1850						502			
1851				69		474			
1852						2230	65		
1853				25		1120			
1854				350		794			
1855						1368			
1856						411			
1857						328			
1858						757			
1859				128		836			
1860						640			
1861				660		341			
1862				390		1129			
1863						709			
1864						574			
1865				700		1269			
1866						1758			
1867				26		398			
1868						478			
1869						716			
1870						842			
1871				780		796			
1872						2315			
1873				192		1682			
1874						652			

	Norway			Great Britan & Ireland		Faroe Islands	Iceland		Greenland
Year	Total catch	Males	Females	Total catch	Stranded	Total catch	Driven	Stranded	Catches
1875						780			
1876				75		802			
1877				80		383			
1878						329	207		
1879				108		1920			
1880				100		628			
1881						390			
1882				154		521			
1883						151			
1884						368			
1885						977			
1886				60		734			
1887						854			
1888				340		476			
1889						695			
1892						34			
1893						840			
1894						498			
1895						542			
1896						128			
1897						342			
1898				600		1336			
1899				71		2377			
1900						797			
1902				166		481			
1903				83		212			
1904						566			
1905						221			
1906						414			
1907						242			
1908						1793			
1909						985			
1910						1324			

	Norway			Great Britan & Ireland		Faroe Islands	Iceland		Greenland
Year	Total catch	Males	Females	Total catch	Stranded	Total catch	Driven	Stranded	Catches
1911				50		1650			
1912						669			
1913						168			
1914						291			
1915						1203			
1916						397			
1917						263			
1918						848			
1919						153			
1920						802			
1921						1076			126
1922						473			
1923						1047			32
1924					1				13
1925						468			
1926						347			200
1927							250		
1928					1	480	5	75	185
1929					500	17	200		
1930						266			
1931					1	2386			415
1932					8	1282			120
1933						959	350		
1934						178	72		
1935						652	219	225	325
1936						1633			
1937						886	68		28
1938	27	20	7			2094	140		
1939	28	21	7			3384	190		400
1940						2847			
1941	4	4				4482	524		
1942	8	8				1864			
1943	8	6	2			1047		700	

	Norway			Great Britan & Ireland		Faroe Islands	Iceland		Greenland
Year	Total catch	Males	Females	Total catch	Stranded	Total catch	Driven	Stranded	Catches
1944	5	1	4		20	1386			
1945	13	11	2			1555			
1946	1	1			200	1040			
1947	7	6	1			1839			
1948	1	1				587			
1949	6	6			450	957			
1950	9		9		249	569			
1951	8	5	3			2786			
1952	2	1	1			1242			
1953	3	2	1			2099			
1954						2015			28
1955	13	10	3		63	885			2
1956	1		1			1843			2
1957	80	53	27		36	2105	105		25
1958	225	167	59			2619	300		48
1959	224	159	65			1428			158
1960	331	228	103			1783	100		10
1961	295	224	71			1892			5
1962	43	32	11			1764			12
1963	71	53	18			2204			
1964	54	44	10			1364			
1965	32	21	11		83	1620			138
1966	339	264	75			1485	3		38
1967	117	111	6			1973			
1968	31	27	4		15	1650			8
1969	27	22	5			1394			
1970	43	32	11			388			10
1971					1	1015			
1972						511			
1973						1050			2
1974	1	1				679			16
1975						1086			108
1976						532			50

	Norway			Great Britan & Ireland		Faroe Islands	Iceland		Greenland
Year	Total catch	Males	Females	Total catch	Stranded	Total catch	Driven	Stranded	Catches
1977						897			138
1978					1	1192			100
1979						1674			50
1980					1	2775			10
1981					1	2909			2
1982					34	2649		280	2
1983					104	1685			
1984						1926			
1985					36	2596			25
1986						1676		148	10
1987						1450			
1988						1738			
1989						1260			
1990						917		22	
1991						722			
1992						1572			
1993						808			100
1994						1201			
1995						228			0

NAMMCO 2025 SC/PWWG/2025-01/7a

On the construction of a Bayesian assessment model for long-finned pilot whales in the North Atlantic

Lars Witting

November 20, 2025

This WP deals with an initial setup of a Bayesian assessment model for long-finned pilot whales in the North Atlantic. The paper is not concerned with the stock structure, priors, and data that should go into the final assessment, but mainly with the prior and likelihood structure needed to best subtract the joint information in the abundance and age data.

The paper is based on the exponential model in the appendix, with preliminary data informed priors on the birth rate and age of reproductive maturity, and uninformed priors on the exponential growth rate, offspring survival (age-class zero), and adult survival (assumed constant from age-class one). I include so far only the catch history from the Faroe Islands, use either a single arbitrary abundance estimate or six agreed absolute abundance estimates from the Iceland / Faroese area from 1987 to 2015, and up to five distributions of age data covering the period from 1986 to 2022.

Given these data and priors, I run the eight models below to illustrate the logic behind the final model, that is suggested as a starting point for the assessment. What is required beyond this for the assessment is that the PWWG agrees on

i) the stuck structure that defines the abundance estimates and catch histories to be included in the model,

ii) if possible, provides additional data to the model on the birth rate and age of reproductive maturity so that these parameters can be fitted directly to the available data (instead of being indirectly updated by the abundance and age data),

iii) considers if the birth and maturity data should be included as timeseries of estimates that allows the model to estimate the development in these parameters over time,

iv) and agrees on the best priors for parameters that are not directly updated by data, which hopefully includes only offspring and adult survival.

The eight populations models are:

Single N; no age data; r prior (i) This exponential model has a single arbitrary abundance estimate of 100,000 (cv:0.25) whales in 2020 as the only data input. Figs. 2 illustrates that this is updating the abundance prior but none of the other parameters. Fig. 10 shows a slight decline due to the catch history (Fig. 1) and the assumed symetrical growth rate (r) prior running from -0.03 to 0.03.

1986 age; r prior (r) Here I have added the age data from 1986, with Fig. 3 illustrating that these data are strongly updating the birth rate (b), age of maturity (m), age-class zero survival (p_0), and a somewhat smaller updating of adult survival (p). The growth rate (r) posterior is dominated by its uniform prior, with Fig. 10 showing an almost identical trajectory compared to the model above. The age data are informative for an interaction between the growth rate and adult survival, with the current model—where a prior-draw of p is estimated from the prior draw of r—results in a posterior update of primarily p.

1986 age; p prior (s) Here I use a prior on p instead of a prior on r, with a prior-draw of r estimated from the prior draws of p. Fig. 4 illustrates that this creates some updating of the growth rate (r) while the adult survival (p) posterior is dominated by its prior, with Fig. 10 showing a slightly increasing, instead of declining, population. The change in the direction of growth is due to the prior on survival that creates a higher growth rate than the r prior of the former model. This shows the importance of having realistic life history priors, and also the importance of estimating the life history data directly from data in the model where possible. As I prefer to specify the biological life history parameters, instead of the resulting growth rate, I use the same p prior in the models below.

All N; no age (n) This model uses the six absolute abundance estimates from the Iceland Faroese survey area from 1987 to 2015, and no age data. In addition to the updating of model abundance, Fig. 5 and 10 illustrate that a slightly negative trend in the abundance data is causing a small updating also of the growth rate and adult survival parameters, but basically no updating of the birth rate, maturity, and age-class zero survival.

All N; all age (a) Compared with the former model, this and the remaining models include also all age-data included as five different dirtributions over the period from 1986 to 2022. Fig. 6 and 10 illustrates a model that is unable to fit to the abundance data, with all posterior distributions being essentially identical to their priors, and this includes also the abundance parameter that is updated in all other models. The combined likelihood signal from the age data is apparently dominating the signal from the abundance data creating a lack of fit to the abundance data. The following three models multiply the log likelihood from the age data by 0.5, 0.25, and 0.10 to downscale the signal from the age data.

All N; all age lnL*=0.5 (aH) This model multiplies the log likelohood of the age data by 0.5, with Fig. 7 and 10 showing that this is not enough to sole the lack of fit problem.

All N; all age lnL*=0.25 (aI) This model multiplies the log likelohood of the age data by 0.25, with Fig. 8 and 10 showing that this allows the model to fit to the data.

All N; all age lnL*=0.1 (aL) This model multiplies the log likelohood of the age data by 0.1, with Fig. 9 and 10 showing that this provides almost the same fit to data as a the former model that multiplies with 0.25. Relative to model n with no age data, this provides a negative updating of adult survival that is growth rate compensated by a positive updating of the birth rate and age-class zero survival, and a negative updating of maturity, with an overall positive updating of the growth rate. Additional data on maturity and births should be included in the model if available, to strengthen the estimates of these parameters.

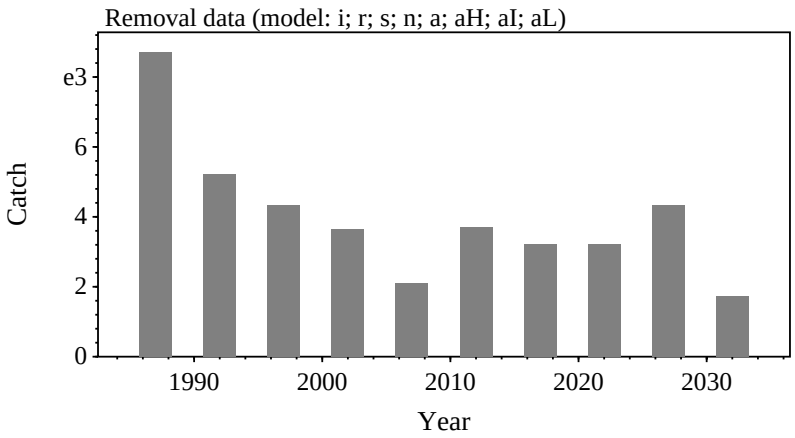

Figure 1: Historical removals in 5 year bins. Data from Mikkelsen et al. (2025).

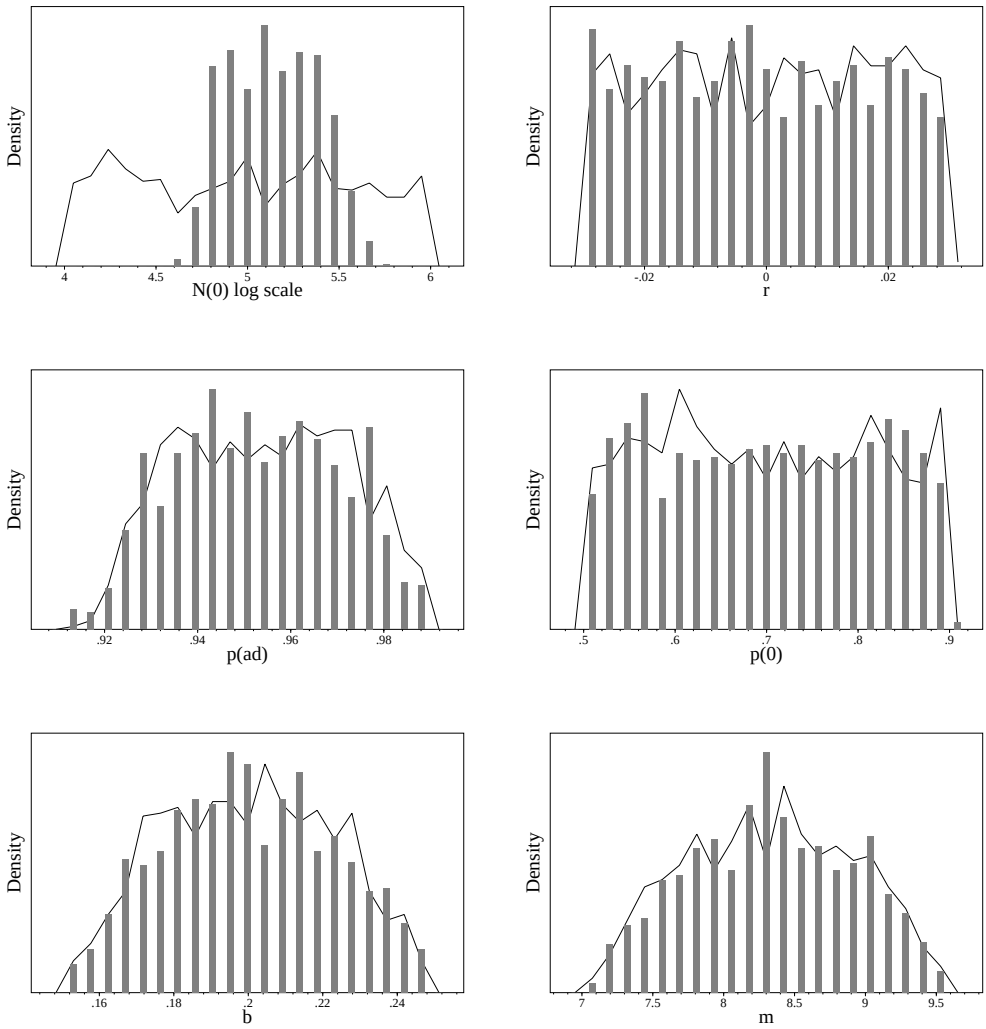

Figure 2: Realised prior (curve) and posterior (bars) distributions for Single N; no age data; r prior (i).

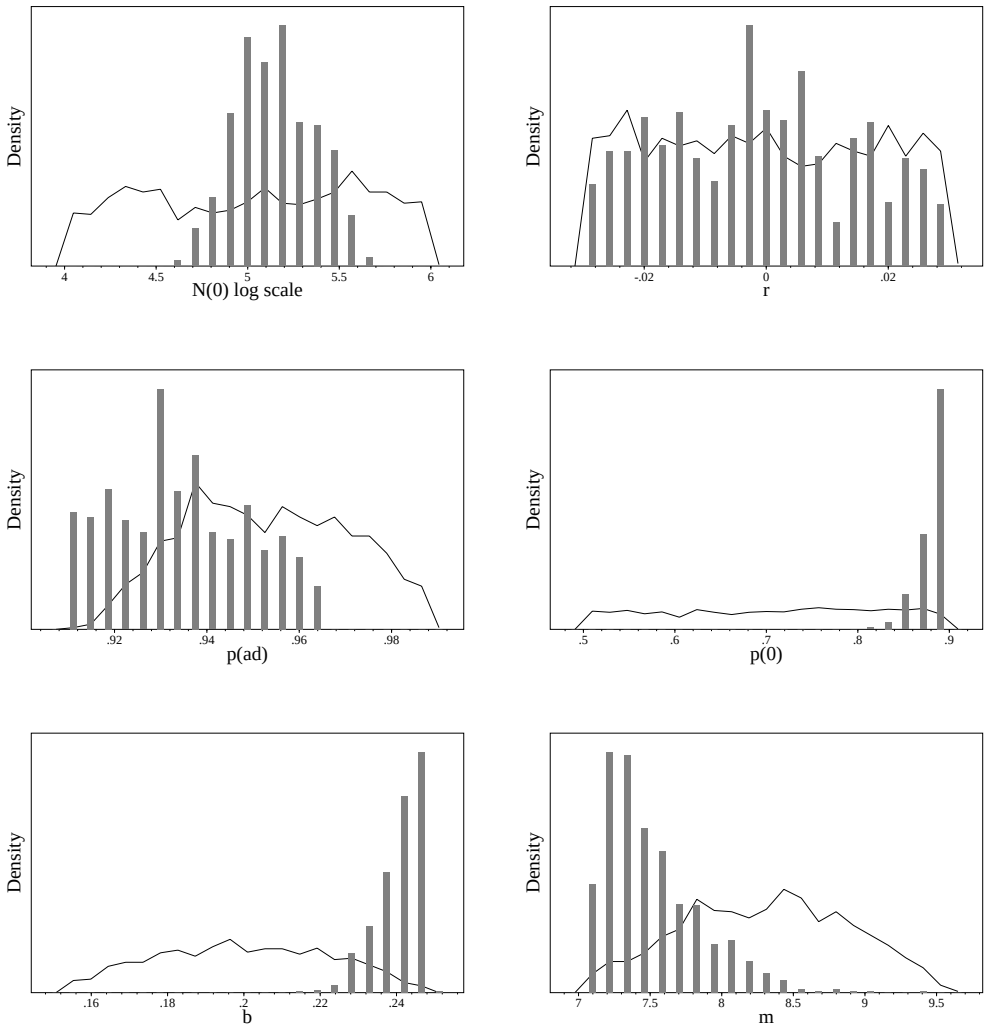

Figure 3: Realised prior (curve) and posterior (bars) distributions for 1986 age; r prior (r).

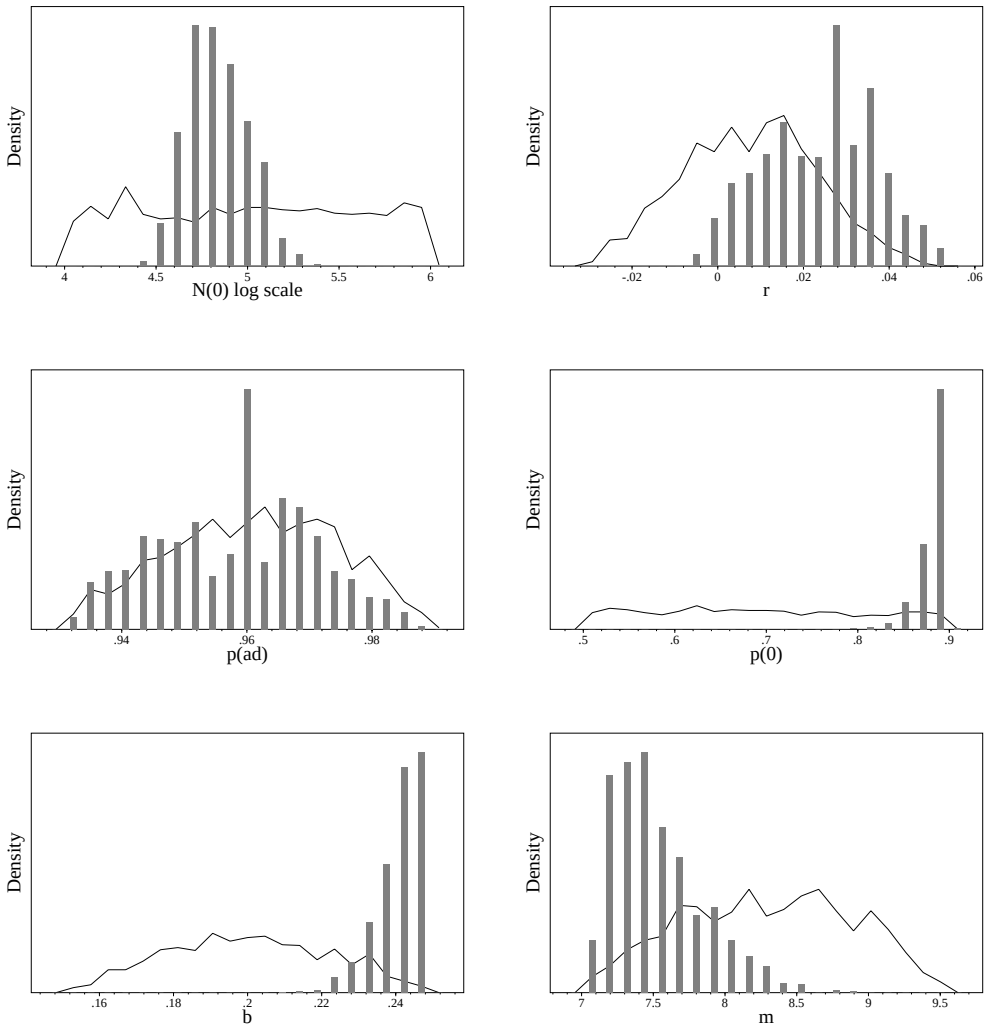

Figure 4: Realised prior (curve) and posterior (bars) distributions for 1986 age; p prior (s).

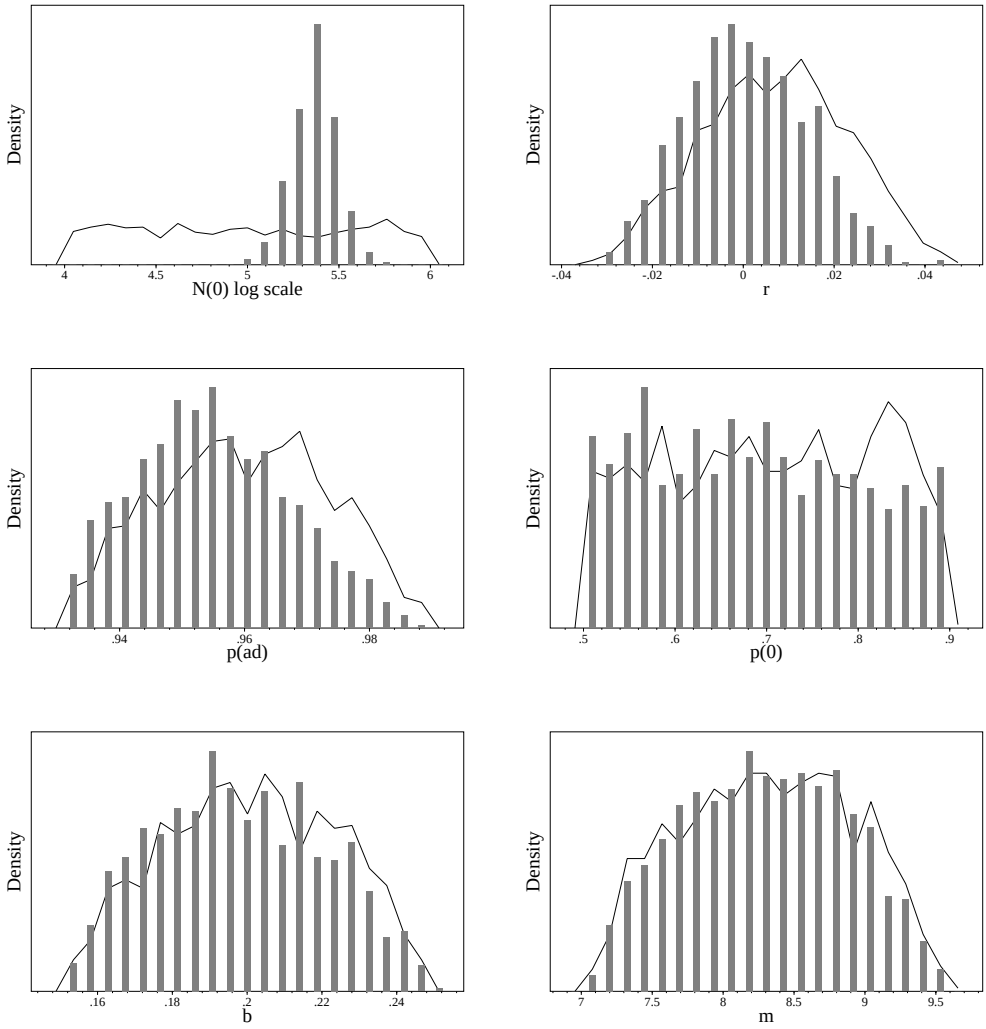

Figure 5: Realised prior (curve) and posterior (bars) distributions for All N; no age (n).

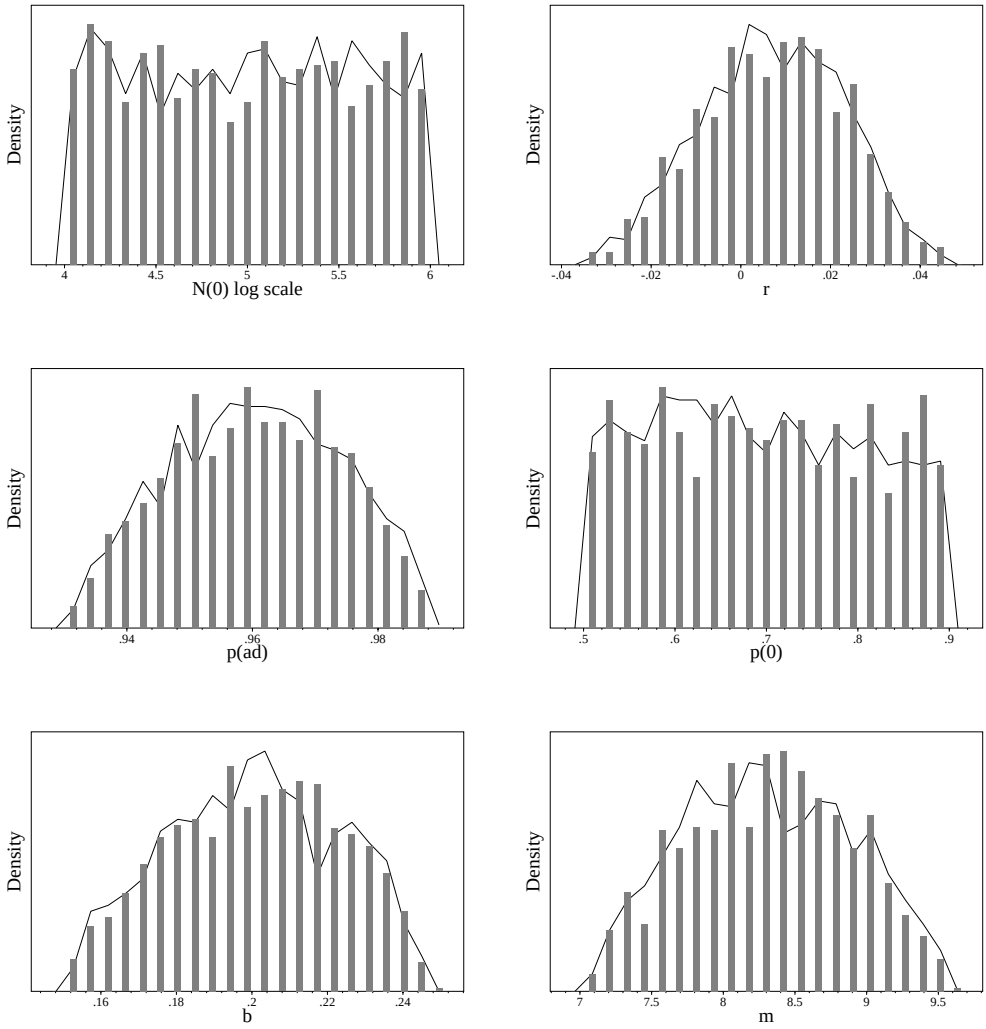

Figure 6: Realised prior (curve) and posterior (bars) distributions for All N; all age (a).

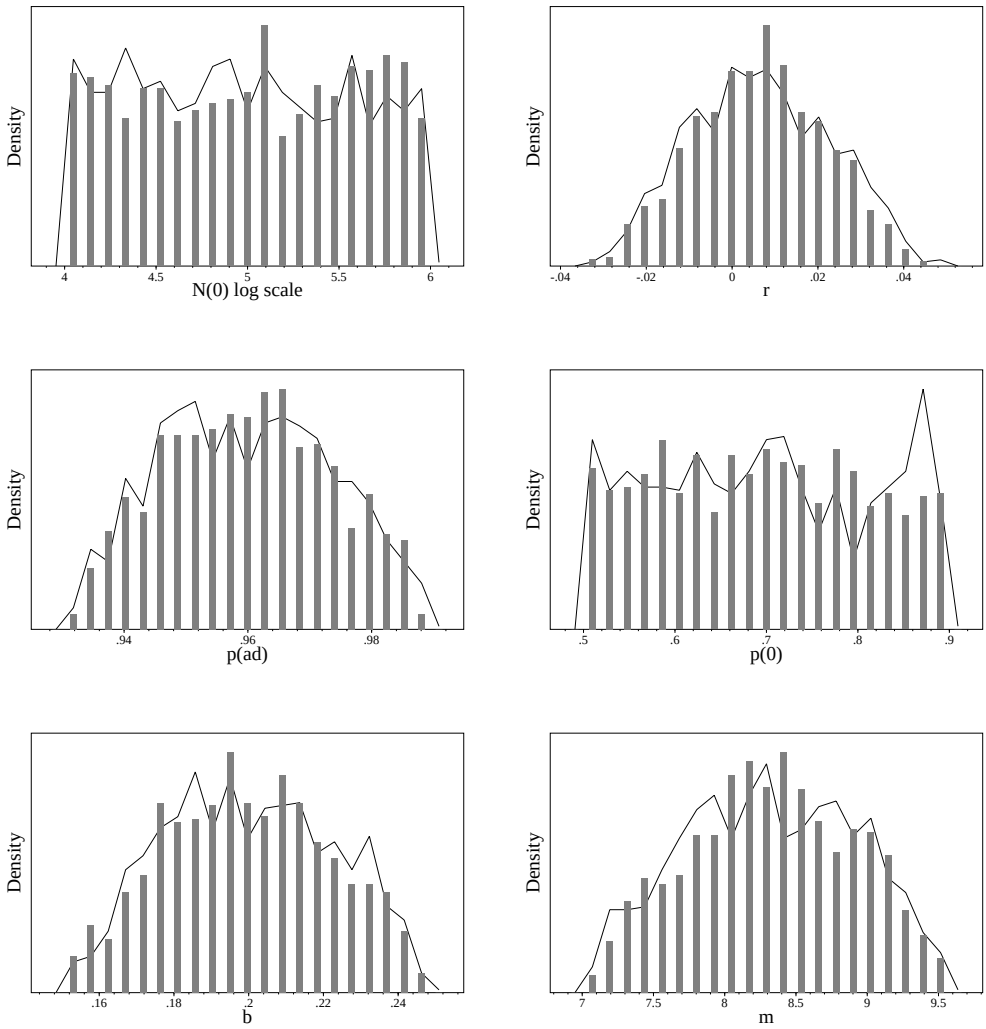

Figure 7: Realised prior (curve) and posterior (bars) distributions for All N; all age lnL*=0.5 (aH).

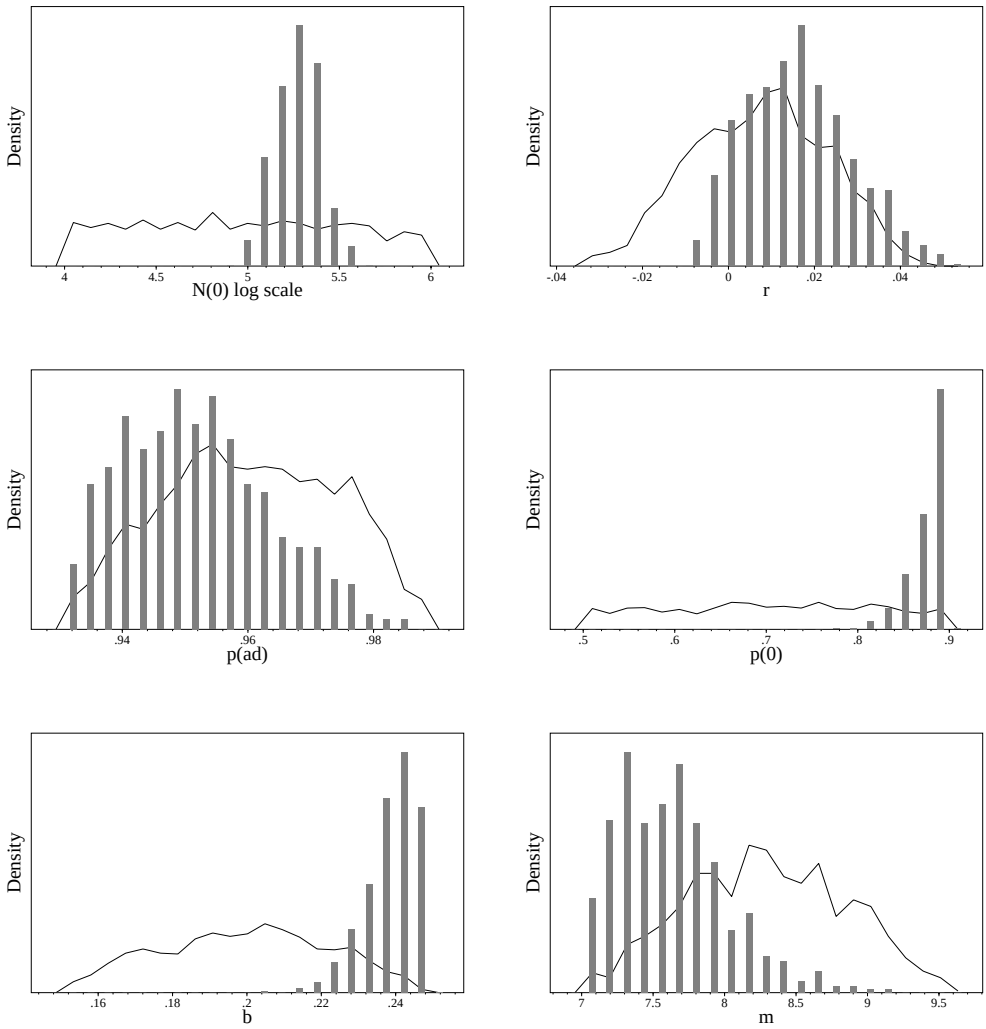

Figure 8: Realised prior (curve) and posterior (bars) distributions for All N; all age lnL*=0.25 (aI).

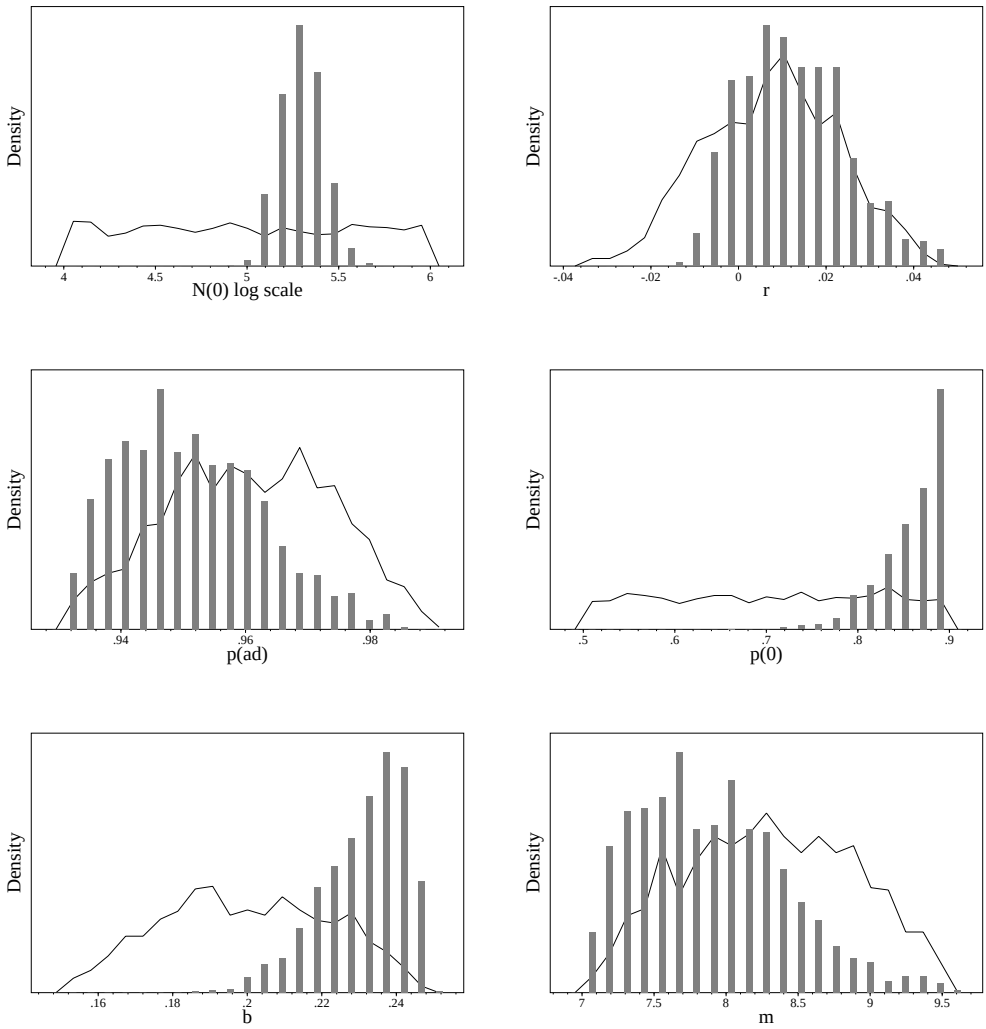

Figure 9: Realised prior (curve) and posterior (bars) distributions for All N; all age lnL*=0.1 (aL).

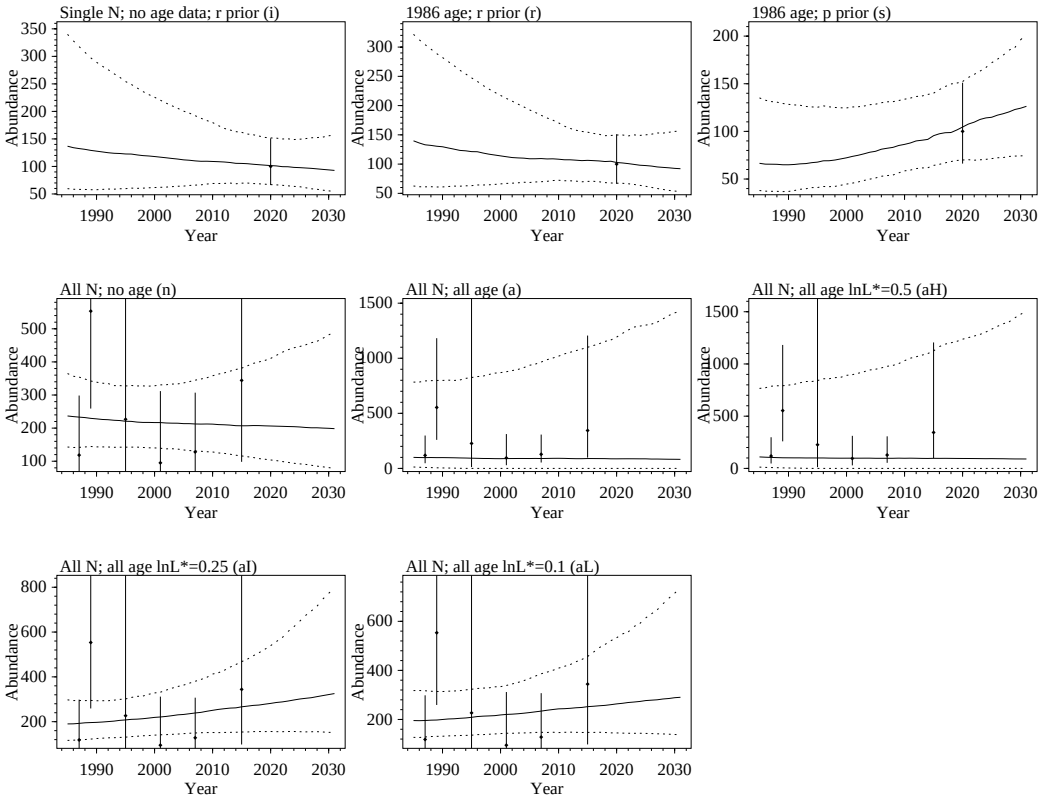

Figure 10: Projected medians and 90% credibility intervals for abundance. Data from NAMMCO (2025).

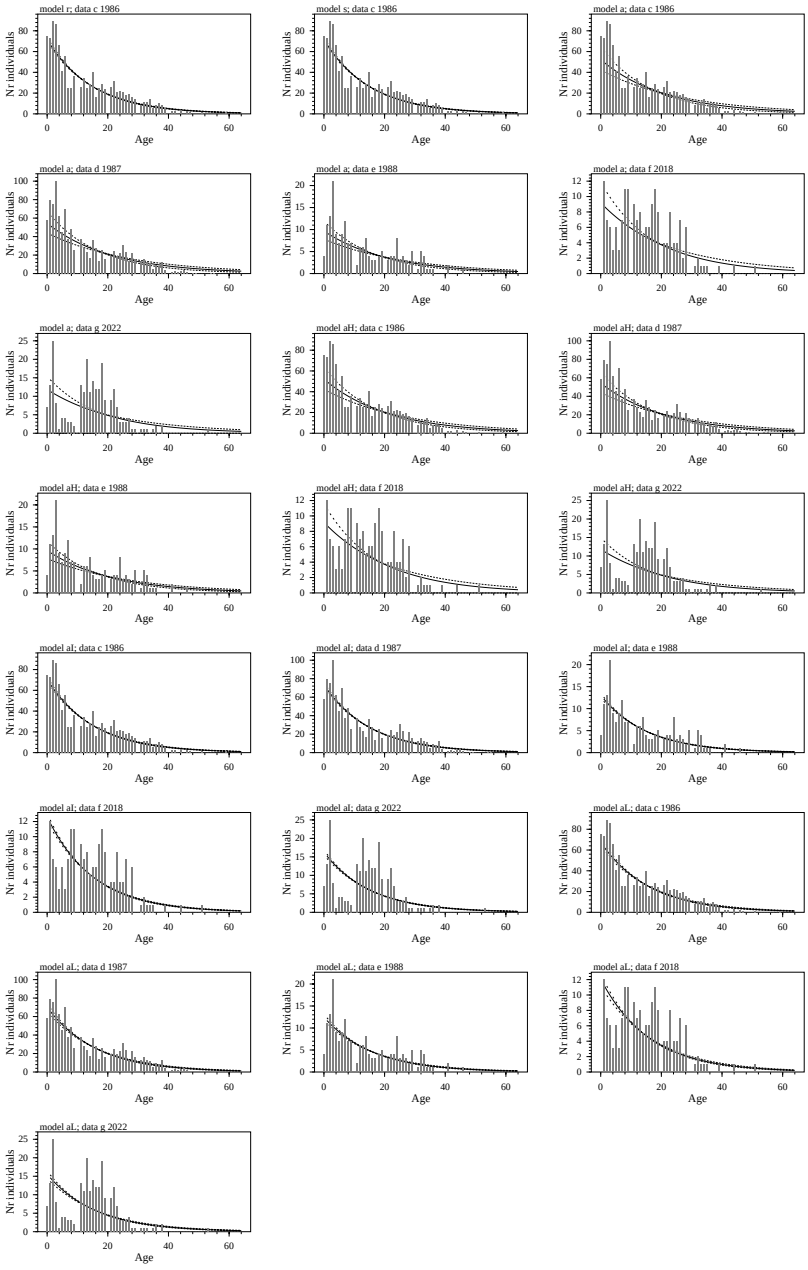

Figure 11: Model fit for age-structure. Data given by bars, and models by the median estimate (solid curve) and 90% credibility interval (dashed curves). Data from Mikkelsen (2025).

	a	c	b	d	e	f	g
i	*	-	-	-	-	-	-
r	*	*	-	-	-	-	-
s	*	*	-	-	-	-	-
n	-	-	*	-	-	-	-
a	-	*	*	*	*	*	*
aH	-	*	*	*	*	*	*
aI	-	*	*	*	*	*	*
aL	-	*	*	*	*	*	*
1986	-	12.4^{17}_{1097}	-	-	-	-	-
1987	-	-	118000^{56}	12.7^{17}_{1121}	-	-	-
1988	-	-	-	-	12.9^{18}_{193}	-	-
1989	-	-	553000^{46}	-	-	-	-
1995	-	-	227000^{178}	-	-	-	-
2001	-	-	95100^{72}	-	-	-	-
2007	-	-	128000^{53}	-	-	-	-
2015	-	-	344000^{76}	-	-	-	-
2018	-	-	-	-	-	14.6^{19}_{183}	-
2020	100000^{25}	-	-	-	-	-	-
2022	-	-	-	-	-	-	13.8^{22}_{243}

Table 1: **Data for likelihood functions.** Their use by models are marked by *. a: Abundance with log normal likelihood [n(1+); $\bar{x}^{cv\%}$]. c: Age structure with multinomial likelihood [population; $\bar{x}_n^{cv\%}$]. b: Abundance with log normal likelihood [n(1+); $\bar{x}^{cv\%}$]. d: Age structure with multinomial likelihood [population; $\bar{x}_n^{cv\%}$]. e: Age structure with multinomial likelihood [population; $\bar{x}_n^{cv\%}$]. f: Age structure with multinomial likelihood [population; $\bar{x}_n^{cv\%}$]. g: Age structure with multinomial likelihood [population; $\bar{x}_n^{cv\%}$]. Data from Mikkelsen (2025) and NAMMCO (2025).

M	N_0	b	ϑ	m	p_0	p	r
i	$10;1000^U$	$^{2;2^b}_{.15;.25}$	$.5^p$	$^{2;2^b}_{7;9.6}$	$.5;.9^u$	-	$-.03;.03^u$
r	$10;1000^U$	$^{2;2^b}_{.15;.25}$	$.5^p$	$^{2;2^b}_{7;9.6}$	$.5;.9^u$	-	$-.03;.03^u$
s	$10;1000^U$	$^{2;2^b}_{.15;.25}$	$.5^p$	$^{2;2^b}_{7;9.6}$	$.5;.9^u$	$^{2;2^b}_{.93;.99}$	-
n	$10;1000^U$	$^{2;2^b}_{.15;.25}$	$.5^p$	$^{2;2^b}_{7;9.6}$	$.5;.9^u$	$^{2;2^b}_{.93;.99}$	-
a	$10;1000^U$	$^{2;2^b}_{.15;.25}$	$.5^p$	$^{2;2^b}_{7;9.6}$	$.5;.9^u$	$^{2;2^b}_{.93;.99}$	-
aH	$10;1000^U$	$^{2;2^b}_{.15;.25}$	$.5^p$	$^{2;2^b}_{7;9.6}$	$.5;.9^u$	$^{2;2^b}_{.93;.99}$	-
aI	$10;1000^U$	$^{2;2^b}_{.15;.25}$	$.5^p$	$^{2;2^b}_{7;9.6}$	$.5;.9^u$	$^{2;2^b}_{.93;.99}$	-
aL	$10;1000^U$	$^{2;2^b}_{.15;.25}$	$.5^p$	$^{2;2^b}_{7;9.6}$	$.5;.9^u$	$^{2;2^b}_{.93;.99}$	-

Table 2: **Priors for the parameters** of the different models (M). N the abundance, b the birth rate, ϑ the female fraction at birth, m the rep. maturity, p_0 the first year survival, p the yearly survival, and r the exp. growth rate (no removal, max or realised). Abundance is given in thousands. The prior probability distribution is given by superscripts; p: fixed value, u: uniform (min;max), U: log uniform (min;max), and b: beta $(^{a;b}_{i;x})$ with i=min and x=max.

M	n_S	n_R	unique	max
i	100	1	972	2
r	1000	1	448	28
s	1000	1	430	34
n	500	1	992	2
a	1000	1	932	6
aH	1000	1	950	4
aI	3000	1	814	7
aL	3000	1	964	2

Table 3: **Sampling statistics** for the different models (M). The number of parameter sets in the sample (n_S) and the resample (n_R), the number of unique parameter sets in the resample, and the maximum number of occurrences of a unique parameter set in the resample. n_S and n_R are given in thousands.

M		N_0	N_t	b	m	p_0	p	r	ry_t
	$x_{.5}$	137	97.8	.199	8.33	.701	.952	-.00164	-157
	$x_{.05}$	59.7	63.2	.165	7.38	.523	.925	-.0275	-2550
i	$x_{.95}$	340	149	.237	9.26	.877	.98	.026	3180
	$x_{.5}$	140	97.5	.242	7.42	.887	.934	-.00264	-205
	$x_{.05}$	62.6	62.1	.23	7.13	.851	.912	-.0257	-2440
r	$x_{.95}$	322	150	.247	8.16	.898	.96	.025	3070
	$x_{.5}$	66.5	115	.242	7.46	.888	.96	.026	2890
	$x_{.05}$	37.9	71.4	.229	7.15	.85	.938	.001	165
s	$x_{.95}$	135	172	.248	8.15	.899	.979	.045	6470
	$x_{.5}$	237	203	.197	8.29	.682	.954	0	5.77
	$x_{.05}$	143	92	.163	7.36	.517	.936	-.0205	-2500
n	$x_{.95}$	365	446	.235	9.24	.878	.977	.023	9360
	$x_{.5}$	100	87	.202	8.34	.693	.96	.008	18.9
	$x_{.05}$	12.8	0	.163	7.37	.522	.938	-.0191	-2590
a	$x_{.95}$	783	1300	.237	9.25	.877	.982	.032	28300
	$x_{.5}$	110	93.7	.199	8.32	.695	.96	.006	28.9
	$x_{.05}$	12.3	0	.164	7.35	.519	.938	-.0189	-2770
aH	$x_{.95}$	766	1330	.237	9.25	.877	.982	.031	30500
	$x_{.5}$	190	301	.24	7.59	.883	.951	.015	4520
	$x_{.05}$	116	155	.225	7.12	.836	.934	-.00273	-444
aI	$x_{.95}$	297	648	.248	8.36	.898	.973	.037	24200
	$x_{.5}$	195	277	.233	7.85	.869	.95	.011	3100
	$x_{.05}$	127	143	.208	7.19	.791	.935	-.00476	-824
aL	$x_{.95}$	318	614	.246	8.83	.898	.972	.034	18700

Table 4: **Parameter estimates** for the different models (M). Estimates are given by the median ($x_{.5}$) and the 90% credibility interval ($x_{.05}$ - $x_{.95}$) of the posterior distributions. N the abundance, b the birth rate, m the rep. maturity, p_0 the first year survival, p the yearly survival, r the exp. growth rate (no removal, max or realised), and ry the replacement yield. Year by subscript: 0:initial and t:2025. Abundance is given in thousands.

Appendix

A Population dynamic model

The population model is an age-structured Bayesian assessments model that is programmed in C++, and which is easily programmed by input files to deal with different species, populations, and situations. Based on the input programming, the model will simulate unregulated exponential growth, density regulated growth, or selection regulated dynamics which is a density regulated population with superimposed selection regulation.

The population dynamic model is structured by gender and age, with x being the maximum lumped age-class. Let the number $N^{m/f}_{a,t+1}$ of males (m) and females (f) in age-classes $0 < a < x$ in year $t+1$ be

$$N^{m/f}_{a+1,t+1} = p^{m/f}_a N^{m/f}_{a,t} - c^{m/f}_{a,t} \tag{1}$$

and the number of animals in age-class x be

$$N^{m/f}_{x,t+1} = p^{m/f}_x N^{m/f}_{x,t} + p^{m/f}_{x-1} N^{m/f}_{x-1,t} - c^{m/f}_{x,t} - c^{m/f}_{x-1,t} \tag{2}$$

where $p^{m/f}_a$ is the age specific survival rate of males/females, and $c^{m/f}_{a,t}$ is the age specific catch of males/females in year t. The age and gender (g) dependent survival rates $p^g_a = p\tilde{p}^g_a$ are given as a product between a survival scalar p and relative ($0 < \tilde{p}^g_a \leq 1$) survival rates. The age and gender specific catches $c^{m/f}_{a,t} = c^{m/f}_t \tilde{c}^{m/f}_{a,t}$ in year t are given as a product between the total catch of males/females ($c^{m/f}_t$), as specified by the catch history, and an age-specific catch selectivity ($\tilde{c}^{m/f}_{a,t}$). The age-specific catch selectivity is listed in Table **??**.

The number of females and males in age-class zero is $N^f_{0,t} = \vartheta N_{0,t}$ and $N^m_{0,t} = (1-\vartheta)N_{0,t}$, where ϑ is the fraction of females at birth, and

$$N_{0,t} = \sum_{a=0}^{x} B_{a,t} \tag{3}$$

where $B_{a,t}$ is the number of births from females in age class a, defined as

$$B_{a,t} = b_{a,t}\, \tilde{b}_a\, M^f_{a,t} \tag{4}$$

where $b_{a,t}$ is the birth rate in year t for age-class a females should they be at their age-specific reproductive peak, $0 < \tilde{b}_a \leq 1$ are the relative age-specific birth rates, and $M^f_{a,t}$ is the number of mature females in age-class a in year t, defined as

$$M^f_{a,t} = \begin{cases} 0 & \text{if } a < m_{0,a,t} \\ \tilde{m}_{a,t} N^f_{a,t} & \text{if } a \geq m_{0,a,t} \end{cases} \tag{5}$$

where

$$\tilde{m}_{a,t} = 1 - e^{-\frac{a-m_{0,a,t}}{m_{a,t}-m_{0,a,t}} \ln 2} \tag{6}$$

is the fraction of females in age-class a in year t that is mature, with $m_{0,a,t}$ being the earliest, and $m_{a,t}$ the median, age of reproductive maturity for females of age a in year t.

Knife-edge maturation, where all females older than m_0 are mature, occurs when $m_0 = m$. Yet, for model versions with knife-edge maturity, the number of mature females is

$$M^f_{a,t} = \min[1, \max(0, a + 1 - m_{a,t})]N^f_{a,t} \tag{7}$$

With adult survival being the life history trait that in most cases is least affected by environmental changes, let the dynamics be regulated by changes in the birth rate

$$b_{a,t} = b^* i_{a,t} f(\hat{N}_t/\hat{N}^*) \tag{8}$$

and/or age of reproductive maturity

$$m_{a,t} = m^*/i_{a,t} f(\hat{N}_t/\hat{N}^*) \tag{9}$$

where b^* and m^* are the birth rate and age of reproductive maturity at the population dynamic equilibrium with no removals, $i_{a,t}$ is the average intrinsic component of the life history (for age-class a individuals in year t) as determined by density dependent natural selection (with $i^{**}_{a,t} = 1$ for all age-classes at the natural selection equilibrium $**$), and $f(\hat{N}_t/\hat{N}^*)$ is density regulation where $f(\hat{N}^*/\hat{N}^*) = 1$, with the one-plus abundance

$$\hat{N}_t = \sum_{a=1}^{x} N^f_t + N^m_t \tag{10}$$

being the component that imposes density regulation.

A.1 Exponential & density regulated growth

A model for exponential growth (given a stable age-structure) does not include the two regulation terms $i_{a,t}$ and $f(\hat{N}_t/\hat{N}^*)$. The birth rate $b_{a,t} = b$ and age of maturity $m_{a,t} = m$ are instead fixed at the same values for all age-classes and years. A density regulated model is another incomplete model, where $i_{a,t} = 1$ for all age-classes and years so that it does not include the selection induced changes in the life history. For this case, I assume a Pella-Tomlinson type of regulation

$$f(\hat{N}_t/\hat{N}^*) = 1 + [b_{max}/b^* - 1][1 - (\hat{N}_t/\hat{N}^*)^\gamma] \tag{11}$$

where the b_{max}/b^* ratio is the phenotypic span between maximal reproduction and reproduction at carrying capacity, and γ is the strength of regulation.

A non-evolving life history with an elastic phenotype that applies, not only to individuals, but also to the population average, is the basic fundament of density regulated growth. It implies that populations have an optimal/maximal growth rate r_{max} at zero density where $b = b_{max}$, and a carrying capacity $\hat{N}^*$ with a sub-optimal phenotype, where the average individuals are short in resources by a factor of b^*/b_{max}. Variation in the growth (and birth) rate is explained exclusively from variation in the environment (at least for large populations with negligible demographic variation), with the full range of phenotypic plasticity being controlled by density regulation [Eq. (11)]. A consequence of the latter, is the concept of optimal harvest with a maximum sustainable yield [msy where $\partial \text{sy}/\partial \hat{N} = 0$ with $\lambda = \hat{N}_t/\hat{N}_{t+1}$] at a specific abundance [$\hat{N}_{\text{msy}}$]; also known by the maximum sustainable yield rate ($\text{msyr} = \text{msy}/\hat{N}_{\text{msy}}$) and the maximum sustainable yield level ($\text{msyl} = \hat{N}_{\text{msy}}/\hat{N}^*$).

A.2 Selection-regulated dynamics

Selection-regulated dynamics is based on a population dynamic feed-back selection that balances two opposing forces of natural selection. The first is selection by the quality-quantity trade-off (Smith and Fretwell, 1974; Stearns, 1992), where e.g. a few large or many small offspring can be produced from the same amount of energy. This selects for increased replication by allocating energy to the demographic traits at the cost of competitive traits like body mass and complex interactive behaviour. The second is selection by interactive competition, where the competitively superior individuals (typically the larger individuals) can dominate the inferior during interactive encounters for limited resources. Yet, before the larger individuals can monopolise resources, there needs to be a certain population density where the individuals meet in interactive competition sufficiently often. This density dependence implies that the resource bias from interactive competition increases with increased population density, with the evolutionary equilibrium being defined by a density that is exactly so large that the resource bias in favour of the larger individuals is balanced against the quality-quantity trade-off, with the rate of replication being independent of mass.

A full description of population dynamic feed-back selection requires an individual based model so that the gradient of resources across the life history variants in the population can be quantified. Yet, for the population level equations of selection-regulated dynamics I use the population level response that Witting (2000a) solved from an underlying individual based model. This formulation combines a density regulation

$$f(\hat{N}_t/\hat{N}^*) = (\hat{N}_t/\hat{N}^*)^{-\gamma} \tag{12}$$

that is linear on log scale, with a similar selection response

$$i_{0,t+1} = \frac{\sum_{a=1}^{x} i_{a,t}\ \tilde{b}_a M_{a,t}^f}{\sum_{a=1}^{x} \tilde{b}_a M_{a,t}^f} \left(\frac{\hat{N}_t}{\hat{N}^*}\right)^{-\iota} \tag{13}$$

where the average intrinsic life history ($i_{0,t+1}$) of offspring born in year t is the weighted average of the intrinsic life histories ($i_{a,t}$) of all mothers, multiplied by the density dependent selection response $[(\hat{N}_t/\hat{N}^*)^{-\iota}]$, with ι being the strength of the response. Assuming that there is no change in the intrinsic life history of a cohort over time, we have that $i_{a+1,t+1} = i_{a,t}$ and

$$i_{x,t+1} = \frac{i_{x,t}(p_x^f N_{x,t}^f - c_{x,t}^f) + i_{x-1,t}(p_{x-1}^f N_{x-1,t}^f - c_{x-1,t}^f)}{N_{x,t+1}^f} \tag{14}$$

While the modelling of the dynamic changes in the intrinsic life history is a relatively small addition to the equation of population regulation [Eqs. (8) and (9)], the conceptual implications for population dynamics are huge (Witting, 2000a,b, 2002, 2013). We have already seen that the equilibrium abundance no longer is determined by density regulation, but by a population dynamic feed-back selection that balance the quality-quantity trade-off against the resource bias of interactive competition across the individuals in the

population. This implies, among others, that the average life history is selected to match the availability of resources at equilibrium, instead of being short in resources by a factor of b^*/b_{max}.

With the optimal life history referring to the ecological conditions at population equilibrium, the focus of the population dynamic formulation moves from the imaginary zero density to the naturally occurring density in an undisturbed population. Because density regulated growth is formulated from the fixpoint of a maximal growth rate (r_{max}; defined here by b_{max}) at zero density, a complete formulation is almost impossible because it requires that we have a full estimation of the density response from zero density to $\hat{N}^*$, while we usually observed densities only in a limited range.

With selection-regulated dynamics being formulated from the population dynamic equilibrium, the regulating equations are primarily intended to describe the behaviour in the surroundings of $\hat{N}^*$. There are no hard r_{max} and b_{max} in selection-regulated dynamics, although I do—for pragmatic reasons—allow for an upper and lower truncation of $i_{a,t}$. The growth rate and birth rate are not even parameters, but initial conditions that cannot be predicted from environmental conditions. Where a given environment has a single explicitly defined growth and birth rate under density regulated growth—for a given environment—the growth rate may take an infinite number of both positive and negative values under selection delayed dynamics. There is no maximum sustainable yield (Witting, 2002), and for given environmental conditions it is possible to predict only the acceleration or deacceleration of growth.

B Bayesian integration

The Bayesian integration between the model and the data is obtained by the sampling-importance-resampling routine (Jeffreys, 1961; Berger, 1985; Rubin, 1988), where n_s random parameterisations θ_i $(1 \leq i \leq n_1)$ are sampled from an importance function $h(\theta)$. This function is a probability distribution function from which a large number, n_s, of independent and identically distributed draws of θ can be taken. $h(\theta)$ shall generally be as close as possible to the posterior, however, the tails of $h(\theta)$ must be no thinner (less dense) than the tails of the posterior (Oh and Berger, 1992). For each drawn parameter set θ_i the population was projected from the first year with a harvest estimate to the present. For each draw an importance weight, or ratio, was then calculated

$$w(\theta_i) = \frac{L(\theta_i)p(\theta_i)}{h(\theta_i)} \tag{15}$$

where $L(\theta_i)$ is the likelihood given the data, and $h(\theta_i)$ and $p(\theta_i)$ are the importance and prior functions evaluated at θ_i. In the present study the importance function is set to the joint prior, so that the importance weight is given simply by the likelihood. The n_s parameter sets were then re-sampled n_r times with replacement, with the sampling probability of the ith parameter set being

$$q_i = \frac{w(\theta_i)}{\sum_{j=1}^{n_s} w(\theta_j)} \tag{16}$$

This generates a random sample of the posterior distribution of size n_r.

The log likelihood is given as a sum ($\ln L = \sum_i \ln L_i$) of the log likelihood of the different data components. The log likelihood of the ith set of the log normally distributed data is calculated as

$$\ln L_n = -\sum_t \frac{[\gamma_s \ln(\hat{x}_{i,t}/\beta_i x_t)]^2}{2\mathrm{cv}_{i,t}^2} + \ln \mathrm{cv}_{i,t} \tag{17}$$

where $\hat{x}_{i,t}$ is the point estimate of the data in year t, x_t the simulated estimate, $\beta_i \neq 1$ a potential bias, $\gamma_s \neq 1$ a potential skew, and $\mathrm{cv}_{i,t} = \sqrt{\hat{\mathrm{cv}}_{i,t}^2 + \sigma_i^2}$ the coefficient of variation, with $\hat{\mathrm{cv}}$ being the cv of the data and σ_i potential overdispersal (additional variance).

The log likelihood of the ith set of the multinomially distributed age data over $\mathbf{n_a}$ age (a) classes is given as

$$\ln L_n = -\sum_t \sum_{a \in \mathbf{n_a}} \frac{(\hat{n}_{i,a,t} - \hat{n}_{i,t} p_{i,a,t})^2}{2\sigma_i^2 \hat{n}_{i,t} p_{i,a,t}(1 - p_{i,a,t})} + \ln[\hat{n}_{i,t} p_{i,a,t}(1 - p_{i,a,t})]/2 + \ln \sigma_i \tag{18}$$

where $\hat{n}_{i,t}$ is the total number of aged individuals in year t, $\hat{n}_{i,a,t}$ the number of individuals in age class a, $p_{i,a,t}$ the simulated probability that an observed individual would be in age class a, β_i a potential bias, and σ_i potential overdispersal.

Year	C	Year	C	Year	C	Year	C	Year	C	Year	C	Year	C
1985	2596	1992	1572	1999	608	2006	856	2013	1104	2020	529	2027	868
1986	1676	1993	808	2000	588	2007	633	2014	48	2021	667	2028	868
1987	1450	1994	1201	2001	918	2008	0	2015	501	2022	528	2029	868
1988	1738	1995	228	2002	626	2009	310	2016	296	2023	896	2030	868
1989	1260	1996	1527	2003	503	2010	1107	2017	1203	2024	598	2031	868
1990	917	1997	1162	2004	1012	2011	726	2018	524	2025	868		
1991	722	1998	815	2005	302	2012	714	2019	682	2026	868		

Table 5: **Catch history** for Single N; no age data; r prior (i), 1986 age; r prior (r), 1986 age; p prior (s), All N; no age (n), All N; all age (a), All N; all age lnL*=0.5 (aH), All N; all age lnL*=0.25 (aI), and All N; all age lnL*=0.1 (aL). From Mikkelsen et al. (2025).

Par	N_0	r	p_0	b	m
N_0	1.00	-0.88	-0.03	-0.02	0.03
r	-0.88	1.00	0.05	0.01	-0.02
p_0	-0.03	0.05	1.00	0.06	0.03
b	-0.02	0.01	0.06	1.00	0.06
m	0.03	-0.02	0.03	0.06	1.00

Table 6: **Correlation matrix** for the posterior parameter estimates of Single N; no age data; r prior (i).

Par	N_0	r	p_0	b	m
N_0	1.00	-0.88	-0.09	-0.02	0.11
r	-0.88	1.00	0.11	0	-0.09
p_0	-0.09	0.11	1.00	-0.05	0.05
b	-0.02	0	-0.05	1.00	0.04
m	0.11	-0.09	0.05	0.04	1.00

Table 7: **Correlation matrix** for the posterior parameter estimates of 1986 age; r prior (r).

Par	N_0	p	p_0	b	m
N_0	1.00	-0.86	0	-0.06	0.09
p	-0.86	1.00	-0.05	0.01	0
p_0	0	-0.05	1.00	-0.10	0.03
b	-0.06	0.01	-0.10	1.00	0.07
m	0.09	0	0.03	0.07	1.00

Table 8: **Correlation matrix** for the posterior parameter estimates of 1986 age; p prior (s).

Par	N_0	p	p_0	b	m
N_0	1.00	-0.44	-0.17	-0.12	-0.02
p	-0.44	1.00	-0.15	-0.07	0.06
p_0	-0.17	-0.15	1.00	-0.07	0
b	-0.12	-0.07	-0.07	1.00	-0.03
m	-0.02	0.06	0	-0.03	1.00

Table 9: **Correlation matrix** for the posterior parameter estimates of All N; no age (n).

Par	N_0	p	p_0	b	m
N_0	1.00	-0.02	-0.02	-0.03	-0.02
p	-0.02	1.00	0.02	0.06	0
p_0	-0.02	0.02	1.00	-0.01	-0.01
b	-0.03	0.06	-0.01	1.00	-0.04
m	-0.02	0	-0.01	-0.04	1.00

Table 10: **Correlation matrix** for the posterior parameter estimates of All N; all age (a).

Par	N_0	p	p_0	b	m
N_0	1.00	0.01	-0.03	0.01	-0.04
p	0.01	1.00	-0.06	-0.03	-0.07
p_0	-0.03	-0.06	1.00	-0.04	0.02
b	0.01	-0.03	-0.04	1.00	0.03
m	-0.04	-0.07	0.02	0.03	1.00

Table 11: **Correlation matrix** for the posterior parameter estimates of All N; all age lnL*=0.5 (aH).

Par	N_0	p	p_0	b	m
N_0	1.00	-0.55	-0.04	-0.04	0.07
p	-0.55	1.00	0.02	0.03	-0.07
p_0	-0.04	0.02	1.00	-0.17	0.06
b	-0.04	0.03	-0.17	1.00	0.13
m	0.07	-0.07	0.06	0.13	1.00

Table 12: **Correlation matrix** for the posterior parameter estimates of All N; all age lnL*=0.25 (aI).

Par	N_0	p	p_0	b	m
N_0	1.00	-0.47	-0.09	-0.07	0.08
p	-0.47	1.00	0.05	-0.06	0.03
p_0	-0.09	0.05	1.00	-0.12	0.05
b	-0.07	-0.06	-0.12	1.00	0.12
m	0.08	0.03	0.05	0.12	1.00

Table 13: **Correlation matrix** for the posterior parameter estimates of All N; all age lnL*=0.1 (aL).

References

Berger, J. O. 1985. Statistical decision theory and Bayesian analysis. Second edn. Springer-Verlag, New York.

Jeffreys, H. 1961. Theory of probability. 3rd edition edn. Clarendon Press, Oxford.

Mikkelsen, B. 2025. Age, growth, and reproduction of long-finned pilot whales in the Faroe Islands. NAMMCO/SC/PWWG/2025-01/10, .

Mikkelsen, B., Ofstad, L. H., and Akralid, R. 2025. Catch history of long-finned pilot whales in the Faroe Islands. NAMMCO/SC/PWWG/2025-01/08, .

NAMMCO 2025. Table of accepted abundance estimates. https://nammco.no/abundance-estimates/, .

Oh, M. S. and Berger, J. O. 1992. Adaptive importance sampling in Monte Carlo integration. Journal of Statistics and Computer Simulation, 41: 143–168.

Rubin, D. B. 1988. Using the SIR algorithm to simulate posterior distributions. In Bayesian Statistics 3: Proceedings of the Third Valencia International Meeting, 1–5 June 1987, pp. 395–402. Ed. by, J. M. Bernardo, M. H. DeGroot, D. V. Lindley, and A. M. Smith. Clarendon Press, Oxford.

Smith, C. C. and Fretwell, S. D. 1974. The optimal balance between size and number of offspring. The American Naturalist, 108: 499–506.

Stearns, S. C. 1992. The evolution of life histories. Oxford University Press, Oxford.

Witting, L. 2000a. Interference competition set limits to the fundamental theorem of natural selection. Acta Biotheoretica, 48: 107–120, https://doi.org/10.1023/A:1002788313345.

Witting, L. 2000b. Population cycles caused by selection by density dependent competitive interactions. Bulletin of Mathematical Biology, 62: 1109–1136, https://doi.org/10.1006/bulm.2000.0200.

Witting, L. 2002. Evolutionary dynamics of exploited populations selected by density dependent competitive interactions. Ecological Modelling, 157: 51–68, https://doi.org/10.1016/S0304–3800(02)00172–2.

Witting, L. 2013. Selection-delayed population dynamics in baleen whales and beyond. Population Ecology, 55: 377–401, https://dx.doi.org/10.1007/s10144–013–0370–9.

NAMMCO 2025 SC/PWWG/2025-01/7b

Bayesian assessment runs for long-finned pilot whales in the North Atlantic

Lars Witting

November 26, 2025

Unless otherwise stated, these models are based on early the age data only, birth rate and reproductive maturity data around 1987 and 2017, allowing also for two independent 1987 and 2017 estimates of offspring survival. Abundance data are the agreed best time series of relative estimates from 1987 to 2015, and absolute estimates from 2007, 2015, and 2024 that all survey comparable areas, and 10% loss is added to the East Greenland catches. The likelihood weight of the age data is multiplied by 0.25, compared with a multiplication factor of unity for the abundance data.

Data model (p) The complete timeseries of relative abundance and all three absolute estimates are used. This however raises the issue that the abundance trend between 2007 and 2015 is weighted twice.

Data model (i) The last index estimate is removed from the data in the p model.

Data model (n) The first absolute estimate (from 2007) is removed from the data in the p model.

Data model (z) Uses the complete index series, and a absolute 2020 estimate calculated as the average of absolute estimates for 2015 and 2024.

Data model (x) As model z, but with the likelihood of the age data multiplied by 0.1.

Data model (u) As model z, but likelihood of age data multiplied by 0.5

Data model (h) As model z but with 30% loss in East Greenland.

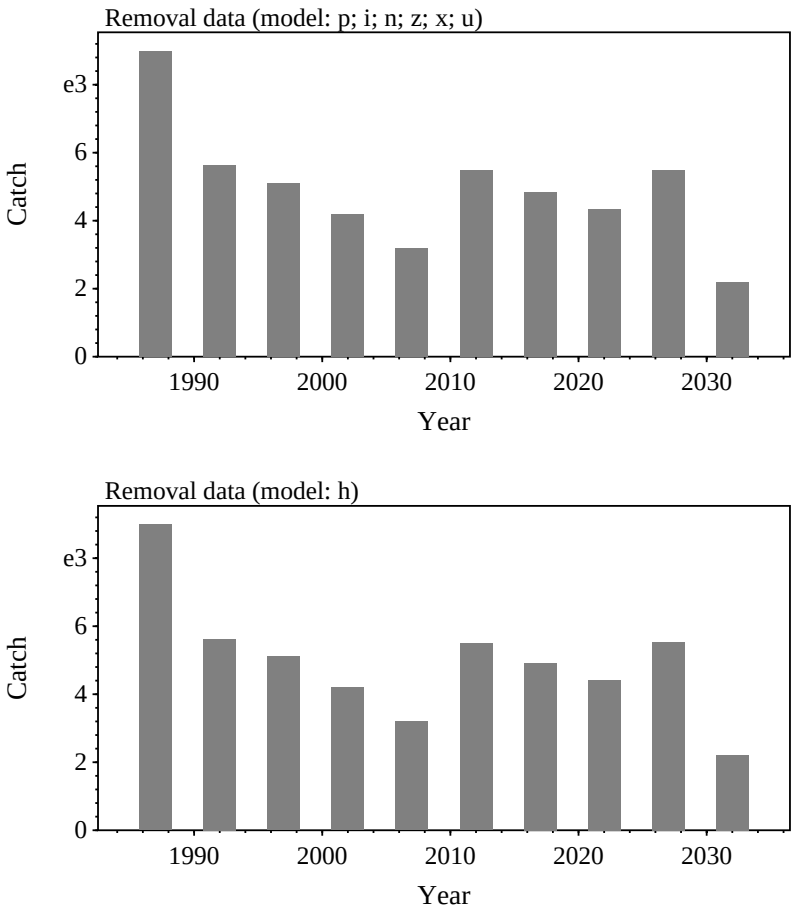

Figure 1: Historical removals in 5 year bins. Data from Mikkelsen et al. (2025).

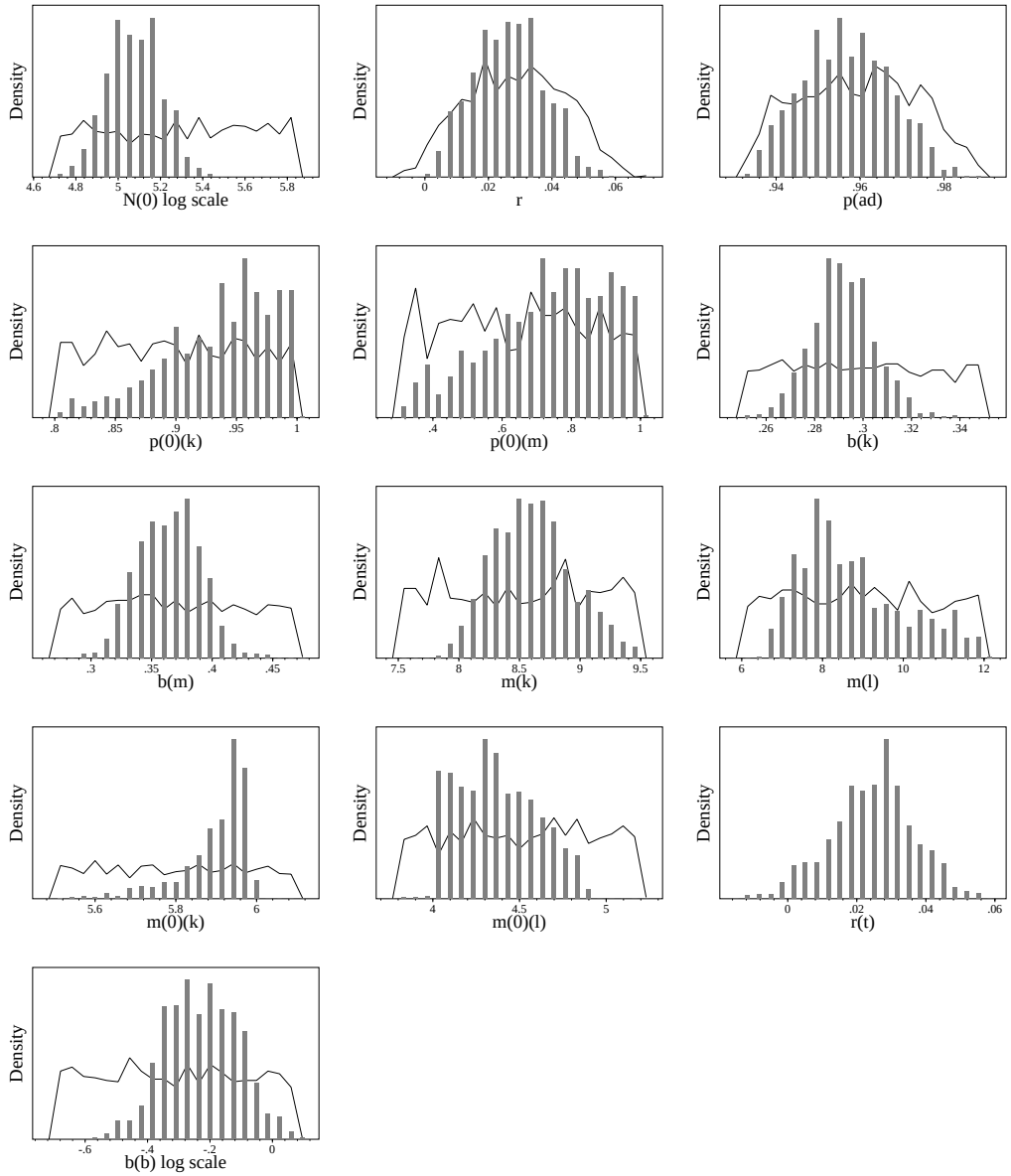

Figure 2: Realised prior (curve) and posterior (bars) distributions for Data model (p).

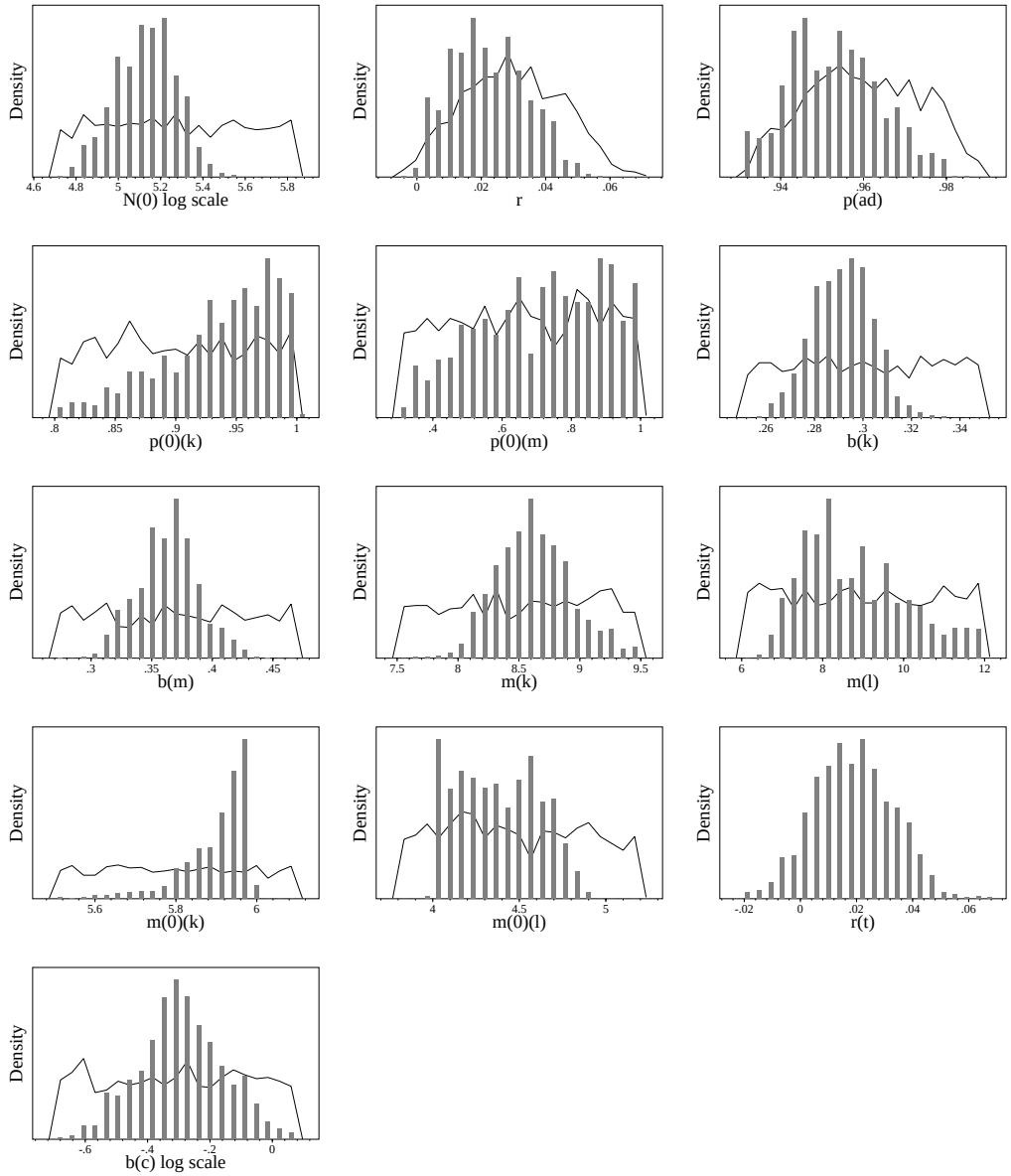

Figure 3: Realised prior (curve) and posterior (bars) distributions for Data model (i).

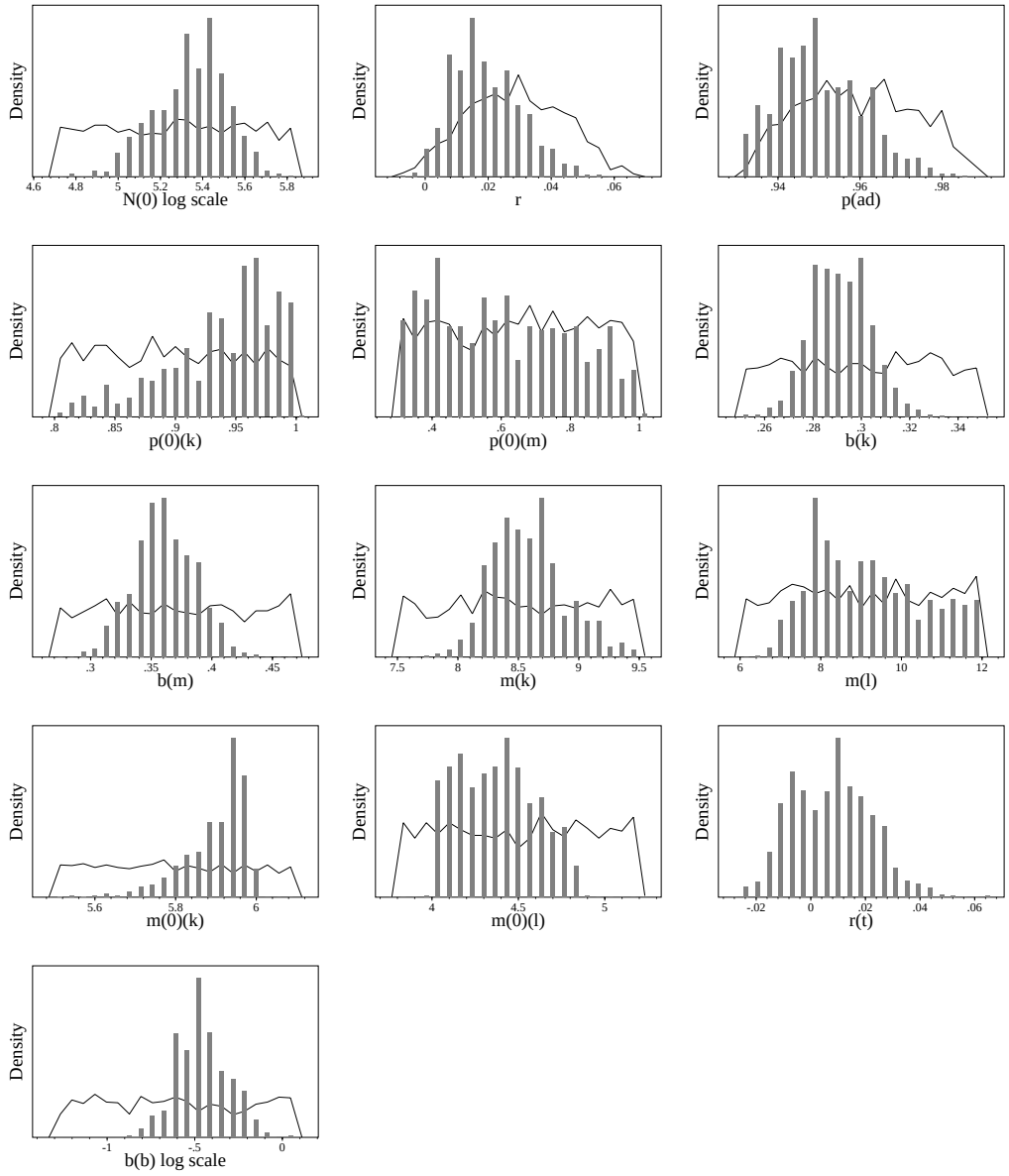

Figure 4: Realised prior (curve) and posterior (bars) distributions for Data model (n).

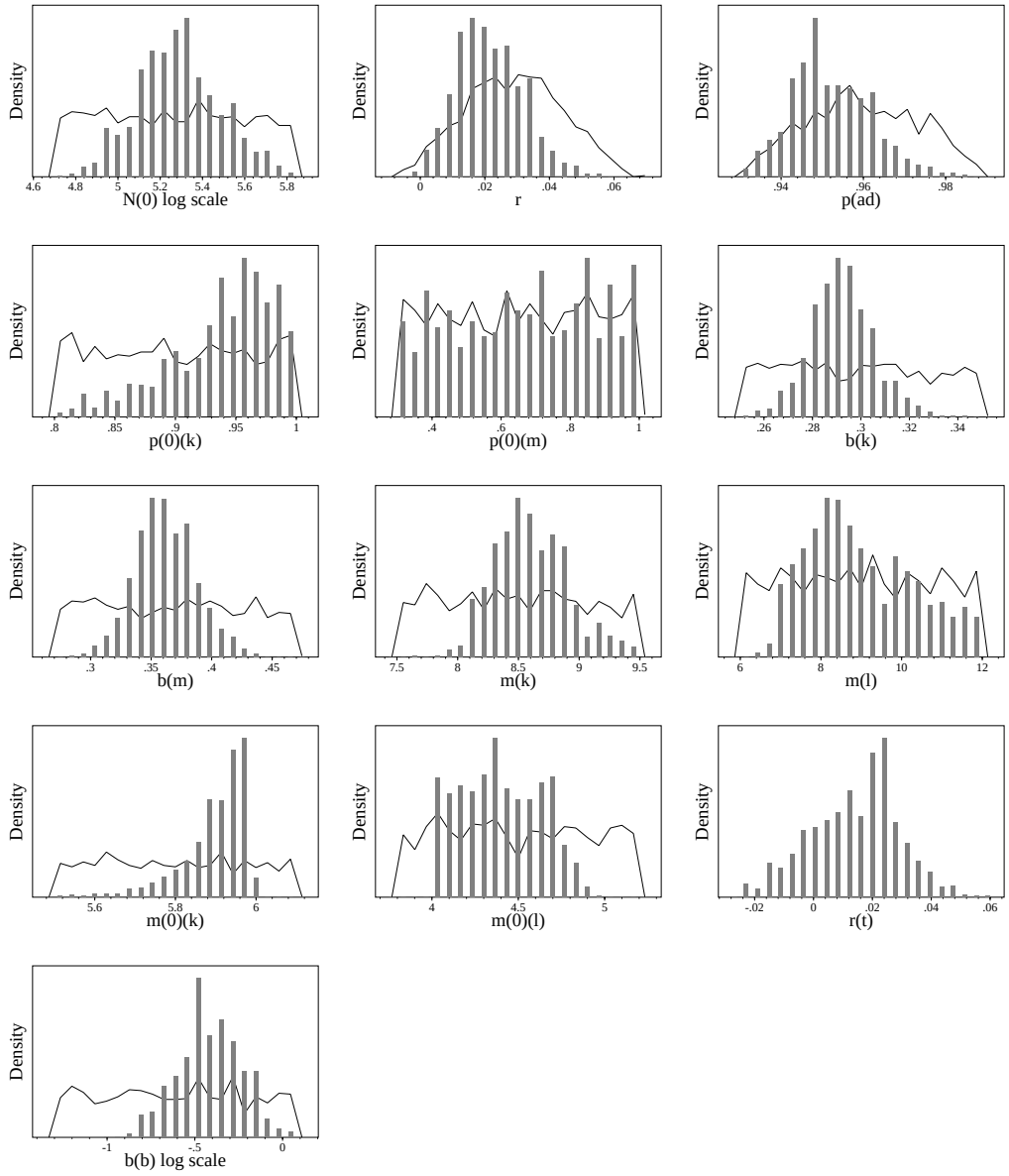

Figure 5: Realised prior (curve) and posterior (bars) distributions for Data model (z).

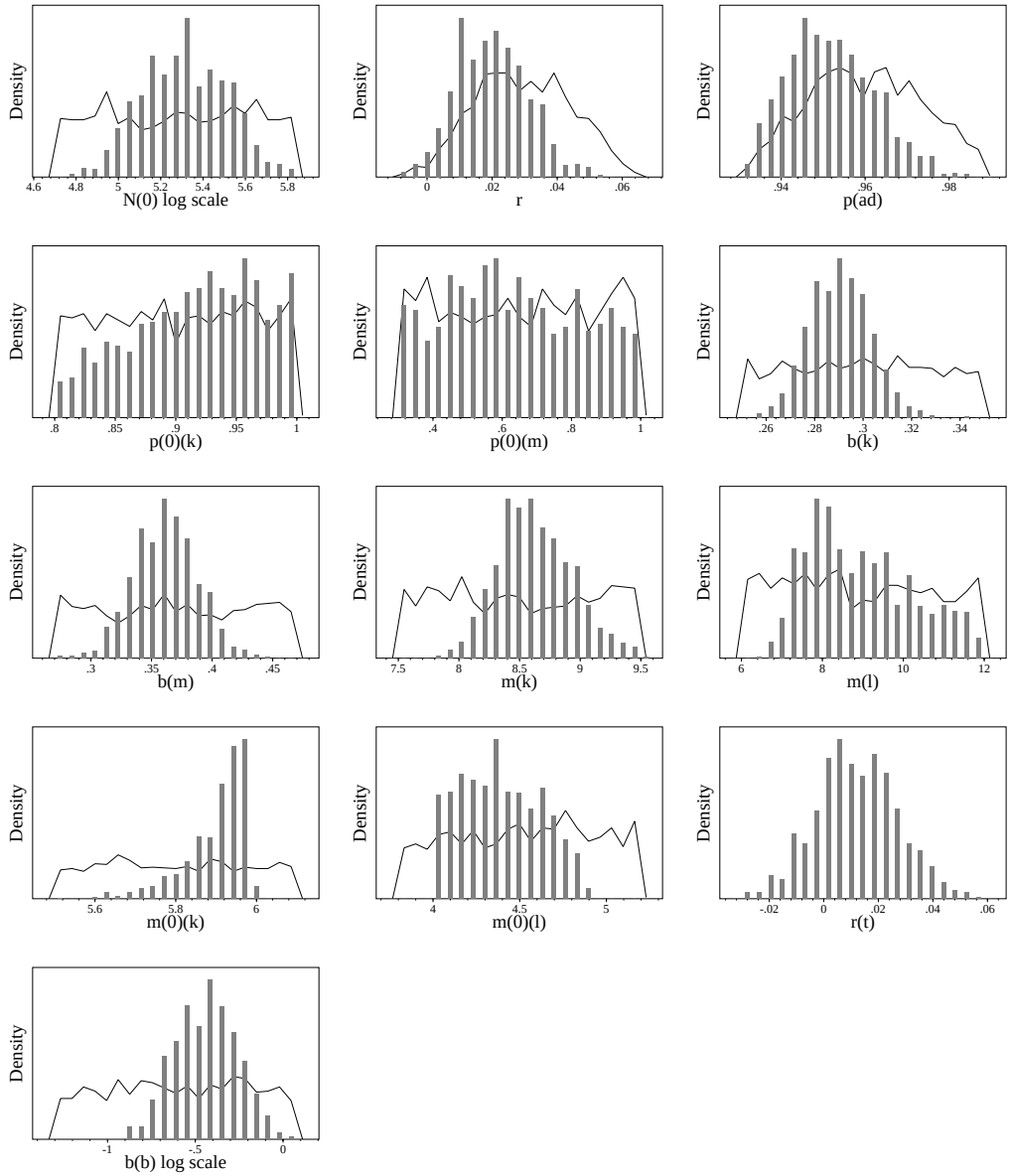

Figure 6: Realised prior (curve) and posterior (bars) distributions for Data model (x).

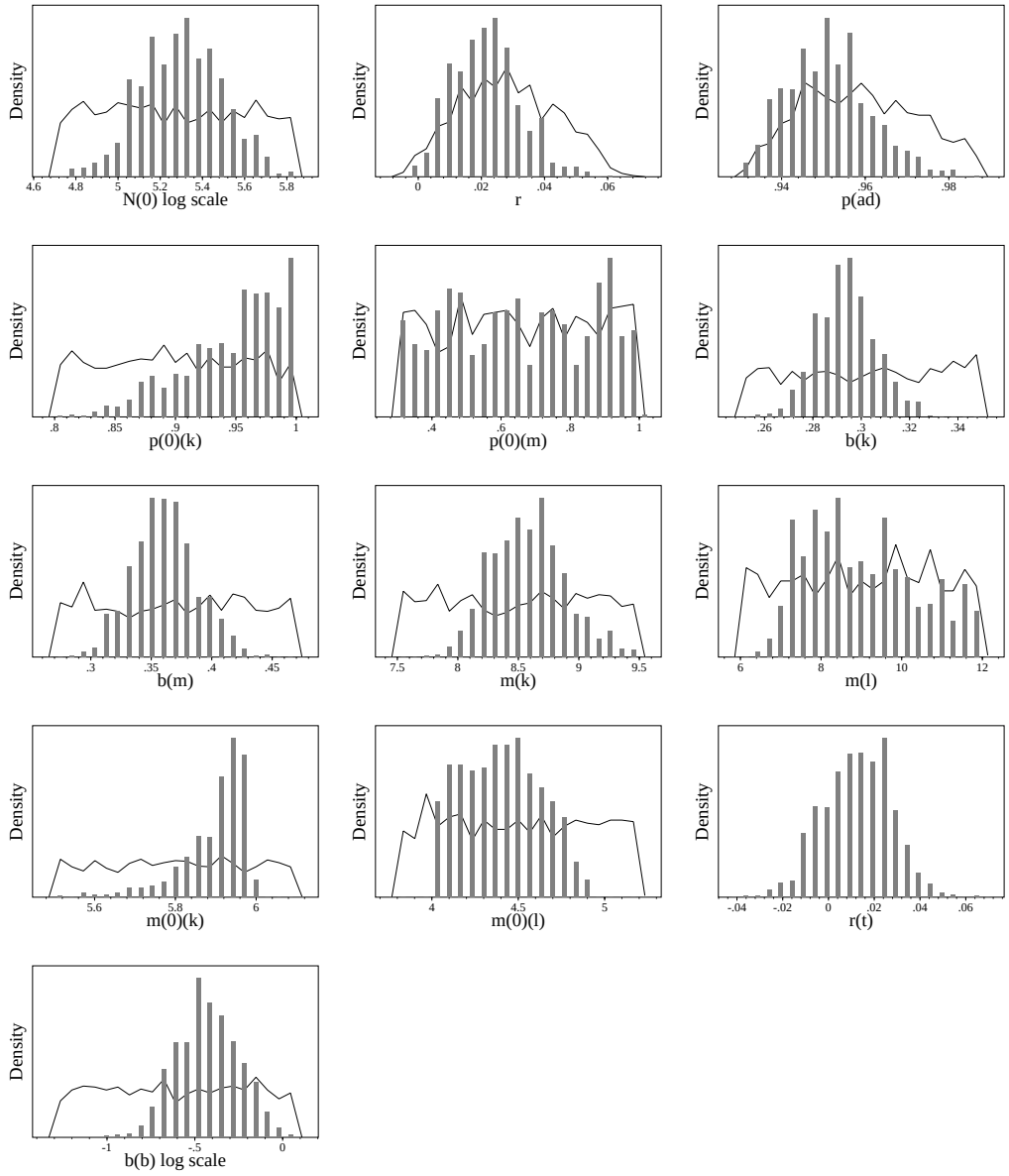

Figure 7: Realised prior (curve) and posterior (bars) distributions for Data model (u).

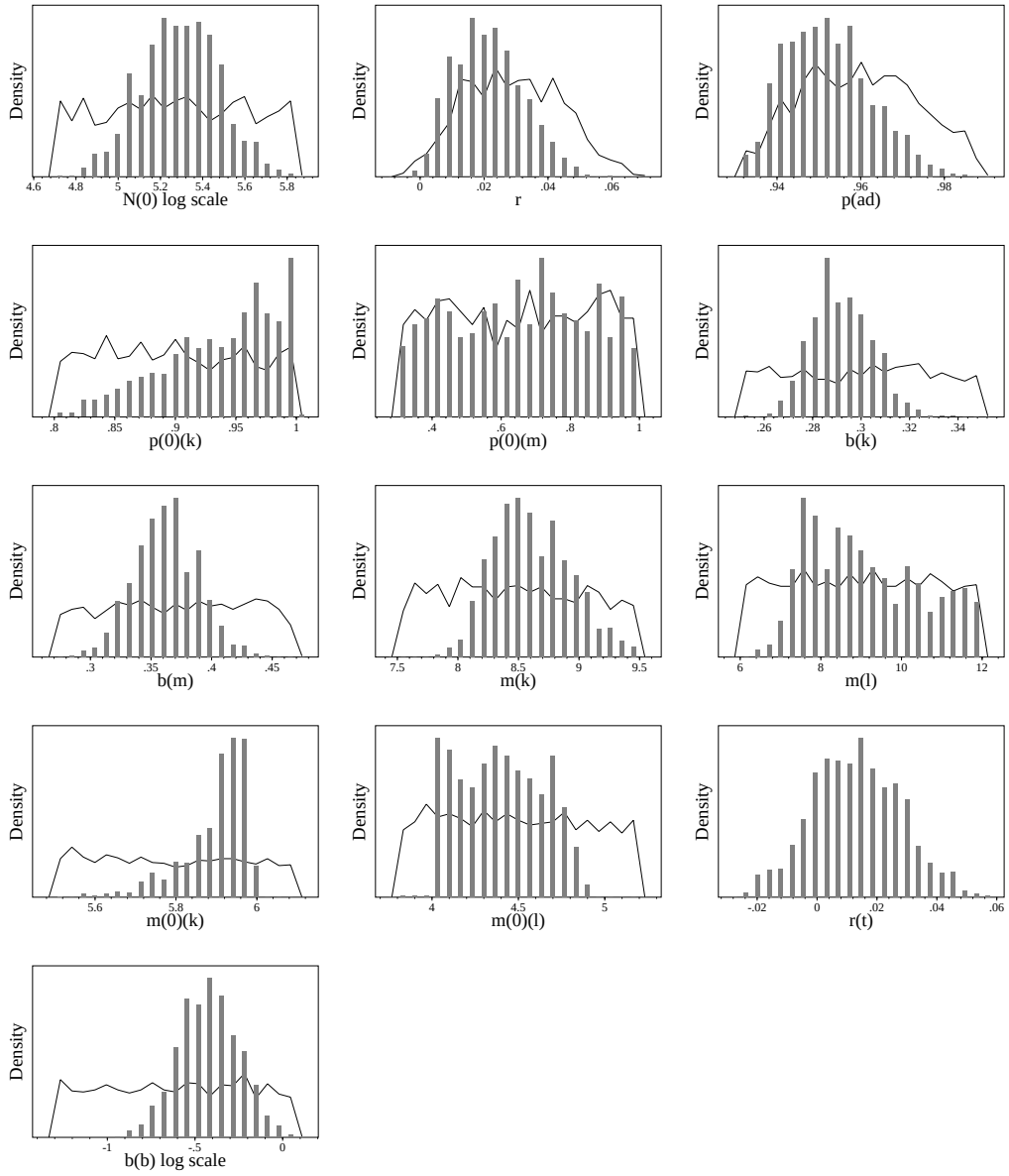

Figure 8: Realised prior (curve) and posterior (bars) distributions for Data model (h).

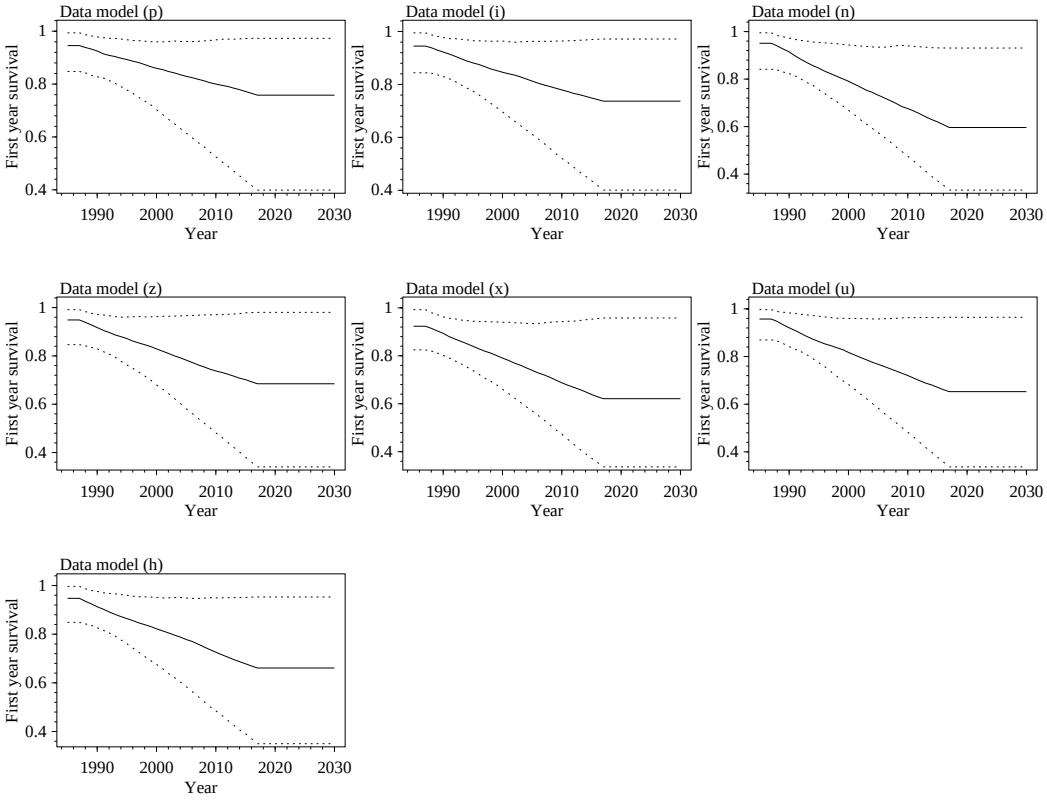

Figure 9: Projected medians and 90% credibility intervals for first year survival.

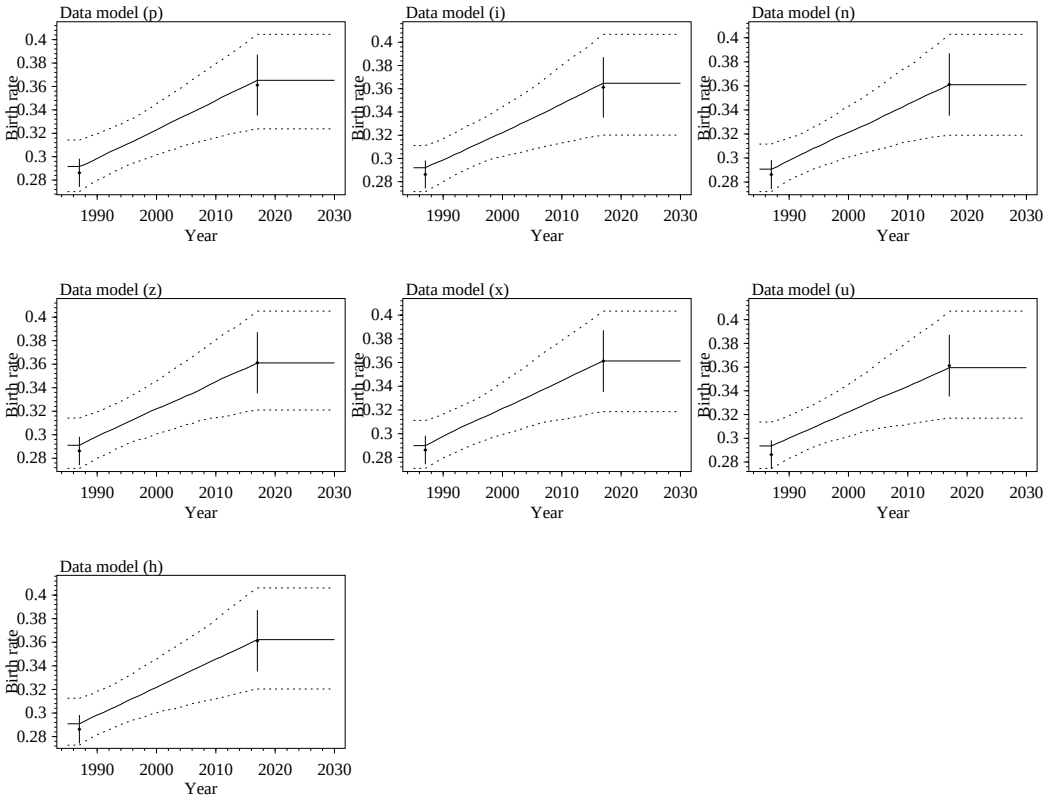

Figure 10: Projected medians and 90% credibility intervals for birth rate. Data from Garde and Heide-Jørgensen (2019).

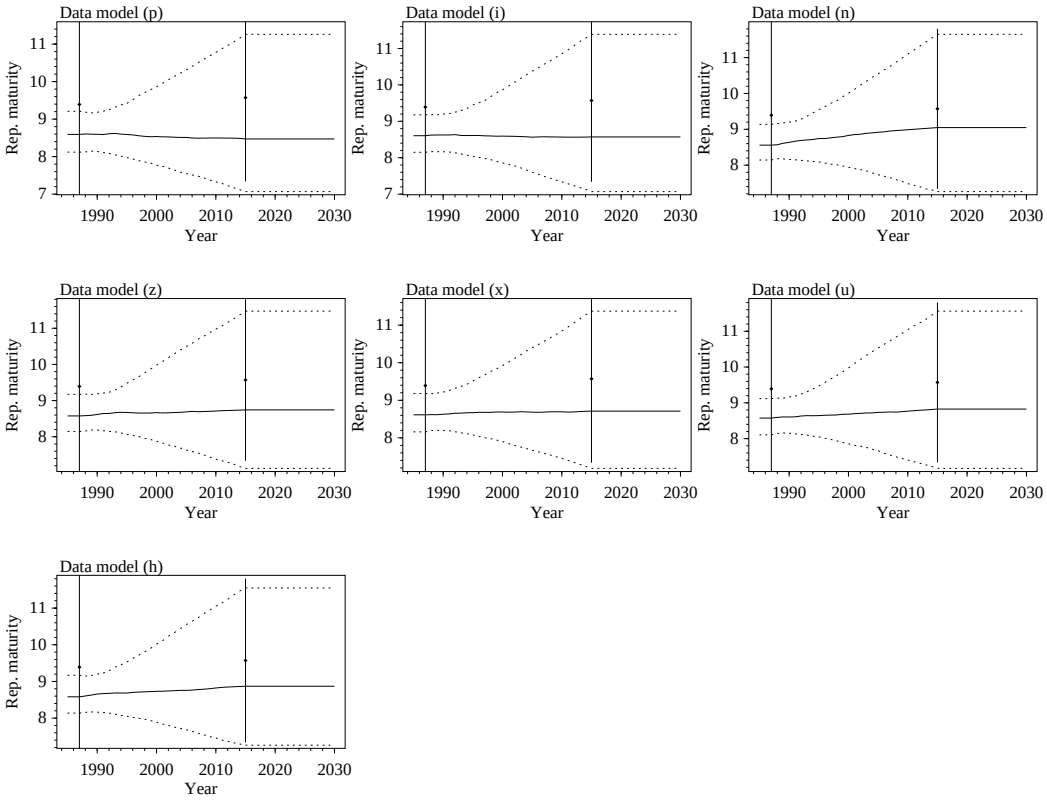

Figure 11: Projected medians and 90% credibility intervals for rep. maturity. Data from Mikkelsen (2025).

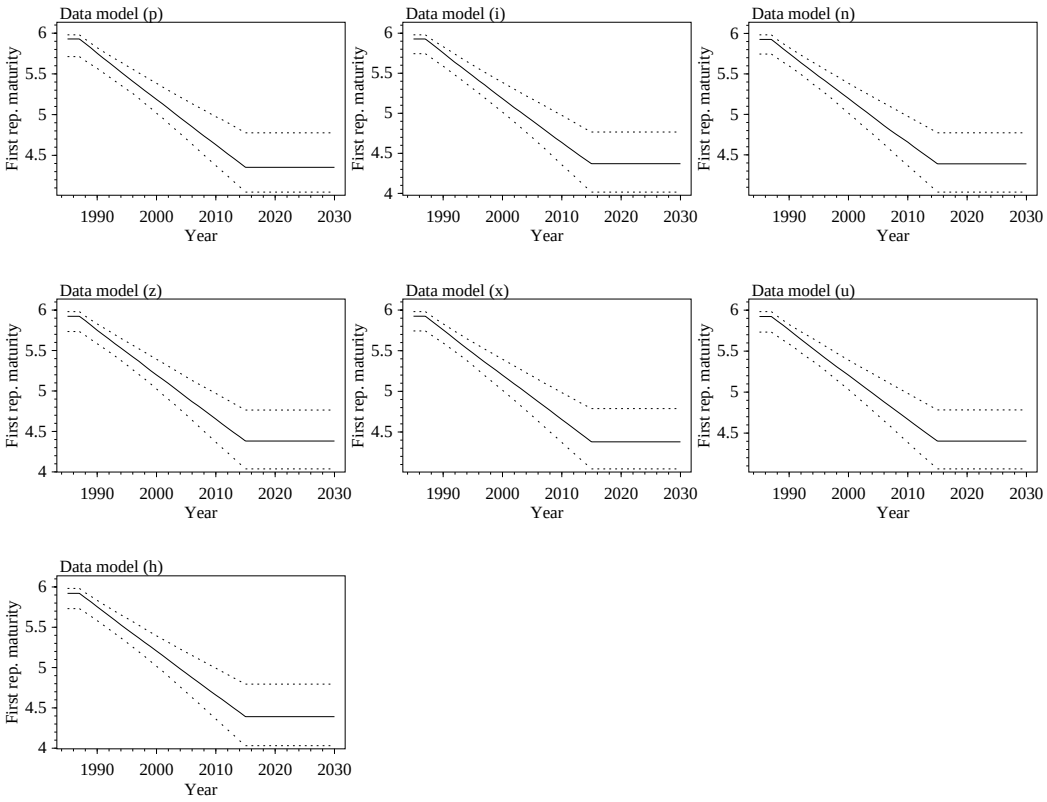

Figure 12: Projected medians and 90% credibility intervals for first rep. maturity.

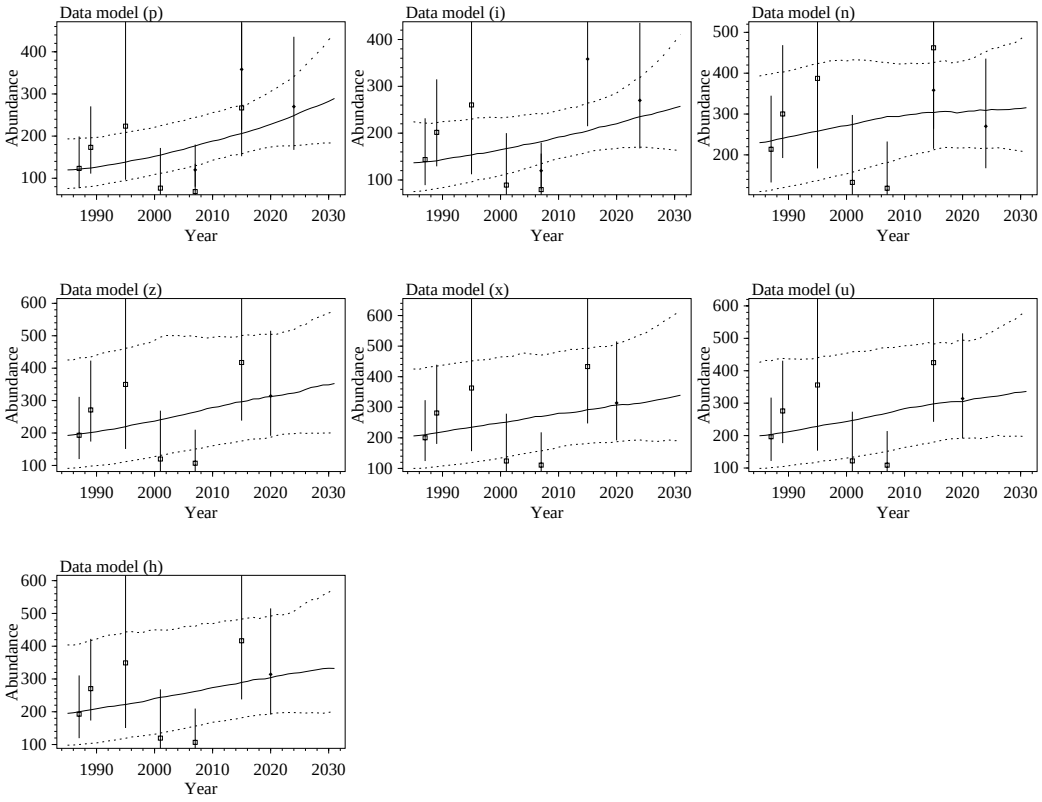

Figure 13: Projected medians and 90% credibility intervals for abundance. Data from NAMMCO (2025).

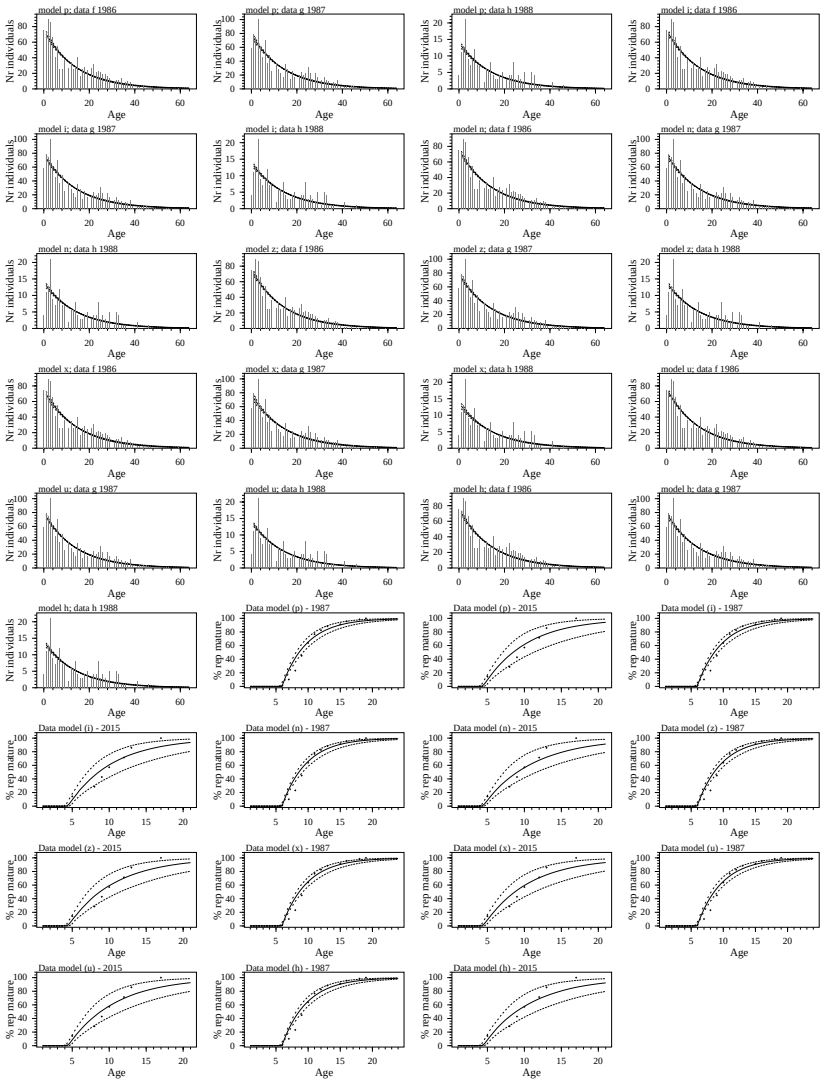

Figure 14: Model fits for age-structure and reproductive maturity. Data given by bars and dots, and models by the median estimate (solid curve) and 90% credibility interval (dashed curves). Data from Mikkelsen (2025).

	a	b	f	g	h	i	j	c	d	e
p	*	*	*	*	*	*	*	-	-	-
i	*	-	*	*	*	*	*	*	-	-
n	-	*	*	*	*	*	*	-	*	-
z	-	*	*	*	*	*	*	-	-	*
x	-	*	*	*	*	*	*	-	-	*
u	-	*	*	*	*	*	*	-	-	*
h	-	*	*	*	*	*	*	-	-	*
1986	-	-	12.4^{17}_{1097}	-	-	-	-	-	-	-
1987	-	73100^{29}	-	12.7^{17}_{1121}	-	0.29^{314}_{1097}	9.39^{32}_{69}	73100^{29}	-	-
1988	-	-	-	-	12.9^{18}_{193}	-	-	-	-	-
1989	-	103000^{27}	-	-	-	-	-	103000^{27}	-	-
1995	-	132000^{51}	-	-	-	-	-	132000^{51}	-	-
2001	-	45400^{49}	-	-	-	-	-	45400^{49}	-	-
2007	120000^{25}	40500^{41}	-	-	-	-	-	40500^{41}	-	-
2015	358000^{31}	158000^{34}	-	-	-	-	9.57^{14}_{7}	-	358000^{31}	-
2017	-	-	-	-	-	0.36^{121}_{335}	-	-	-	-
2020	-	-	-	-	-	-	-	-	-	314000^{30}
2024	270000^{29}	-	-	-	-	-	-	-	270000^{29}	-

Table 1: **Data for likelihood functions.** Their use by models are marked by *. a: Abundance with log normal likelihood [n(1+); $\bar{x}^{cv\%}$]. b: Abundance with log normal likelihood [n(1+); relative; $\bar{x}^{cv\%}$]. f: Age structure with multinomial likelihood [population; $\bar{x}_n^{cv\%}$]. g: Age structure with multinomial likelihood [population; $\bar{x}_n^{cv\%}$]. h: Age structure with multinomial likelihood [population; $\bar{x}_n^{cv\%}$]. i: Birth rate with binomial likelihood [$\bar{x}^{n_1}_{n_0+n_1}$]. j: Age of first reproduction with multinomial likelihood [$\bar{x}_n^{cv\%}$]. c: Abundance with log normal likelihood [n(1+); relative; $\bar{x}^{cv\%}$]. d: Abundance with log normal likelihood [n(1+); $\bar{x}^{cv\%}$]. e: Abundance with log normal likelihood [n(1+); $\bar{x}^{cv\%}$]. Data from Garde and Heide-Jørgensen (2019), Mikkelsen (2025), and NAMMCO (2025).

M	N_0	b_k	b_m	ϑ	m_{0k}	m_{0l}	m_k	m_l	p_{0k}	p_{0m}	p
p	$50;700^U$	$.25;.35^u$	$.27;.47^u$	$.5^p$	$5.5;6.1^u$	$3.8;5.2^u$	$7.5;9.5^u$	$6;12^u$	$.8;1^u$	$.3;1^u$	$^{2;2^b}_{.93;.99}$
i	$50;700^U$	$.25;.35^u$	$.27;.47^u$	$.5^p$	$5.5;6.1^u$	$3.8;5.2^u$	$7.5;9.5^u$	$6;12^u$	$.8;1^u$	$.3;1^u$	$^{2;2^b}_{.93;.99}$
n	$50;700^U$	$.25;.35^u$	$.27;.47^u$	$.5^p$	$5.5;6.1^u$	$3.8;5.2^u$	$7.5;9.5^u$	$6;12^u$	$.8;1^u$	$.3;1^u$	$^{2;2^b}_{.93;.99}$
z	$50;700^U$	$.25;.35^u$	$.27;.47^u$	$.5^p$	$5.5;6.1^u$	$3.8;5.2^u$	$7.5;9.5^u$	$6;12^u$	$.8;1^u$	$.3;1^u$	$^{2;2^b}_{.93;.99}$
x	$50;700^U$	$.25;.35^u$	$.27;.47^u$	$.5^p$	$5.5;6.1^u$	$3.8;5.2^u$	$7.5;9.5^u$	$6;12^u$	$.8;1^u$	$.3;1^u$	$^{2;2^b}_{.93;.99}$
u	$50;700^U$	$.25;.35^u$	$.27;.47^u$	$.5^p$	$5.5;6.1^u$	$3.8;5.2^u$	$7.5;9.5^u$	$6;12^u$	$.8;1^u$	$.3;1^u$	$^{2;2^b}_{.93;.99}$
h	$50;700^U$	$.25;.35^u$	$.27;.47^u$	$.5^p$	$5.5;6.1^u$	$3.8;5.2^u$	$7.5;9.5^u$	$6;12^u$	$.8;1^u$	$.3;1^u$	$^{2;2^b}_{.93;.99}$

Table 2: **Priors for the model parameters** of the different models (M). N the abundance, b the birth rate, ϑ the female fraction at birth, m_0 the first rep. maturity, m the rep. maturity, p_0 the first year survival, and p the yearly survival. Year by subscript: 0:initial, k:1987, l:2015, and m:2017. Abundance is given in thousands. The prior probability distribution is given by superscripts; p: fixed value, u: uniform (min;max), U: log uniform (min;max), and b: beta $(^{a;b}_{i;x})$ with i=min and x=max.

M	β_b	β_c
p	$.2;1.2^U$	-
i	-	$.2;1.2^U$
n	$.05;1.2^U$	-
z	$.05;1.2^U$	-
x	$.05;1.2^U$	-
u	$.05;1.2^U$	-
h	$.05;1.2^U$	-

Table 3: **Priors for the data parameters** of the different models (M). β_i the abundance estimate bias (i: data reference). The prior probability distribution is given by superscripts; U: log uniform (min;max).

M	n_S	n_R	unique	max
p	2000	1	716	26
i	2000	1	686	17
n	2000	1	631	21
z	2000	1	691	19
x	2000	1	768	8
u	2000	1	683	20
h	2000	1	726	17

Table 4: **Sampling statistics** for the different models (M). The number of parameter sets in the sample (n_S) and the resample (n_R), the number of unique parameter sets in the resample, and the maximum number of occurrences of a unique parameter set in the resample. n_S and n_R are given in thousands.

M		N_0	N_t	b_k	b_m	m_{0k}	m_{0l}	m_k	m_l	p_{0k}	p_{0m}	p	r	r_t
	$x_{.5}$	120	255	.292	.365	5.93	4.35	8.59	8.47	.946	.758	.956	.026	.025
	$x_{.05}$	75.7	178	.27	.324	5.71	4.05	8.12	7.07	.848	.399	.94	.008	.002
p	$x_{.95}$	193	354	.314	.405	5.98	4.78	9.21	11.3	.994	.973	.974	.044	.043
	$x_{.5}$	137	238	.292	.365	5.93	4.37	8.6	8.57	.945	.737	.953	.021	.018
	$x_{.05}$	75.2	170	.271	.32	5.74	4.02	8.15	7.07	.844	.401	.936	.003	-.0049
i	$x_{.95}$	224	330	.311	.407	5.98	4.77	9.18	11.4	.995	.972	.972	.042	.041
	$x_{.5}$	230	311	.291	.361	5.93	4.39	8.56	9.05	.951	.596	.949	.017	.008
	$x_{.05}$	110	216	.272	.319	5.75	4.04	8.14	7.26	.841	.333	.935	.003	-.014
n	$x_{.95}$	393	460	.312	.403	5.98	4.77	9.14	11.6	.995	.931	.969	.039	.029
	$x_{.5}$	192	327	.291	.361	5.92	4.38	8.58	8.74	.949	.685	.951	.02	.016
	$x_{.05}$	90.9	200	.271	.321	5.73	4.04	8.15	7.12	.847	.341	.937	.005	-.0118
z	$x_{.95}$	425	530	.314	.405	5.98	4.76	9.17	11.5	.992	.98	.969	.038	.036
	$x_{.5}$	206	316	.29	.361	5.92	4.38	8.61	8.71	.923	.621	.951	.019	.011
	$x_{.05}$	100	190	.271	.319	5.74	4.05	8.16	7.19	.825	.337	.937	.002	-.0128
x	$x_{.95}$	425	543	.311	.403	5.98	4.79	9.18	11.4	.993	.958	.97	.038	.037
	$x_{.5}$	199	320	.294	.36	5.92	4.4	8.57	8.83	.957	.653	.951	.021	.013
	$x_{.05}$	98.8	197	.275	.317	5.73	4.06	8.11	7.17	.87	.337	.936	.005	-.0115
u	$x_{.95}$	426	519	.314	.407	5.98	4.78	9.12	11.6	.997	.965	.969	.038	.035
	$x_{.5}$	195	319	.291	.362	5.92	4.39	8.58	8.87	.947	.661	.951	.020	.012
	$x_{.05}$	98	197	.273	.32	5.73	4.03	8.14	7.26	.849	.35	.938	.006	-.0106
h	$x_{.95}$	404	519	.313	.406	5.98	4.79	9.17	11.5	.996	.953	.97	.040	.037

Table 5: **Model parameter estimates** for the different models (M). Estimates are given by the median ($x_{.5}$) and the 90% credibility interval ($x_{.05}$ - $x_{.95}$) of the posterior distributions. N the abundance, b the birth rate, m_0 the first rep. maturity, m the rep. maturity, p_0 the first year survival, p the yearly survival, and r the exp. growth rate (no removal, max or realised). Year by subscript: 0:initial, k:1987, l:2015, m:2017, and t:2025. Abundance is given in thousands.

M		β_b	β_c
	$x_{.5}$	.592	-
	$x_{.05}$	.387	-
p	$x_{.95}$	.903	-
	$x_{.5}$	-	.509
	$x_{.05}$	-	.302
i	$x_{.95}$	-	.868
	$x_{.5}$	.342	-
	$x_{.05}$	.198	-
n	$x_{.95}$	.636	-
	$x_{.5}$	.379	-
	$x_{.05}$	.188	-
z	$x_{.95}$	.721	-
	$x_{.5}$	.365	-
	$x_{.05}$	.19	-
x	$x_{.95}$	.687	-
	$x_{.5}$	.372	-
	$x_{.05}$	.193	-
u	$x_{.95}$	.738	-
	$x_{.5}$	.379	-
	$x_{.05}$	.196	-
h	$x_{.95}$	.724	-

Table 6: **Data parameter estimates** for the different models (M). Estimates are given by the median ($x_{.5}$) and the 90% credibility interval ($x_{.05}$ - $x_{.95}$) of the posterior distributions. β_i the abundance estimate bias (i: data reference).

P	p	i	n	z	x	u	h
F	0.50	0.50	0.50	0.50	0.50	0.50	0.50
0.50	6621	4499	2541	4966	3569	4170	4068
0.55	6209	3995	1843	4256	2921	3296	3343
0.60	5573	3492	1035	3463	2300	2632	2552
0.65	5047	2977	134	2720	1682	2096	1923
0.70	4567	2446	-499	2068	1169	1475	1290
0.75	4086	1926	-1140	1133	503	606	618
0.80	3399	1458	-1729	111	-89	-649	138
0.85	2762	835	-2326	-937	-1023	-1322	-539
0.90	1681	242	-2951	-2012	-2291	-2148	-1627
0.95	613	-887	-4101	-4006	-3614	-3599	-3249

Table 7: **Catch objective trade-off per stock.** The annual total removals per stock that meet given probabilities (P) of meeting management objectives. The simulated period is from 2026 to 2031, and F is the assumed fraction of females in the catch.

Appendix

A Population dynamic model

The population model is an age-structured Bayesian assessments model that is programmed in C++, and which is easily programmed by input files to deal with different species, populations, and situations. Based on the input programming, the model will simulate unregulated exponential growth, density regulated growth, or selection regulated dynamics which is a density regulated population with superimposed selection regulation.

The population dynamic model is structured by gender and age, with x being the maximum lumped age-class. Let the number $N^{m/f}_{a,t+1}$ of males (m) and females (f) in age-classes $0 < a < x$ in year $t+1$ be

$$N^{m/f}_{a+1,t+1} = p^{m/f}_a N^{m/f}_{a,t} - c^{m/f}_{a,t} \tag{1}$$

and the number of animals in age-class x be

$$N^{m/f}_{x,t+1} = p^{m/f}_x N^{m/f}_{x,t} + p^{m/f}_{x-1} N^{m/f}_{x-1,t} - c^{m/f}_{x,t} - c^{m/f}_{x-1,t} \tag{2}$$

where $p^{m/f}_a$ is the age specific survival rate of males/females, and $c^{m/f}_{a,t}$ is the age specific catch of males/females in year t. The age and gender (g) dependent survival rates $p^g_a = p\tilde{p}^g_a$ are given as a product between a survival scalar p and relative ($0 < \tilde{p}^g_a \leq 1$) survival rates. The age and gender specific catches $c^{m/f}_{a,t} = c^{m/f}_t \tilde{c}^{m/f}_{a,t}$ in year t are given as a product between the total catch of males/females ($c^{m/f}_t$), as specified by the catch history, and an age-specific catch selectivity ($\tilde{c}^{m/f}_{a,t}$). The age-specific catch selectivity is listed in Table **??**.

The number of females and males in age-class zero is $N^f_{0,t} = \vartheta N_{0,t}$ and $N^m_{0,t} = (1-\vartheta)N_{0,t}$, where ϑ is the fraction of females at birth, and

$$N_{0,t} = \sum_{a=0}^{x} B_{a,t} \tag{3}$$

where $B_{a,t}$ is the number of births from females in age class a, defined as

$$B_{a,t} = b_{a,t}\, \tilde{b}_a\, M^f_{a,t} \tag{4}$$

where $b_{a,t}$ is the birth rate in year t for age-class a females should they be at their age-specific reproductive peak, $0 < \tilde{b}_a \leq 1$ are the relative age-specific birth rates, and $M^f_{a,t}$ is the number of mature females in age-class a in year t, defined as

$$M^f_{a,t} = \begin{cases} 0 & \text{if } a < m_{0,a,t} \\ \tilde{m}_{a,t} N^f_{a,t} & \text{if } a \geq m_{0,a,t} \end{cases} \tag{5}$$

where

$$\tilde{m}_{a,t} = 1 - e^{-\frac{a-m_{0,a,t}}{m_{a,t}-m_{0,a,t}} \ln 2} \tag{6}$$

is the fraction of females in age-class a in year t that is mature, with $m_{0,a,t}$ being the earliest, and $m_{a,t}$ the median, age of reproductive maturity for females of age a in year t.

Knife-edge maturation, where all females older than m_0 are mature, occurs when $m_0 = m$. Yet, for model versions with knife-edge maturity, the number of mature females is

$$M^f_{a,t} = \min[1, \max(0, a + 1 - m_{a,t})]N^f_{a,t} \tag{7}$$

With adult survival being the life history trait that in most cases is least affected by environmental changes, let the dynamics be regulated by changes in the birth rate

$$b_{a,t} = b^* i_{a,t} f(\hat{N}_t/\hat{N}^*) \tag{8}$$

and/or age of reproductive maturity

$$m_{a,t} = m^*/i_{a,t} f(\hat{N}_t/\hat{N}^*) \tag{9}$$

where b^* and m^* are the birth rate and age of reproductive maturity at the population dynamic equilibrium with no removals, $i_{a,t}$ is the average intrinsic component of the life history (for age-class a individuals in year t) as determined by density dependent natural selection (with $i^{**}_{a,t} = 1$ for all age-classes at the natural selection equilibrium $**$), and $f(\hat{N}_t/\hat{N}^*)$ is density regulation where $f(\hat{N}^*/\hat{N}^*) = 1$, with the one-plus abundance

$$\hat{N}_t = \sum_{a=1}^{x} N^f_t + N^m_t \tag{10}$$

being the component that imposes density regulation.

A.1 Exponential & density regulated growth

A model for exponential growth (given a stable age-structure) does not include the two regulation terms $i_{a,t}$ and $f(\hat{N}_t/\hat{N}^*)$. The birth rate $b_{a,t} = b$ and age of maturity $m_{a,t} = m$ are instead fixed at the same values for all age-classes and years. A density regulated model is another incomplete model, where $i_{a,t} = 1$ for all age-classes and years so that it does not include the selection induced changes in the life history. For this case, I assume a Pella-Tomlinson type of regulation

$$f(\hat{N}_t/\hat{N}^*) = 1 + [b_{max}/b^* - 1][1 - (\hat{N}_t/\hat{N}^*)^\gamma] \tag{11}$$

where the b_{max}/b^* ratio is the phenotypic span between maximal reproduction and reproduction at carrying capacity, and γ is the strength of regulation.

A non-evolving life history with an elastic phenotype that applies, not only to individuals, but also to the population average, is the basic fundament of density regulated growth. It implies that populations have an optimal/maximal growth rate r_{max} at zero density where $b = b_{max}$, and a carrying capacity $\hat{N}^*$ with a sub-optimal phenotype, where the average individuals are short in resources by a factor of b^*/b_{max}. Variation in the growth (and birth) rate is explained exclusively from variation in the environment (at least for large populations with negligible demographic variation), with the full range of phenotypic plasticity being controlled by density regulation [Eq. (11)]. A consequence of the latter, is the concept of optimal harvest with a maximum sustainable yield [msy where $\partial \text{sy}/\partial \hat{N} = 0$ with $\lambda = \hat{N}_t/\hat{N}_{t+1}$] at a specific abundance [$\hat{N}_{\text{msy}}$]; also known by the maximum sustainable yield rate ($\text{msyr} = \text{msy}/\hat{N}_{\text{msy}}$) and the maximum sustainable yield level ($\text{msyl} = \hat{N}_{\text{msy}}/\hat{N}^*$).

A.2 Selection-regulated dynamics

Selection-regulated dynamics is based on a population dynamic feed-back selection that balances two opposing forces of natural selection. The first is selection by the quality-quantity trade-off (Smith and Fretwell, 1974; Stearns, 1992), where e.g. a few large or many small offspring can be produced from the same amount of energy. This selects for increased replication by allocating energy to the demographic traits at the cost of competitive traits like body mass and complex interactive behaviour. The second is selection by interactive competition, where the competitively superior individuals (typically the larger individuals) can dominate the inferior during interactive encounters for limited resources. Yet, before the larger individuals can monopolise resources, there needs to be a certain population density where the individuals meet in interactive competition sufficiently often. This density dependence implies that the resource bias from interactive competition increases with increased population density, with the evolutionary equilibrium being defined by a density that is exactly so large that the resource bias in favour of the larger individuals is balanced against the quality-quantity trade-off, with the rate of replication being independent of mass.

A full description of population dynamic feed-back selection requires an individual based model so that the gradient of resources across the life history variants in the population can be quantified. Yet, for the population level equations of selection-regulated dynamics I use the population level response that Witting (2000a) solved from an underlying individual based model. This formulation combines a density regulation

$$f(\hat{N}_t/\hat{N}^*) = (\hat{N}_t/\hat{N}^*)^{-\gamma} \tag{12}$$

that is linear on log scale, with a similar selection response

$$i_{0,t+1} = \frac{\sum_{a=1}^{x} i_{a,t}\ \tilde{b}_a M_{a,t}^f}{\sum_{a=1}^{x} \tilde{b}_a M_{a,t}^f} \left(\frac{\hat{N}_t}{\hat{N}^*}\right)^{-\iota} \tag{13}$$

where the average intrinsic life history ($i_{0,t+1}$) of offspring born in year t is the weighted average of the intrinsic life histories ($i_{a,t}$) of all mothers, multiplied by the density dependent selection response $[(\hat{N}_t/\hat{N}^*)^{-\iota}]$, with ι being the strength of the response. Assuming that there is no change in the intrinsic life history of a cohort over time, we have that $i_{a+1,t+1} = i_{a,t}$ and

$$i_{x,t+1} = \frac{i_{x,t}(p_x^f N_{x,t}^f - c_{x,t}^f) + i_{x-1,t}(p_{x-1}^f N_{x-1,t}^f - c_{x-1,t}^f)}{N_{x,t+1}^f} \tag{14}$$

While the modelling of the dynamic changes in the intrinsic life history is a relatively small addition to the equation of population regulation [Eqs. (8) and (9)], the conceptual implications for population dynamics are huge (Witting, 2000a,b, 2002, 2013). We have already seen that the equilibrium abundance no longer is determined by density regulation, but by a population dynamic feed-back selection that balance the quality-quantity trade-off against the resource bias of interactive competition across the individuals in the

population. This implies, among others, that the average life history is selected to match the availability of resources at equilibrium, instead of being short in resources by a factor of b^*/b_{max}.

With the optimal life history referring to the ecological conditions at population equilibrium, the focus of the population dynamic formulation moves from the imaginary zero density to the naturally occurring density in an undisturbed population. Because density regulated growth is formulated from the fixpoint of a maximal growth rate (r_{max}; defined here by b_{max}) at zero density, a complete formulation is almost impossible because it requires that we have a full estimation of the density response from zero density to $\hat{N}^*$, while we usually observed densities only in a limited range.

With selection-regulated dynamics being formulated from the population dynamic equilibrium, the regulating equations are primarily intended to describe the behaviour in the surroundings of $\hat{N}^*$. There are no hard r_{max} and b_{max} in selection-regulated dynamics, although I do—for pragmatic reasons—allow for an upper and lower truncation of $i_{a,t}$. The growth rate and birth rate are not even parameters, but initial conditions that cannot be predicted from environmental conditions. Where a given environment has a single explicitly defined growth and birth rate under density regulated growth—for a given environment—the growth rate may take an infinite number of both positive and negative values under selection delayed dynamics. There is no maximum sustainable yield (Witting, 2002), and for given environmental conditions it is possible to predict only the acceleration or deacceleration of growth.

B Bayesian integration

The Bayesian integration between the model and the data is obtained by the sampling-importance-resampling routine (Jeffreys, 1961; Berger, 1985; Rubin, 1988), where n_s random parameterisations θ_i $(1 \leq i \leq n_1)$ are sampled from an importance function $h(\theta)$. This function is a probability distribution function from which a large number, n_s, of independent and identically distributed draws of θ can be taken. $h(\theta)$ shall generally be as close as possible to the posterior, however, the tails of $h(\theta)$ must be no thinner (less dense) than the tails of the posterior (Oh and Berger, 1992). For each drawn parameter set θ_i the population was projected from the first year with a harvest estimate to the present. For each draw an importance weight, or ratio, was then calculated

$$w(\theta_i) = \frac{L(\theta_i)p(\theta_i)}{h(\theta_i)} \tag{15}$$

where $L(\theta_i)$ is the likelihood given the data, and $h(\theta_i)$ and $p(\theta_i)$ are the importance and prior functions evaluated at θ_i. In the present study the importance function is set to the joint prior, so that the importance weight is given simply by the likelihood. The n_s parameter sets were then re-sampled n_r times with replacement, with the sampling probability of the ith parameter set being

$$q_i = \frac{w(\theta_i)}{\sum_{j=1}^{n_s} w(\theta_j)} \tag{16}$$

This generates a random sample of the posterior distribution of size n_r.

The log likelihood is given as a sum ($\ln L = \sum_i \ln L_i$) of the log likelihood of the different data components. The log likelihood of the ith set of the log normally distributed data is calculated as

$$\ln L_n = -\sum_t \frac{[\gamma_s \ln(\hat{x}_{i,t}/\beta_i x_t)]^2}{2\mathrm{cv}_{i,t}^2} + \ln \mathrm{cv}_{i,t} \tag{17}$$

where $\hat{x}_{i,t}$ is the point estimate of the data in year t, x_t the simulated estimate, $\beta_i \neq 1$ a potential bias, $\gamma_s \neq 1$ a potential skew, and $\mathrm{cv}_{i,t} = \sqrt{\hat{\mathrm{cv}}_{i,t}^2 + \sigma_i^2}$ the coefficient of variation, with $\hat{\mathrm{cv}}$ being the cv of the data and σ_i potential overdispersal (additional variance).

The log likelihood of the ith set of the binomially distributed data is calculated as

$$\ln L_n = -\sum_t \frac{(\hat{n}_{i,1,t}/\beta_i - \hat{n}_{i,t} p_{i,1,t})^2}{2\sigma_i^2 \hat{n}_{i,t} p_{i,1,t}(1-p_{i,1,t})} + \ln[\hat{n}_{i,t} p_{i,1,t}(1-p_{i,1,t})]/2 + \ln \sigma_i \tag{18}$$

where $\hat{n}_{i,t}$ is the total number of data observations in year t, $\hat{n}_{i,1,t}$ the number of positive observations, $p_{i,1,t}$ the simulated probability of a positive observation, β_i a potential bias, and σ_i potential overdispersal.

The log likelihood of the ith set of the multinomially distributed age data over $\mathbf{n_a}$ age (a) classes is given as

$$\ln L_n = -\sum_t \sum_{a \in \mathbf{n_a}} \frac{(\hat{n}_{i,a,t} - \hat{n}_{i,t} p_{i,a,t})^2}{2\sigma_i^2 \hat{n}_{i,t} p_{i,a,t}(1-p_{i,a,t})} + \ln[\hat{n}_{i,t} p_{i,a,t}(1-p_{i,a,t})]/2 + \ln \sigma_i \tag{19}$$

where $\hat{n}_{i,t}$ is the total number of aged individuals in year t, $\hat{n}_{i,a,t}$ the number of individuals in age class a, $p_{i,a,t}$ the simulated probability that an observed individual would be in age class a, β_i a potential bias, and σ_i potential overdispersal.

Year	C	Year	C	Year	C	Year	C	Year	C	Year	C	Year	C
1985	2622	1992	1652	1999	721	2006	901	2013	1419	2020	768	2027	1095
1986	1686	1993	888	2000	593	2007	920	2014	481	2021	959	2028	1095
1987	1530	1994	1281	2001	980	2008	182	2015	785	2022	842	2029	1095
1988	1818	1995	229	2002	665	2009	548	2016	494	2023	1070	2030	1095
1989	1340	1996	1600	2003	696	2010	1445	2017	1594	2024	713	2031	1095
1990	997	1997	1380	2004	1264	2011	1000	2018	1027	2025	1095		
1991	802	1998	1176	2005	644	2012	1147	2019	942	2026	1095		

Table 8: **Catch history** for Data model (p), Data model (i), Data model (n), Data model (z), Data model (x), and Data model (u). From Mikkelsen et al. (2025).

Year	C	Year	C	Year	C	Year	C	Year	C	Year	C	Year	C
1985	2622	1992	1652	1999	721	2006	901	2013	1419	2020	792	2027	1108
1986	1686	1993	888	2000	593	2007	924	2014	481	2021	974	2028	1108
1987	1530	1994	1281	2001	980	2008	182	2015	786	2022	849	2029	1108
1988	1818	1995	229	2002	668	2009	548	2016	499	2023	1081	2030	1108
1989	1340	1996	1600	2003	698	2010	1445	2017	1607	2024	722	2031	1108
1990	997	1997	1380	2004	1266	2011	1001	2018	1054	2025	1108		
1991	802	1998	1176	2005	644	2012	1148	2019	973	2026	1108		

Table 9: **Catch history** for Data model (h). From Mikkelsen et al. (2025).

Par	N_0	p	p_{0k}	p_{0m}	b_k	b_m	m_k	m_l	m_{0k}	m_{0l}
N_0	1.00	-0.75	-0.01	-0.05	-0.04	-0.06	-0.03	-0.04	-0.05	-0.03
p	-0.75	1.00	-0.09	-0.39	0.01	-0.15	0.10	0.16	0.02	0.08
p_{0k}	-0.01	-0.09	1.00	0.06	-0.32	0.07	0.07	0.07	-0.01	-0.06
p_{0m}	-0.05	-0.39	0.06	1.00	-0.01	0.05	-0.08	0.05	0.01	-0.06
b_k	-0.04	0.01	-0.32	-0.01	1.00	0.01	0.13	0.02	0.02	0.01
b_m	-0.06	-0.15	0.07	0.05	0.01	1.00	0.01	0.01	0.04	-0.01
m_k	-0.03	0.10	0.07	-0.08	0.13	0.01	1.00	0	0.10	-0.03
m_l	-0.04	0.16	0.07	0.05	0.02	0.01	0	1.00	0.01	-0.08
m_{0k}	-0.05	0.02	-0.01	0.01	0.02	0.04	0.10	0.01	1.00	-0.04
m_{0l}	-0.03	0.08	-0.06	-0.06	0.01	-0.01	-0.03	-0.08	-0.04	1.00

Table 10: **Correlation matrix** for the posterior parameter estimates of Data model (p).

Par	N_0	p	p_{0k}	p_{0m}	b_k	b_m	m_k	m_l	m_{0k}	m_{0l}
N_0	1.00	-0.79	-0.03	-0.15	-0.06	-0.09	0.04	0.05	0.02	-0.02
p	-0.79	1.00	-0.06	-0.24	0.04	-0.01	-0.02	0.13	-0.01	0.06
p_{0k}	-0.03	-0.06	1.00	0.03	-0.36	0	0.15	-0.03	0.08	0.01
p_{0m}	-0.15	-0.24	0.03	1.00	0	-0.02	0.03	0.04	0.01	-0.08
b_k	-0.06	0.04	-0.36	0	1.00	-0.02	0.10	0.03	0.05	0.05
b_m	-0.09	-0.01	0	-0.02	-0.02	1.00	0.03	0.02	0.02	0.03
m_k	0.04	-0.02	0.15	0.03	0.10	0.03	1.00	-0.01	0.12	0.04
m_l	0.05	0.13	-0.03	0.04	0.03	0.02	-0.01	1.00	0.02	-0.01
m_{0k}	0.02	-0.01	0.08	0.01	0.05	0.02	0.12	0.02	1.00	0.06
m_{0l}	-0.02	0.06	0.01	-0.08	0.05	0.03	0.04	-0.01	0.06	1.00

Table 11: **Correlation matrix** for the posterior parameter estimates of Data model (i).

Par	N_0	p	p_{0k}	p_{0m}	b_k	b_m	m_k	m_l	m_{0k}	m_{0l}
N_0	1.00	-0.70	0.13	-0.22	-0.03	-0.03	0.05	0.10	0.03	0.02
p	-0.70	1.00	-0.18	-0.26	-0.03	-0.07	-0.05	0.10	-0.04	0.03
p_{0k}	0.13	-0.18	1.00	-0.03	-0.34	0.04	0.13	-0.04	0.09	0.01
p_{0m}	-0.22	-0.26	-0.03	1.00	0.04	-0.05	-0.04	0.05	0.02	-0.12
b_k	-0.03	-0.03	-0.34	0.04	1.00	-0.08	0.11	-0.06	-0.03	-0.02
b_m	-0.03	-0.07	0.04	-0.05	-0.08	1.00	0.01	0.03	-0.03	-0.08
m_k	0.05	-0.05	0.13	-0.04	0.11	0.01	1.00	-0.02	0.07	-0.01
m_l	0.10	0.10	-0.04	0.05	-0.06	0.03	-0.02	1.00	0	-0.13
m_{0k}	0.03	-0.04	0.09	0.02	-0.03	-0.03	0.07	0	1.00	0.02
m_{0l}	0.02	0.03	0.01	-0.12	-0.02	-0.08	-0.01	-0.13	0.02	1.00

Table 12: **Correlation matrix** for the posterior parameter estimates of Data model (n).

Par	N_0	p	p_{0k}	p_{0m}	b_k	b_m	m_k	m_l	m_{0k}	m_{0l}
N_0	1.00	-0.58	-0.05	-0.33	0.01	-0.09	0.01	0.15	-0.03	0
p	-0.58	1.00	0.01	-0.21	-0.06	-0.05	0.01	0.14	0.05	0.02
p_{0k}	-0.05	0.01	1.00	-0.02	-0.36	0.09	0.13	0.04	-0.01	-0.04
p_{0m}	-0.33	-0.21	-0.02	1.00	-0.03	-0.02	-0.02	-0.01	-0.01	0.04
b_k	0.01	-0.06	-0.36	-0.03	1.00	0.01	0.09	-0.04	0.01	-0.03
b_m	-0.09	-0.05	0.09	-0.02	0.01	1.00	-0.04	-0.04	0	-0.01
m_k	0.01	0.01	0.13	-0.02	0.09	-0.04	1.00	0	0.03	-0.01
m_l	0.15	0.14	0.04	-0.01	-0.04	-0.04	0	1.00	0.06	-0.06
m_{0k}	-0.03	0.05	-0.01	-0.01	0.01	0	0.03	0.06	1.00	0.02
m_{0l}	0	0.02	-0.04	0.04	-0.03	-0.01	-0.01	-0.06	0.02	1.00

Table 13: **Correlation matrix** for the posterior parameter estimates of Data model (z).

Par	N_0	p	p_{0k}	p_{0m}	b_k	b_m	m_k	m_l	m_{0k}	m_{0l}
N_0	1.00	-0.63	-0.11	-0.29	0.01	-0.02	0.02	0.11	0.01	-0.08
p	-0.63	1.00	-0.02	-0.16	0	-0.11	0.03	0.05	-0.03	0.06
p_{0k}	-0.11	-0.02	1.00	-0.06	-0.15	0.06	0.10	-0.02	0.01	0.06
p_{0m}	-0.29	-0.16	-0.06	1.00	-0.06	-0.01	0.01	0.05	0.01	0.04
b_k	0.01	0	-0.15	-0.06	1.00	-0.01	0.07	0.09	0.01	-0.03
b_m	-0.02	-0.11	0.06	-0.01	-0.01	1.00	0.04	0.03	-0.04	-0.03
m_k	0.02	0.03	0.10	0.01	0.07	0.04	1.00	0.02	0.08	0.02
m_l	0.11	0.05	-0.02	0.05	0.09	0.03	0.02	1.00	0.03	-0.04
m_{0k}	0.01	-0.03	0.01	0.01	0.01	-0.04	0.08	0.03	1.00	0.03
m_{0l}	-0.08	0.06	0.06	0.04	-0.03	-0.03	0.02	-0.04	0.03	1.00

Table 14: **Correlation matrix** for the posterior parameter estimates of Data model (x).

Par	N_0	p	p_{0k}	p_{0m}	b_k	b_m	m_k	m_l	m_{0k}	m_{0l}
N_0	1.00	-0.61	-0.03	-0.30	0.01	-0.13	0.05	0.02	-0.08	-0.02
p	-0.61	1.00	-0.05	-0.21	-0.01	0	-0.02	0.17	0.06	-0.04
p_{0k}	-0.03	-0.05	1.00	-0.04	-0.41	0.06	0.16	-0.01	0.01	0.11
p_{0m}	-0.30	-0.21	-0.04	1.00	-0.01	-0.04	-0.06	0	0.05	0.06
b_k	0.01	-0.01	-0.41	-0.01	1.00	-0.03	0.19	-0.02	-0.01	-0.11
b_m	-0.13	0	0.06	-0.04	-0.03	1.00	0.08	0.05	0.04	-0.03
m_k	0.05	-0.02	0.16	-0.06	0.19	0.08	1.00	-0.03	0.15	0.04
m_l	0.02	0.17	-0.01	0	-0.02	0.05	-0.03	1.00	0.02	-0.08
m_{0k}	-0.08	0.06	0.01	0.05	-0.01	0.04	0.15	0.02	1.00	0.02
m_{0l}	-0.02	-0.04	0.11	0.06	-0.11	-0.03	0.04	-0.08	0.02	1.00

Table 15: **Correlation matrix** for the posterior parameter estimates of Data model (u).

Par	N_0	p	p_{0k}	p_{0m}	b_k	b_m	m_k	m_l	m_{0k}	m_{0l}
N_0	1.00	-0.60	-0.02	-0.31	0.02	-0.11	0.08	0.06	0.04	0.01
p	-0.60	1.00	-0.05	-0.18	-0.05	-0.06	-0.05	0.10	-0.01	-0.03
p_{0k}	-0.02	-0.05	1.00	-0.02	-0.35	-0.03	0.18	-0.03	0.03	0.07
p_{0m}	-0.31	-0.18	-0.02	1.00	0.01	-0.03	-0.03	0.05	-0.04	-0.04
b_k	0.02	-0.05	-0.35	0.01	1.00	0.01	0.09	0.10	-0.02	0.07
b_m	-0.11	-0.06	-0.03	-0.03	0.01	1.00	-0.07	0.02	-0.02	0.02
m_k	0.08	-0.05	0.18	-0.03	0.09	-0.07	1.00	0.03	0.11	0.10
m_l	0.06	0.10	-0.03	0.05	0.10	0.02	0.03	1.00	-0.04	-0.11
m_{0k}	0.04	-0.01	0.03	-0.04	-0.02	-0.02	0.11	-0.04	1.00	0.06
m_{0l}	0.01	-0.03	0.07	-0.04	0.07	0.02	0.10	-0.11	0.06	1.00

Table 16: **Correlation matrix** for the posterior parameter estimates of Data model (h).

References

Berger, J. O. 1985. Statistical decision theory and Bayesian analysis. Second edn. Springer-Verlag, New York.

Jeffreys, H. 1961. Theory of probability. 3rd edition edn. Clarendon Press, Oxford.

Mikkelsen, B. 2025. Age, growth, and reproduction of long-finned pilot whales in the Faroe Islands. NAMMCO/SC/PWWG/2025-01/10, .

Mikkelsen, B., Ofstad, L. H., and Akralid, R. 2025. Catch history of long-finned pilot whales in the Faroe Islands. NAMMCO/SC/PWWG/2025-01/08, .

NAMMCO 2025. Table of accepted abundance estimates. https://nammco.no/abundance-estimates/, .

Oh, M. S. and Berger, J. O. 1992. Adaptive importance sampling in Monte Carlo integration. Journal of Statistics and Computer Simulation, 41: 143–168.

Rubin, D. B. 1988. Using the SIR algorithm to simulate posterior distributions. In Bayesian Statistics 3: Proceedings of the Third Valencia International Meeting, 1–5 June 1987, pp. 395–402. Ed. by, J. M. Bernardo, M. H. DeGroot, D. V. Lindley, and A. M. Smith. Clarendon Press, Oxford.

Smith, C. C. and Fretwell, S. D. 1974. The optimal balance between size and number of offspring. The American Naturalist, 108: 499–506.

Stearns, S. C. 1992. The evolution of life histories. Oxford University Press, Oxford.

Witting, L. 2000a. Interference competition set limits to the fundamental theorem of natural selection. Acta Biotheoretica, 48: 107–120, https://doi.org/10.1023/A:1002788313345.

Witting, L. 2000b. Population cycles caused by selection by density dependent competitive interactions. Bulletin of Mathematical Biology, 62: 1109–1136, https://doi.org/10.1006/bulm.2000.0200.

Witting, L. 2002. Evolutionary dynamics of exploited populations selected by density dependent competitive interactions. Ecological Modelling, 157: 51–68, https://doi.org/10.1016/S0304–3800(02)00172–2.

Witting, L. 2013. Selection-delayed population dynamics in baleen whales and beyond. Population Ecology, 55: 377–401, https://dx.doi.org/10.1007/s10144–013–0370–9.

NAMMCO 2025 SC/PWWG/2025-01/7c

Density regulated models for long-finned pilot whales in the North Atlantic

Lars Witting

November 26, 2025

This working paper constructs two density regulated models for long-finned pilot whales in the North Atlantic, using the data and likelihood scaling setup of the exponential model z.

The main purpose of this is to show that the historical hunts on the Faroese Islands and in Greenland have in no way depleted the population, yet the paper does not include other removals in the North Atlantic.

The paper includes a long forward projection from a pre-exploited population dynamic equilibrium abundance around year 1700, and a model that is initiated in the 1980s attempting to provide an estimate of the current equilibrium abundance.

The two models are:

Data model (dB) Projection from assumed pre-exploitation population dynamic equilibrium in year 1708.

Data model (dE) Short-term density regulated model.

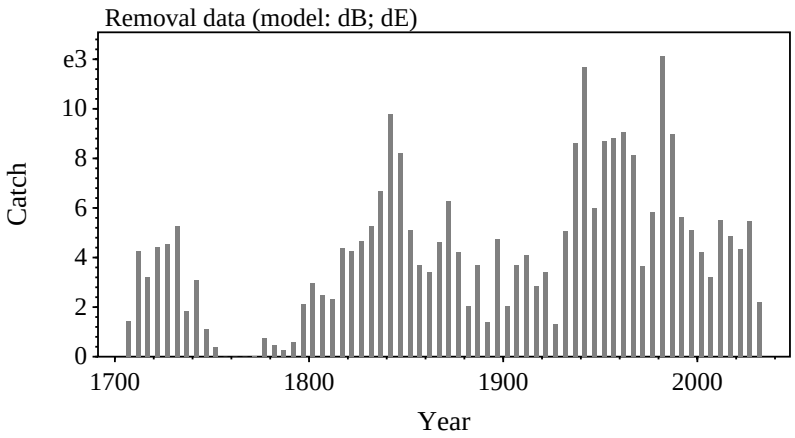

Figure 1: Historical removals in 5 year bins. Data from Mikkelsen et al. (2025).

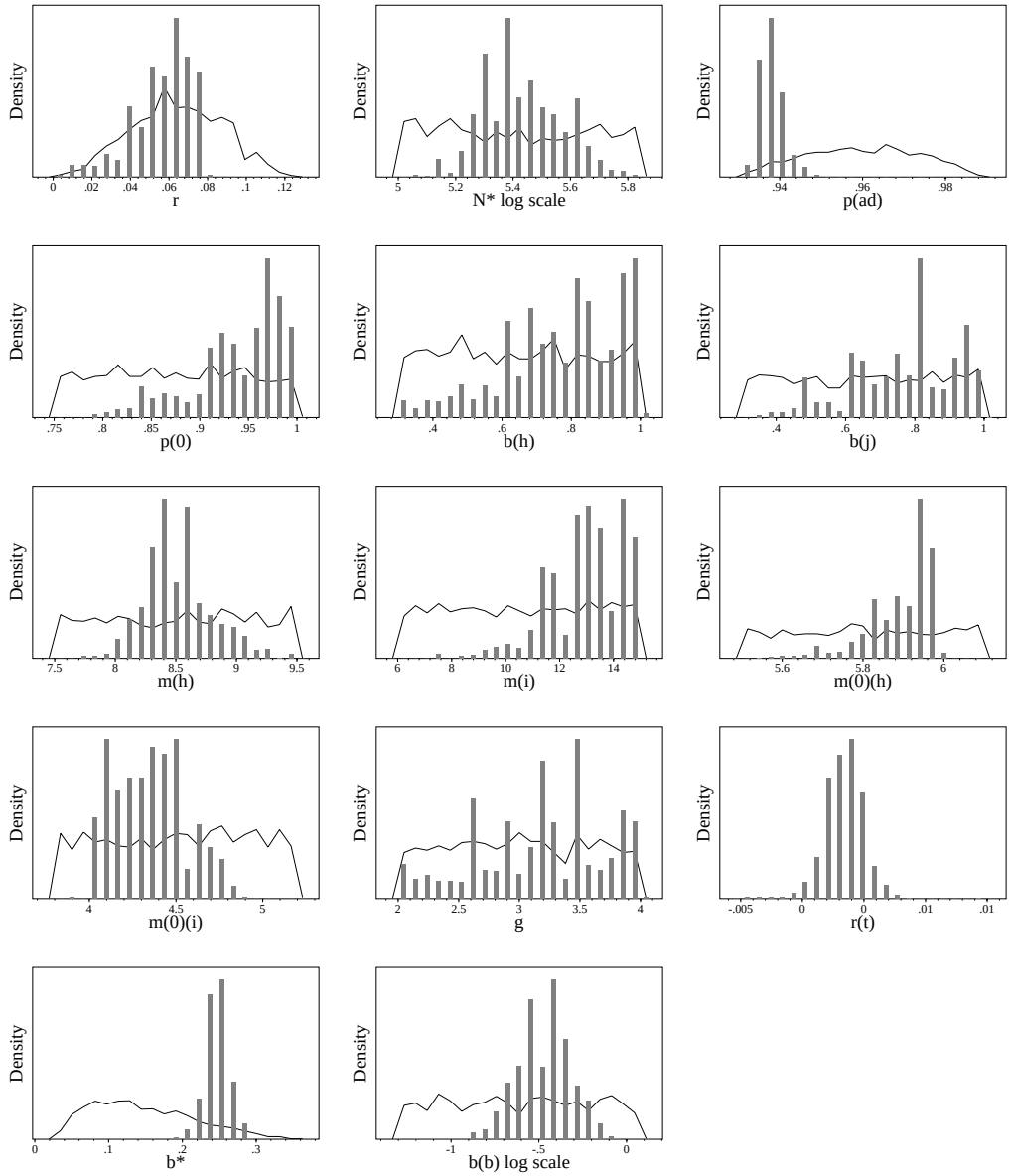

Figure 2: Realised prior (curve) and posterior (bars) distributions for Data model (dB).

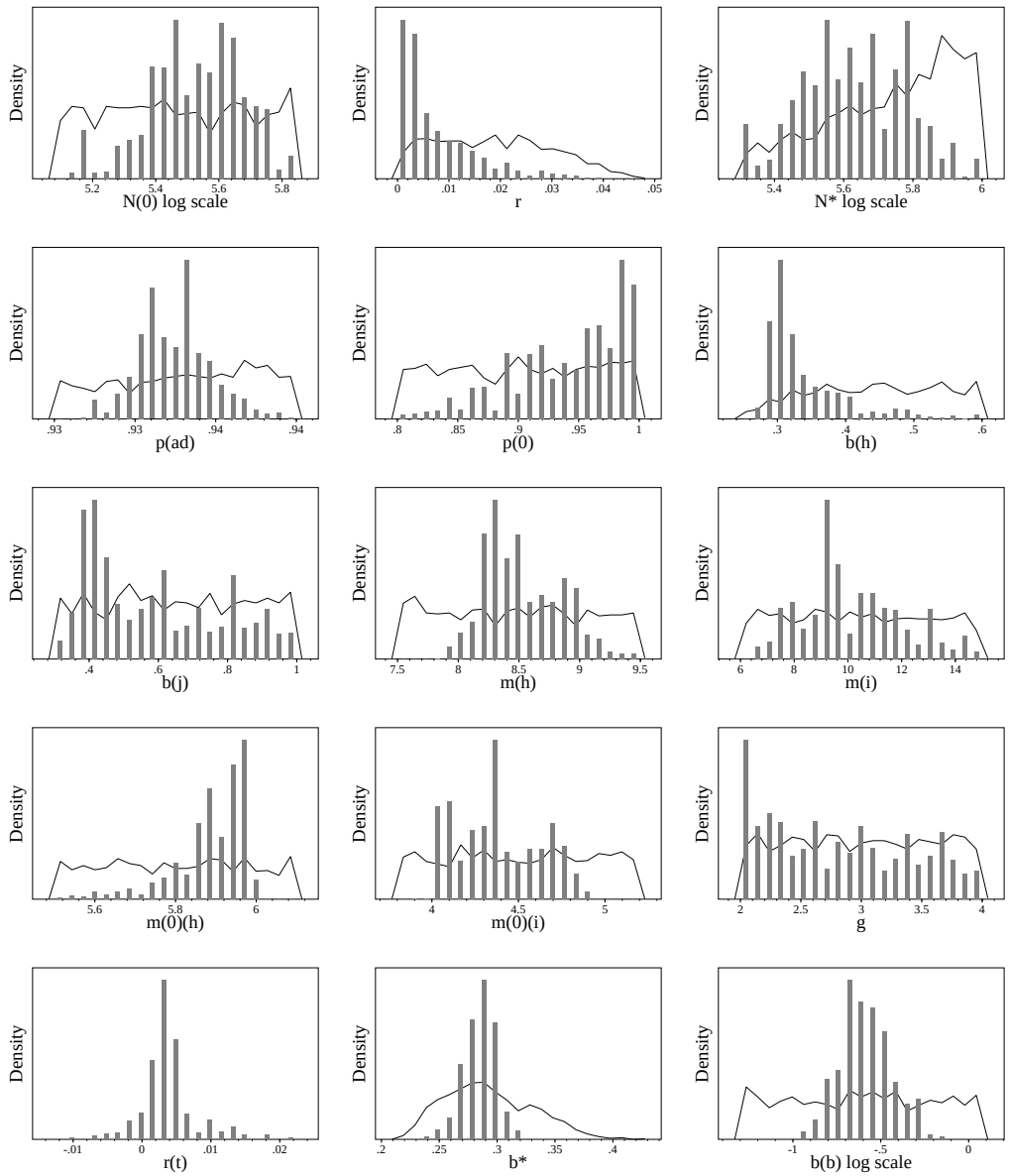

Figure 3: Realised prior (curve) and posterior (bars) distributions for Data model (dE).

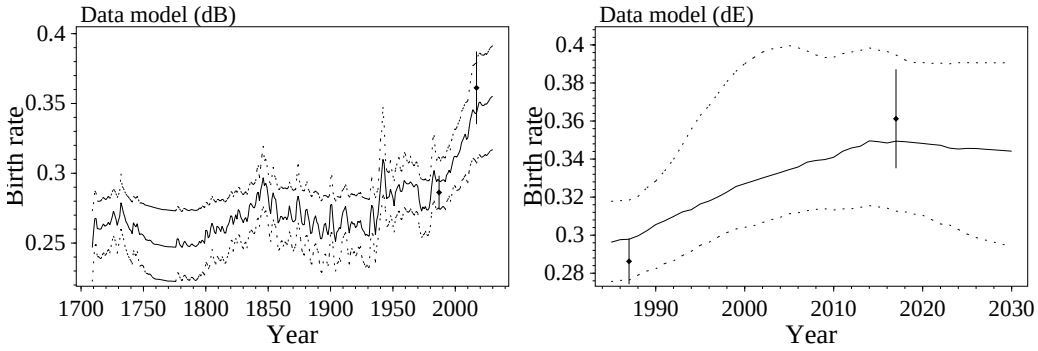

Figure 4: Projected medians and 90% credibility intervals for birth rate. Data from Garde and Heide-Jørgensen (2019).

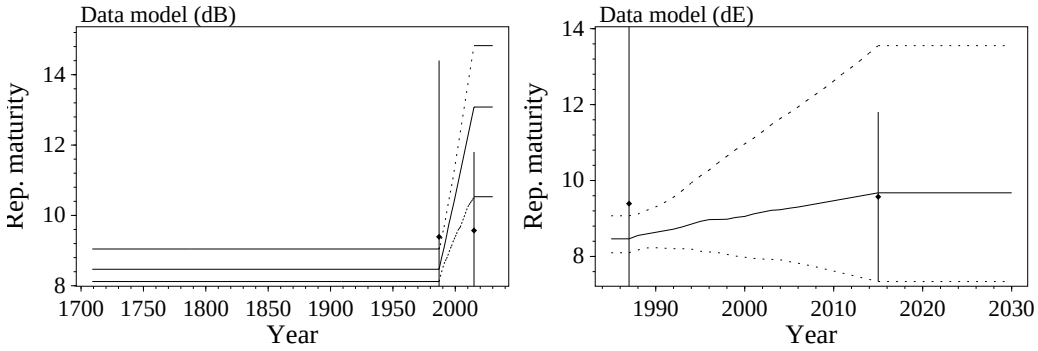

Figure 5: Projected medians and 90% credibility intervals for rep. maturity. Data from Mikkelsen (2025).

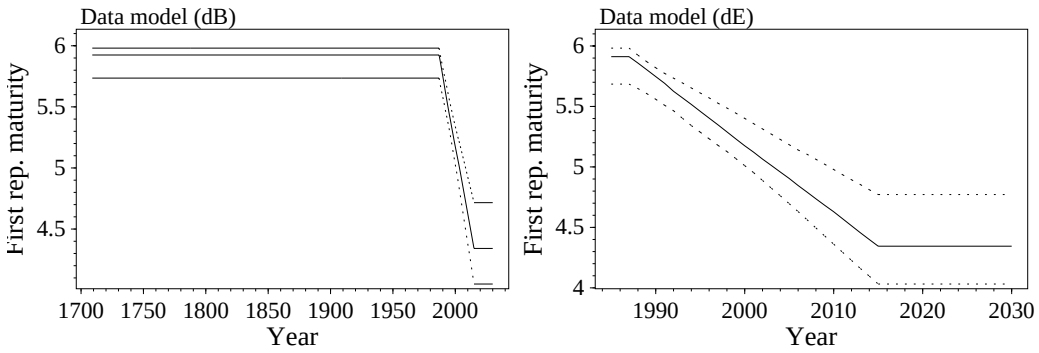

Figure 6: Projected medians and 90% credibility intervals for first rep. maturity.

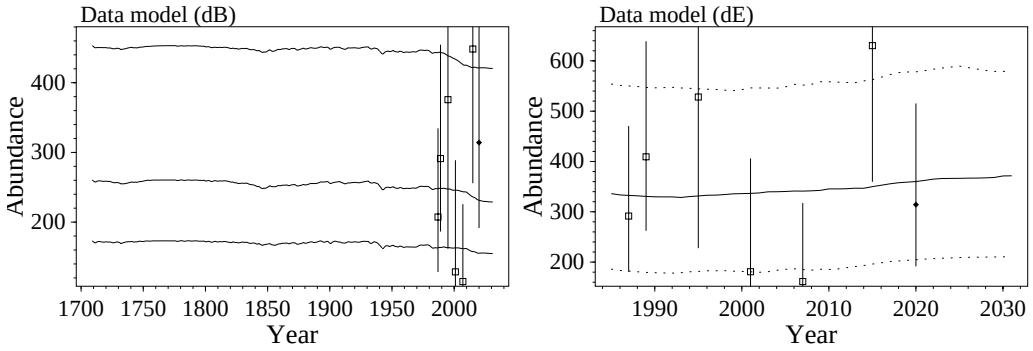

Figure 7: Projected medians and 90% credibility intervals for abundance. Data from NAMMCO (2025).

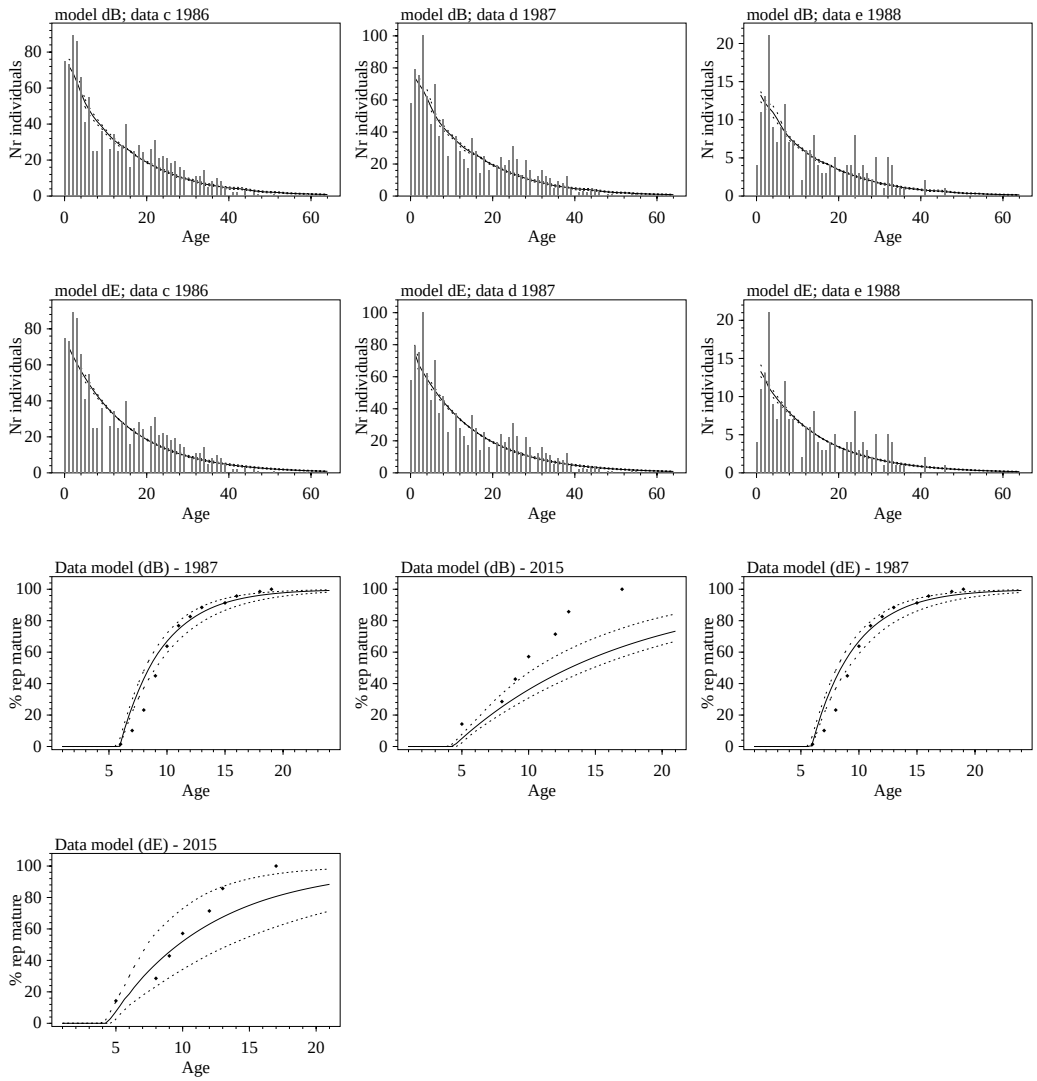

Figure 8: Model fits for age-structure and reproductive maturity. Data given by bars and dots, and models by the median estimate (solid curve) and 90% credibility interval (dashed curves). Data from Mikkelsen (2025).

	a	b	c	d	e	f	g
dB	*	*	*	*	*	*	*
dE	*	*	*	*	*	*	*
1986	-	-	12.4^{17}_{1097}	-	-	-	-
1987	-	73100^{29}	-	12.7^{17}_{1121}	-	0.29^{314}_{1097}	9.39^{32}_{69}
1988	-	-	-	-	12.9^{18}_{193}	-	-
1989	-	103000^{27}	-	-	-	-	-
1995	-	132000^{51}	-	-	-	-	-
2001	-	45400^{49}	-	-	-	-	-
2007	-	40500^{41}	-	-	-	-	-
2015	-	158000^{34}	-	-	-	-	9.57^{14}_{7}
2017	-	-	-	-	-	0.36^{121}_{335}	-
2020	314000^{30}	-	-	-	-	-	-

Table 1: **Data for likelihood functions.** Their use by models are marked by *. a: Abundance with log normal likelihood [n(1+); $\bar{x}^{cv\%}$]. b: Abundance with log normal likelihood [n(1+); relative; $\bar{x}^{cv\%}$]. c: Age structure with multinomial likelihood [population; $\bar{x}_n^{cv\%}$]. d: Age structure with multinomial likelihood [population; $\bar{x}_n^{cv\%}$]. e: Age structure with multinomial likelihood [population; $\bar{x}_n^{cv\%}$]. f: Birth rate with binomial likelihood [$\bar{x}^{n_1}_{n_0+n_1}$]. g: Age of first reproduction with multinomial likelihood [$\bar{x}_n^{cv\%}$]. Data from Garde and Heide-Jørgensen (2019), Mikkelsen (2025), and NAMMCO (2025).

M	N_0	N^*	b_h	b_j	ϑ	γ	m_{0h}	m_{0i}	m_h	m_i	p_0	p
dB	-	$100;700^U$	$.3;1^u$	$.3;1^u$	$.5^p$	$2;4^u$	$5.5;6.1^u$	$3.8;5.2^u$	$7.5;9.5^u$	$6;15^u$	$.75;1^u$	$^{2;2^b}_{.93;.99}$
dE	$120;700^U$	$200;1000^U$	$.1;.6^u$	$.3;1^u$	$.5^p$	$2;4^u$	$5.5;6.1^u$	$3.8;5.2^u$	$7.5;9.5^u$	$6;15^u$	$.8;1^u$	$.93;.94^u$

Table 2: **Priors for the model parameters** of the different models (M). N the abundance, b the birth rate, ϑ the female fraction at birth, γ the density regulation, m_0 the first rep. maturity, m the rep. maturity, p_0 the first year survival, p the yearly survival, and $*$ denotes population dynamic equilibrium. Year by subscript: 0:initial, h:1987, i:2015, and j:2017. Abundance is given in thousands. The prior probability distribution is given by superscripts; p: fixed value, u: uniform (min;max), U: log uniform (min;max), and b: beta $\binom{a;b}{i;x}$ with i=min and x=max.

M	β_b
dB	.05;1.2^U
dE	.05;1.2^U

Table 3: **Priors for the data parameters** of the different models (M). β_i the abundance estimate bias (i: data reference). The prior probability distribution is given by superscripts; U: log uniform (min;max).

M	n_S	n_R	unique	max
dB	1000	1	317	72
dE	500	1	380	41

Table 4: **Sampling statistics** for the different models (M). The number of parameter sets in the sample (n_S) and the resample (n_R), the number of unique parameter sets in the resample, and the maximum number of occurrences of a unique parameter set in the resample. n_S and n_R are given in thousands.

M		N_0	N_t	N^*	b_h	b_j	b^*	d_t	γ	m_{0h}	m_{0i}	m_h	m_i	p_0	p	r	r_t
	$x_{.5}$	-	230	260	.81	.813	.247	.93	3.23	5.92	4.34	8.47	13.1	.953	.938	.059	.003
	$x_{.05}$	-	156	173	.446	.488	.222	.856	2.2	5.74	4.05	8.12	10.5	.84	.934	.025	.001
dB	$x_{.95}$	-	421	453	.975	.973	.273	.963	3.93	5.98	4.72	9.05	14.8	.993	.944	.073	.005
	$x_{.5}$	336	366	422	.317	.554	.286	.891	2.77	5.91	4.34	8.46	9.68	.954	.933	.004	.003
	$x_{.05}$	186	209	245	.288	.363	.262	.519	2.02	5.68	4.03	8.1	7.34	.853	.929	0	-.00236
dE	$x_{.95}$	554	590	728	.471	.925	.306	.988	3.79	5.98	4.77	9.07	13.6	.997	.936	.023	.012

Table 5: **Model parameter estimates** for the different models (M). Estimates are given by the median ($x_{.5}$) and the 90% credibility interval ($x_{.05}$ - $x_{.95}$) of the posterior distributions. N the abundance, b the birth rate, d the depletion ratio, γ the density regulation, m_0 the first rep. maturity, m the rep. maturity, p_0 the first year survival, p the yearly survival, r the exp. growth rate (no removal, max or realised), and $*$ denotes population dynamic equilibrium. Year by subscript: 0:initial, h:1987, i:2015, j:2017, and t:2025. Abundance is given in thousands.

M		β_b
	$x_{.5}$	.353
	$x_{.05}$	.187
dB	$x_{.95}$	.595
	$x_{.5}$	.251
	$x_{.05}$	.15
dE	$x_{.95}$	.491

Table 6: **Data parameter estimates** for the different models (M). Estimates are given by the median ($x_{.5}$) and the 90% credibility interval ($x_{.05}$ - $x_{.95}$) of the posterior distributions. β_i the abundance estimate bias (i: data reference).

Appendix

A Population dynamic model

The population model is an age-structured Bayesian assessments model that is programmed in C++, and which is easily programmed by input files to deal with different species, populations, and situations. Based on the input programming, the model will simulate unregulated exponential growth, density regulated growth, or selection regulated dynamics which is a density regulated population with superimposed selection regulation.

The population dynamic model is structured by gender and age, with x being the maximum lumped age-class. Let the number $N^{m/f}_{a,t+1}$ of males (m) and females (f) in age-classes $0 < a < x$ in year $t+1$ be

$$N^{m/f}_{a+1,t+1} = p^{m/f}_a N^{m/f}_{a,t} - c^{m/f}_{a,t} \tag{1}$$

and the number of animals in age-class x be

$$N^{m/f}_{x,t+1} = p^{m/f}_x N^{m/f}_{x,t} + p^{m/f}_{x-1} N^{m/f}_{x-1,t} - c^{m/f}_{x,t} - c^{m/f}_{x-1,t} \tag{2}$$

where $p^{m/f}_a$ is the age specific survival rate of males/females, and $c^{m/f}_{a,t}$ is the age specific catch of males/females in year t. The age and gender (g) dependent survival rates $p^g_a = p\tilde{p}^g_a$ are given as a product between a survival scalar p and relative ($0 < \tilde{p}^g_a \leq 1$) survival rates. The age and gender specific catches $c^{m/f}_{a,t} = c^{m/f}_t \tilde{c}^{m/f}_{a,t}$ in year t are given as a product between the total catch of males/females ($c^{m/f}_t$), as specified by the catch history, and an age-specific catch selectivity ($\tilde{c}^{m/f}_{a,t}$). The age-specific catch selectivity is listed in Table **??**.

The number of females and males in age-class zero is $N^f_{0,t} = \vartheta N_{0,t}$ and $N^m_{0,t} = (1-\vartheta)N_{0,t}$, where ϑ is the fraction of females at birth, and

$$N_{0,t} = \sum_{a=0}^{x} B_{a,t} \tag{3}$$

where $B_{a,t}$ is the number of births from females in age class a, defined as

$$B_{a,t} = b_{a,t}\, \tilde{b}_a\, M^f_{a,t} \tag{4}$$

where $b_{a,t}$ is the birth rate in year t for age-class a females should they be at their age-specific reproductive peak, $0 < \tilde{b}_a \leq 1$ are the relative age-specific birth rates, and $M^f_{a,t}$ is the number of mature females in age-class a in year t, defined as

$$M^f_{a,t} = \begin{cases} 0 & \text{if } a < m_{0,a,t} \\ \tilde{m}_{a,t} N^f_{a,t} & \text{if } a \geq m_{0,a,t} \end{cases} \tag{5}$$

where

$$\tilde{m}_{a,t} = 1 - e^{-\frac{a - m_{0,a,t}}{m_{a,t} - m_{0,a,t}} \ln 2} \tag{6}$$

is the fraction of females in age-class a in year t that is mature, with $m_{0,a,t}$ being the earliest, and $m_{a,t}$ the median, age of reproductive maturity for females of age a in year t.

Knife-edge maturation, where all females older than m_0 are mature, occurs when $m_0 = m$. Yet, for model versions with knife-edge maturity, the number of mature females is

$$M^f_{a,t} = \min[1, \max(0, a + 1 - m_{a,t})]N^f_{a,t} \tag{7}$$

With adult survival being the life history trait that in most cases is least affected by environmental changes, let the dynamics be regulated by changes in the birth rate

$$b_{a,t} = b^* i_{a,t} f(\hat{N}_t/\hat{N}^*) \tag{8}$$

and/or age of reproductive maturity

$$m_{a,t} = m^*/i_{a,t} f(\hat{N}_t/\hat{N}^*) \tag{9}$$

where b^* and m^* are the birth rate and age of reproductive maturity at the population dynamic equilibrium with no removals, $i_{a,t}$ is the average intrinsic component of the life history (for age-class a individuals in year t) as determined by density dependent natural selection (with $i^{**}_{a,t} = 1$ for all age-classes at the natural selection equilibrium $**$), and $f(\hat{N}_t/\hat{N}^*)$ is density regulation where $f(\hat{N}^*/\hat{N}^*) = 1$, with the one-plus abundance

$$\hat{N}_t = \sum_{a=1}^{x} N^f_t + N^m_t \tag{10}$$

being the component that imposes density regulation.

A.1 Exponential & density regulated growth

A model for exponential growth (given a stable age-structure) does not include the two regulation terms $i_{a,t}$ and $f(\hat{N}_t/\hat{N}^*)$. The birth rate $b_{a,t} = b$ and age of maturity $m_{a,t} = m$ are instead fixed at the same values for all age-classes and years. A density regulated model is another incomplete model, where $i_{a,t} = 1$ for all age-classes and years so that it does not include the selection induced changes in the life history. For this case, I assume a Pella-Tomlinson type of regulation

$$f(\hat{N}_t/\hat{N}^*) = 1 + [b_{max}/b^* - 1][1 - (\hat{N}_t/\hat{N}^*)^\gamma] \tag{11}$$

where the b_{max}/b^* ratio is the phenotypic span between maximal reproduction and reproduction at carrying capacity, and γ is the strength of regulation.

A non-evolving life history with an elastic phenotype that applies, not only to individuals, but also to the population average, is the basic fundament of density regulated growth. It implies that populations have an optimal/maximal growth rate r_{max} at zero density where $b = b_{max}$, and a carrying capacity $\hat{N}^*$ with a sub-optimal phenotype, where the average individuals are short in resources by a factor of b^*/b_{max}. Variation in the growth (and birth) rate is explained exclusively from variation in the environment (at least for large populations with negligible demographic variation), with the full range of phenotypic plasticity being controlled by density regulation [Eq. (11)]. A consequence of the latter, is the concept of optimal harvest with a maximum sustainable yield [msy where $\partial \text{sy}/\partial \hat{N} = 0$ with $\lambda = \hat{N}_t/\hat{N}_{t+1}$] at a specific abundance [$\hat{N}_{\text{msy}}$]; also known by the maximum sustainable yield rate ($\text{msyr} = \text{msy}/\hat{N}_{\text{msy}}$) and the maximum sustainable yield level ($\text{msyl} = \hat{N}_{\text{msy}}/\hat{N}^*$).

A.2 Selection-regulated dynamics

Selection-regulated dynamics is based on a population dynamic feed-back selection that balances two opposing forces of natural selection. The first is selection by the quality-quantity trade-off (Smith and Fretwell, 1974; Stearns, 1992), where e.g. a few large or many small offspring can be produced from the same amount of energy. This selects for increased replication by allocating energy to the demographic traits at the cost of competitive traits like body mass and complex interactive behaviour. The second is selection by interactive competition, where the competitively superior individuals (typically the larger individuals) can dominate the inferior during interactive encounters for limited resources. Yet, before the larger individuals can monopolise resources, there needs to be a certain population density where the individuals meet in interactive competition sufficiently often. This density dependence implies that the resource bias from interactive competition increases with increased population density, with the evolutionary equilibrium being defined by a density that is exactly so large that the resource bias in favour of the larger individuals is balanced against the quality-quantity trade-off, with the rate of replication being independent of mass.

A full description of population dynamic feed-back selection requires an individual based model so that the gradient of resources across the life history variants in the population can be quantified. Yet, for the population level equations of selection-regulated dynamics I use the population level response that Witting (2000a) solved from an underlying individual based model. This formulation combines a density regulation

$$f(\hat{N}_t/\hat{N}^*) = (\hat{N}_t/\hat{N}^*)^{-\gamma} \tag{12}$$

that is linear on log scale, with a similar selection response

$$i_{0,t+1} = \frac{\sum_{a=1}^{x} i_{a,t}\ \tilde{b}_a M_{a,t}^f}{\sum_{a=1}^{x} \tilde{b}_a M_{a,t}^f} \left(\frac{\hat{N}_t}{\hat{N}^*}\right)^{-\iota} \tag{13}$$

where the average intrinsic life history ($i_{0,t+1}$) of offspring born in year t is the weighted average of the intrinsic life histories ($i_{a,t}$) of all mothers, multiplied by the density dependent selection response $[(\hat{N}_t/\hat{N}^*)^{-\iota}]$, with ι being the strength of the response. Assuming that there is no change in the intrinsic life history of a cohort over time, we have that $i_{a+1,t+1} = i_{a,t}$ and

$$i_{x,t+1} = \frac{i_{x,t}(p_x^f N_{x,t}^f - c_{x,t}^f) + i_{x-1,t}(p_{x-1}^f N_{x-1,t}^f - c_{x-1,t}^f)}{N_{x,t+1}^f} \tag{14}$$

While the modelling of the dynamic changes in the intrinsic life history is a relatively small addition to the equation of population regulation [Eqs. (8) and (9)], the conceptual implications for population dynamics are huge (Witting, 2000a,b, 2002, 2013). We have already seen that the equilibrium abundance no longer is determined by density regulation, but by a population dynamic feed-back selection that balance the quality-quantity trade-off against the resource bias of interactive competition across the individuals in the

population. This implies, among others, that the average life history is selected to match the availability of resources at equilibrium, instead of being short in resources by a factor of b^*/b_{max}.

With the optimal life history referring to the ecological conditions at population equilibrium, the focus of the population dynamic formulation moves from the imaginary zero density to the naturally occurring density in an undisturbed population. Because density regulated growth is formulated from the fixpoint of a maximal growth rate (r_{max}; defined here by b_{max}) at zero density, a complete formulation is almost impossible because it requires that we have a full estimation of the density response from zero density to $\hat{N}^*$, while we usually observed densities only in a limited range.

With selection-regulated dynamics being formulated from the population dynamic equilibrium, the regulating equations are primarily intended to describe the behaviour in the surroundings of $\hat{N}^*$. There are no hard r_{max} and b_{max} in selection-regulated dynamics, although I do—for pragmatic reasons—allow for an upper and lower truncation of $i_{a,t}$. The growth rate and birth rate are not even parameters, but initial conditions that cannot be predicted from environmental conditions. Where a given environment has a single explicitly defined growth and birth rate under density regulated growth—for a given environment—the growth rate may take an infinite number of both positive and negative values under selection delayed dynamics. There is no maximum sustainable yield (Witting, 2002), and for given environmental conditions it is possible to predict only the acceleration or deacceleration of growth.

B Bayesian integration

The Bayesian integration between the model and the data is obtained by the sampling-importance-resampling routine (Jeffreys, 1961; Berger, 1985; Rubin, 1988), where n_s random parameterisations θ_i $(1 \leq i \leq n_1)$ are sampled from an importance function $h(\theta)$. This function is a probability distribution function from which a large number, n_s, of independent and identically distributed draws of θ can be taken. $h(\theta)$ shall generally be as close as possible to the posterior, however, the tails of $h(\theta)$ must be no thinner (less dense) than the tails of the posterior (Oh and Berger, 1992). For each drawn parameter set θ_i the population was projected from the first year with a harvest estimate to the present. For each draw an importance weight, or ratio, was then calculated

$$w(\theta_i) = \frac{L(\theta_i)p(\theta_i)}{h(\theta_i)} \tag{15}$$

where $L(\theta_i)$ is the likelihood given the data, and $h(\theta_i)$ and $p(\theta_i)$ are the importance and prior functions evaluated at θ_i. In the present study the importance function is set to the joint prior, so that the importance weight is given simply by the likelihood. The n_s parameter sets were then re-sampled n_r times with replacement, with the sampling probability of the ith parameter set being

$$q_i = \frac{w(\theta_i)}{\sum_{j=1}^{n_s} w(\theta_j)} \tag{16}$$

This generates a random sample of the posterior distribution of size n_r.

The log likelihood is given as a sum ($\ln L = \sum_i \ln L_i$) of the log likelihood of the different data components. The log likelihood of the ith set of the log normally distributed data is calculated as

$$\ln L_n = -\sum_t \frac{[\gamma_s \ln(\hat{x}_{i,t}/\beta_i x_t)]^2}{2\mathrm{cv}_{i,t}^2} + \ln \mathrm{cv}_{i,t} \tag{17}$$

where $\hat{x}_{i,t}$ is the point estimate of the data in year t, x_t the simulated estimate, $\beta_i \neq 1$ a potential bias, $\gamma_s \neq 1$ a potential skew, and $\mathrm{cv}_{i,t} = \sqrt{\hat{\mathrm{cv}}_{i,t}^2 + \sigma_i^2}$ the coefficient of variation, with $\hat{\mathrm{cv}}$ being the cv of the data and σ_i potential overdispersal (additional variance).

The log likelihood of the ith set of the binomially distributed data is calculated as

$$\ln L_n = -\sum_t \frac{(\hat{n}_{i,1,t}/\beta_i - \hat{n}_{i,t} p_{i,1,t})^2}{2\sigma_i^2 \hat{n}_{i,t} p_{i,1,t}(1-p_{i,1,t})} + \ln[\hat{n}_{i,t} p_{i,1,t}(1-p_{i,1,t})]/2 + \ln \sigma_i \tag{18}$$

where $\hat{n}_{i,t}$ is the total number of data observations in year t, $\hat{n}_{i,1,t}$ the number of positive observations, $p_{i,1,t}$ the simulated probability of a positive observation, β_i a potential bias, and σ_i potential overdispersal.

The log likelihood of the ith set of the multinomially distributed age data over $\mathbf{n_a}$ age (a) classes is given as

$$\ln L_n = -\sum_t \sum_{a \in \mathbf{n_a}} \frac{(\hat{n}_{i,a,t} - \hat{n}_{i,t} p_{i,a,t})^2}{2\sigma_i^2 \hat{n}_{i,t} p_{i,a,t}(1-p_{i,a,t})} + \ln[\hat{n}_{i,t} p_{i,a,t}(1-p_{i,a,t})]/2 + \ln \sigma_i \tag{19}$$

where $\hat{n}_{i,t}$ is the total number of aged individuals in year t, $\hat{n}_{i,a,t}$ the number of individuals in age class a, $p_{i,a,t}$ the simulated probability that an observed individual would be in age class a, β_i a potential bias, and σ_i potential overdispersal.

Year	C	Year	C	Year	C	Year	C	Year	C	Year	C	Year	C
1709	1448	1756	0	1803	1063	1850	502	1897	342	1944	1386	1991	802
1710	1430	1757	0	1804	953	1851	474	1898	1336	1945	1558	1992	1652
1711	715	1758	0	1805	206	1852	2230	1899	2380	1946	1040	1993	888
1712	385	1759	0	1806	550	1853	1120	1900	797	1947	1839	1994	1281
1713	1090	1760	0	1807	367	1854	794	1901	0	1948	587	1995	229
1714	635	1761	0	1808	1145	1855	1368	1902	481	1949	955	1996	1600
1715	625	1762	0	1809	226	1856	411	1903	212	1950	560	1997	1380
1716	728	1763	0	1810	429	1857	328	1904	566	1951	2794	1998	1176
1717	720	1764	0	1811	510	1858	757	1905	221	1952	1242	1999	721
1718	409	1765	0	1812	834	1859	836	1906	414	1953	2100	2000	593
1719	726	1766	0	1813	281	1860	640	1907	267	1954	2010	2001	980
1720	803	1767	0	1814	261	1861	341	1908	1793	1955	885	2002	665
1721	905	1768	0	1815	543	1862	1129	1909	985	1956	1816	2003	696
1722	317	1769	0	1816	812	1863	709	1910	1324	1957	2085	2004	1264
1723	1320	1770	16	1817	652	1864	574	1911	1650	1958	2619	2005	644
1724	1063	1771	0	1818	917	1865	1269	1912	669	1959	1426	2006	901
1725	1359	1772	0	1819	1448	1866	1758	1913	168	1960	1795	2007	920
1726	688	1773	0	1820	787	1867	398	1914	291	1961	1892	2008	182
1727	835	1774	0	1821	263	1868	478	1915	1203	1962	1813	2009	548
1728	236	1775	0	1822	1647	1869	716	1916	397	1963	2204	2010	1445
1729	1423	1776	743	1823	1098	1870	842	1917	263	1964	1364	2011	1000
1730	915	1777	0	1824	442	1871	796	1918	848	1965	1620	2012	1147
1731	2188	1778	0	1825	1935	1872	2315	1919	153	1966	1485	2013	1419
1732	277	1779	0	1826	714	1873	1670	1920	802	1967	1973	2014	481
1733	1186	1780	0	1827	711	1874	652	1921	1076	1968	1650	2015	785
1734	696	1781	434	1828	725	1875	780	1922	473	1969	1395	2016	494
1735	559	1782	50	1829	556	1876	797	1923	1047	1970	388	2017	1594
1736	391	1783	0	1830	1149	1877	383	1924	0	1971	1015	2018	1027
1737	350	1784	0	1831	695	1878	329	1925	468	1972	511	2019	942
1738	214	1785	0	1832	391	1879	1930	1926	347	1973	1052	2020	768
1739	313	1786	0	1833	1455	1880	615	1927	0	1974	695	2021	959
1740	0	1787	262	1834	1569	1881	390	1928	480	1975	1194	2022	842
1741	1460	1788	0	1835	1338	1882	521	1929	17	1976	582	2023	1070
1742	0	1789	0	1836	1183	1883	135	1930	266	1977	1035	2024	713
1743	622	1790	0	1837	1221	1884	368	1931	2386	1978	1292	2025	1095
1744	1017	1791	0	1838	1332	1885	977	1932	1282	1979	1724	2026	1095
1745	0	1792	152	1839	1614	1886	723	1933	959	1980	2785	2027	1095

Par	N^*	p	p_0	b_h	b_j	m_h	m_i	m_{0h}	m_{0i}	γ
N^*	1.00	-0.48	-0.12	-0.29	-0.20	0.15	-0.16	-0.25	-0.04	-0.10
p	-0.48	1.00	-0.56	-0.03	0.02	0.08	0.23	0.16	0.05	-0.03
p_0	-0.12	-0.56	1.00	0.15	0.21	0.15	0.08	0.02	0.06	-0.03
b_h	-0.29	-0.03	0.15	1.00	0.15	-0.17	0.19	0.04	-0.01	0.17
b_j	-0.20	0.02	0.21	0.15	1.00	-0.09	0.09	0.12	0.15	-0.10
m_h	0.15	0.08	0.15	-0.17	-0.09	1.00	0.05	0.05	0.08	-0.14
m_i	-0.16	0.23	0.08	0.19	0.09	0.05	1.00	0.16	-0.07	-0.06
m_{0h}	-0.25	0.16	0.02	0.04	0.12	0.05	0.16	1.00	-0.07	0.10
m_{0i}	-0.04	0.05	0.06	-0.01	0.15	0.08	-0.07	-0.07	1.00	-0.08
γ	-0.10	-0.03	-0.03	0.17	-0.10	-0.14	-0.06	0.10	-0.08	1.00

Table 8: **Correlation matrix** for the posterior parameter estimates of Data model (dB).

Par	N_0	N^*	p	p_0	b_h	b_j	m_h	m_i	m_{0h}	m_{0i}	γ
N_0	1.00	0.55	-0.05	-0.15	0.28	0.01	-0.19	0.38	-0.04	-0.17	0.08
N^*	0.55	1.00	-0.07	0.01	-0.12	-0.33	-0.16	0.04	-0.04	-0.08	0.02
p	-0.05	-0.07	1.00	-0.54	0.04	0.17	0.16	0.22	-0.04	-0.16	0
p_0	-0.15	0.01	-0.54	1.00	-0.13	-0.11	0.12	-0.07	0.03	0.10	0.03
b_h	0.28	-0.12	0.04	-0.13	1.00	0.19	0.04	0.30	-0.02	0	0.03
b_j	0.01	-0.33	0.17	-0.11	0.19	1.00	0.01	0.06	-0.01	-0.07	0.02
m_h	-0.19	-0.16	0.16	0.12	0.04	0.01	1.00	0	0.12	0.03	0.02
m_i	0.38	0.04	0.22	-0.07	0.30	0.06	0	1.00	0.06	-0.18	0.06
m_{0h}	-0.04	-0.04	-0.04	0.03	-0.02	-0.01	0.12	0.06	1.00	-0.03	-0.12
m_{0i}	-0.17	-0.08	-0.16	0.10	0	-0.07	0.03	-0.18	-0.03	1.00	0.08
γ	0.08	0.02	0	0.03	0.03	0.02	0.02	0.06	-0.12	0.08	1.00

Table 9: **Correlation matrix** for the posterior parameter estimates of Data model (dE).

References

Berger, J. O. 1985. Statistical decision theory and Bayesian analysis. Second edn. Springer-Verlag, New York.

Jeffreys, H. 1961. Theory of probability. 3rd edition edn. Clarendon Press, Oxford.

Mikkelsen, B. 2025. Age, growth, and reproduction of long-finned pilot whales in the Faroe Islands. NAMMCO/SC/PWWG/2025-01/10, .

Mikkelsen, B., Ofstad, L. H., and Akralid, R. 2025. Catch history of long-finned pilot whales in the Faroe Islands. NAMMCO/SC/PWWG/2025-01/08, .

NAMMCO 2025. Table of accepted abundance estimates. https://nammco.no/abundance-estimates/, .

Oh, M. S. and Berger, J. O. 1992. Adaptive importance sampling in Monte Carlo integration. Journal of Statistics and Computer Simulation, 41: 143–168.

Rubin, D. B. 1988. Using the SIR algorithm to simulate posterior distributions. In Bayesian Statistics 3: Proceedings of the Third Valencia International Meeting, 1–5 June 1987, pp. 395–402. Ed. by, J. M. Bernardo, M. H. DeGroot, D. V. Lindley, and A. M. Smith. Clarendon Press, Oxford.

Smith, C. C. and Fretwell, S. D. 1974. The optimal balance between size and number of offspring. The American Naturalist, 108: 499–506.

Stearns, S. C. 1992. The evolution of life histories. Oxford University Press, Oxford.

Witting, L. 2000a. Interference competition set limits to the fundamental theorem of natural selection. Acta Biotheoretica, 48: 107–120, https://doi.org/10.1023/A:1002788313345.

Witting, L. 2000b. Population cycles caused by selection by density dependent competitive interactions. Bulletin of Mathematical Biology, 62: 1109–1136, https://doi.org/10.1006/bulm.2000.0200.

Witting, L. 2002. Evolutionary dynamics of exploited populations selected by density dependent competitive interactions. Ecological Modelling, 157: 51–68, https://doi.org/10.1016/S0304–3800(02)00172–2.

Witting, L. 2013. Selection-delayed population dynamics in baleen whales and beyond. Population Ecology, 55: 377–401, https://dx.doi.org/10.1007/s10144–013–0370–9.